

Ricardo Delgado de Souza

DEVELOPMENT OF A DIAMOND WIRE WELDING DEVICE

Dissertação submetida ao Programa de Pós-Graduação em Engenharia Mecânica para a obtenção do Grau de Mestre em Engenharia Mecânica.

Orientador: Prof. Fabio Antonio Xavier,
Dr. Eng.

Coorientador: Prof. Walter L. Weingaertner,
Dr.-Ing.

Florianópolis

2019

Ficha de identificação da obra elaborada pelo autor, através do Programa de Geração Automática da Biblioteca Universitária da UFSC.

Souza, Ricardo Delgado de
Development of a diamond wire welding device /
Ricardo Delgado de Souza ; orientador, Fabio Antonio Xavier,
coorientador, Walter Lindolfo Weingaertner, 2019.
162 p.

Dissertação (mestrado) - Universidade Federal de Santa Catarina,
Centro Tecnológico, Programa de Pós Graduação em Engenharia
Mecânica,
Florianópolis, 2019.

Inclui referências.

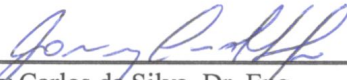
1. Engenharia Mecânica. 2. Desenvolvimento de produto industrial. 3. Metodologia de projetos. 4. Soldagem de fio diamantado. 5. Serra de fio sem fim. I. Xavier, Fabio Antonio . II. Weingaertner, Walter Lindolfo. III. Universidade Federal de Santa Catarina. Programa de Pós-Graduação em Engenharia Mecânica. IV. Título.

Ricardo Delgado de Souza

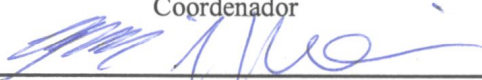
DEVELOPMENT OF A DIAMOND WIRE WELDING DEVICE

Esta dissertação foi julgada aprovada para a obtenção do Título de “Mestre em Engenharia Mecânica”, e aprovada em sua forma final pelo Programa de Pós-Graduação em Engenharia Mecânica.

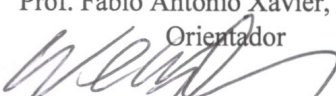
Florianópolis, 20 de Fevereiro de 2019.



Prof. Jonny Carlos da Silva, Dr. Eng.
Coordenador




Prof. Fabio Antonio Xavier, Dr. Eng.
Orientador

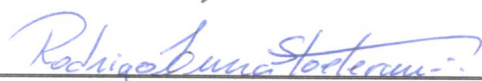


Prof. Dr.-Ing. Walter L. Weingaertner
Coorientador

Banca Examinadora:



Prof. Milton Pereira, Dr. Eng.
Universidade Federal de Santa Catarina – UFSC



Prof. Rodrigo Lima Stoeterau, Dr. Eng.
Universidade de São Paulo – USP

À minha família e à minha noiva Amanda, por
todo amor e carinho.

AGRADECIMENTOS

Com a entrega deste trabalho, uma grande etapa da minha vida é concluída. Desta forma, devo agradecer a todos aqueles que, de alguma forma, contribuíram neste percurso.

A Deus, pelo dom da vida.

Aos meus pais Evanir José de Souza, Neusa Maria Delgado de Souza pelo incentivo e apoio em todos os momentos, pelo amor e carinho incondicional. Agradeço eternamente por terem dedicados suas vidas a mim.

Aos meu avós, que me educaram e sempre se orgulharam de mim.

Ao meu irmão Leandro Delgado de Souza pelo apoio, amizade e diversão que sempre me proporcionou, e pelo caráter e valores que adquiri de ti.

À minha noiva Amanda Legnani, pelo incentivo nesta etapa, por me apoiar em cada decisão, por se dedicar à nossa felicidade, e pelo imenso amor. Seu esforço e carinho deram sentido a este passo da minha vida. Cada sorriso seu me dava forças para continuar.

Meus sinceros agradecimentos ao Prof. Walter L. Weingaertner pelo conhecimento transmitido e pela oportunidade de desempenhar meu trabalho. Ao professor Fabio A. Xavier pela confiança, orientação e oportunidades proporcionadas. Aos demais professores do LMP pela amizade e pelo ambiente de aprendizado.

Gostaria de agradecer o Prof. Celso Salamon da UTFPR pela doação de componentes que foram essenciais para a realização deste trabalho.

Minha gratidão se estende aos meus colegas de laboratório, Ricardo Knoblauch, Francisco Ratusznei, Jurandir Marcos e Gabriel Barbosa, que proporcionaram um ambiente descontraído e me ajudaram em diversos momentos deste trabalho.

Por fim agradeço à CAPES pela bolsa fornecida para o desenvolvimento deste trabalho.

You're here for a good time, not a long time.

Colin McRae

RESUMO

O Serramento com Fio Diamantado (DWS) é a tecnologia mais promissora utilizada atualmente para fatiar *wafers* de silício (Si) para a indústria foto-voltaica. No DWS, o fio diamantado é alimentado de um carretel de fornecimento para um carretel de recolhimento, formando uma rede de múltiplos fios, fatiando o lingote de Si em centenas de *wafers* pelo movimento recíprocante do fio. O modo de operação recíprocante impossibilita a investigação dos parâmetros do processo e do desgaste da ferramenta. Baseado nisso, no Laboratório de Mecânica de Precisão (LMP) foi desenvolvida uma bancada experimental de serramento que utiliza um único fio diamantado em formato de *loop* para cortar materiais frágeis. Desta forma, com uma serra de fio de apenas um metro operando em velocidade constante em apenas uma direção, é possível observar o desgaste do fio e investigar melhor o processo. Para a fabricação dos fios diamantados em *loop*, dispositivos de soldagem por resistência foram inicialmente desenvolvidos, e embora tenham atingido seus objetivos, apresentaram diversos problemas de desempenho. Desta maneira, o objetivo deste trabalho consiste no desenvolvimento de um dispositivo de soldagem de fios diamantados que apresentasse conceitos inovadores, alta eficiência e facilidade de operação. Portanto, o dispositivo de solda foi desenvolvido utilizando uma metodologia de desenvolvimento de produtos industriais (PRODIP). O dispositivo foi fabricado no LMP, testado e utilizado para a concretização de diversos procedimentos de soldagem, fornecendo ao laboratório serras de fio contínuas. Também foram realizados experimentos para caracterizar a qualidade das soldas, como examinação visual, ensaio de flexão, ensaio de tensão de ruptura, metalografia, microdureza e medição da excentricidade da junta de solda. Primeiramente foi notado a importância da utilização de uma metodologia sistemática para o desenvolvimento de um produto industrial. Através dos experimentos, foram encontrados os parâmetros de soldagem e tratamento térmico para atingir soldas de alta qualidade. Os perfis de microdureza das juntas de solda foram caracterizados e a zona afetada termicamente foi definida. Nos experimentos de medição da excentricidade foi encontrado que as soldas possuem um desalinhamento médio de apenas 6,36% do diâmetro do fio, alcançado por fatores construtivos do dispositivo. Assim, o dispositivo de soldagem desenvolvido desempenhou suas funções com sucesso, portanto foi submetido à patente como modelo de utilidade.

Palavras-chave: Metodologia de projeto. Desenvolvimento de produtos industriais. Fio diamantado. Soldagem de topo. Serra de fio contínuo.

RESUMO EXPANDIDO

Introdução

A indústria de energia solar fotovoltaica apresenta uma das tecnologias mais promissoras para suprir a demanda mundial por energia limpa e renovável. No ano de 2017 foram instalados mais de 99 Gigawatts de painéis solares fotovoltaicos pelo mundo. No entanto, o custo da energia solar fotovoltaica ainda é elevado devido ao alto custo de fabricação dos painéis solares, que são fabricados principalmente de silício monocristalino. O custo de fabricação pode representar até 40% do custo total de uma célula solar, sendo que o processo de *wafering* representa até 26% do custo total da célula. Desta forma, o serramento de silício com fio diamantado, é um assunto muito importante de ser pesquisado, visto que a indústria busca reduzir os custos de fabricação dos painéis solares para aumentar a viabilidade econômica desta tecnologia. Os dois principais métodos utilizados na indústria para o fatiamento de silício é o serramento com múltiplos fios diamantados e o serramento com múltiplos fios com pasta abrasiva. Como o processo de serramento com fio diamantado apresenta algumas vantagens, ele se consolidou como a tecnologia mais promissora. Embora venha sendo empregado na indústria de *wafering* por um longo tempo, a pesquisa deste processo ainda é limitada. O princípio de operação de uma serra de múltiplos fios impossibilita uma melhor investigação do processo, devido ao movimento recíprocante do fio. Para superar esta barreira no Laboratório de Mecânica de Precisão da Universidade Federal de Santa Catarina foi desenvolvida uma bancada de serramento com fio diamantado, neste equipamento é utilizado um segmento de fio diamantado contínuo, em formato de laço de apenas um metro de comprimento, assim pode-se utilizar velocidades de corte e avanços contínuos e rastrear um conjunto de grãos abrasivos para monitorar o desgaste dos diamantes. No entanto, para fabricar a serra contínua é necessário soldar as extremidades do fio diamantado, que possui cerca de 0,3 mm de diâmetro, sendo um processo muito difícil de ser executado. Para isso foram desenvolvidos diversos dispositivos de soldagem, que apesar de funcionarem, apresentavam baixas taxas de consolidação do procedimento e dificuldade de operação. Desta forma, no presente trabalho foi desenvolvido um novo dispositivo de soldagem de fios diamantados pelo processo de soldagem de topo por resistência.

Objetivos

O objetivo principal deste trabalho é desenvolver um dispositivo capaz de soldar fios diamantados pelo processo de soldagem de topo por resistência com baixa taxa de falha e baixa dependência do operador. Assim, determinou-se os seguintes objetivos específicos: Aplicar o conhecimento de

metodologia de projeto desenvolvido no POSMEC; Fabricar um dispositivo com conceitos inovadores; Promover avanços na pesquisa de serramento com fio diamantado; Apresentar as características das juntas soldadas.

Metodologia

A metodologia utilizada para a estruturação do processo de projeto do dispositivo foi a PRODIP (Projeto de Desenvolvimento Integrado do Produto). A primeira etapa foi o desenvolvimento do projeto informacional, no qual foram estabelecidos os problemas do projeto, realizou-se uma pesquisa por informações técnicas, estabeleceu-se o ciclo de vida do produto e os usuários. Assim, obteve-se as necessidades dos usuários, que foram transformadas em requisitos dos usuários, e quando combinados com os requisitos do projeto através do método QFD originaram as especificações do projeto. A segunda etapa foi a fase de projeto conceitual, na qual o projeto foi desenvolvido em termos de formas, materiais e funções. A terceira etapa foi o projeto preliminar, na qual projetou-se definitivamente o dispositivo e fabricou-se as peças e montou-se o dispositivo, estando pronto para testes. Na metodologia experimental primeiro foram realizados experimentos para avaliar o desempenho do dispositivo de soldagem. Em seguida definiu-se os parâmetros de soldagem e por fim realizou-se experimentos para avaliar a qualidade das soldas e a caracterizar a junta soldada.

Resultados e Discussão

O dispositivo apresentou bom desempenho em suas funções. Inicialmente foi avaliado a capacidade do mecanismo de usinagem de ranhuras, pelo qual foram fabricadas duas ranhuras para posicionamento das pontas do fio diamantado para soldar. O formato e dimensão das ranhuras usinadas pelo mecanismo apresentaram-se melhores do que as ranhuras feitas anteriormente por disco abrasivo e manualmente com fio diamantado. O eletrodo de cobre utilizado apresentou bom desempenho conduzindo eletricidade para a junta de solda. Os componentes de movimentação e posicionamento da junta de solda foram fabricados em aço ao invés de alumínio, isso contribuiu para a consolidação dos procedimentos de soldagem. Os conceitos inovadores do dispositivo de soldagem, principalmente a ausência de atrito estático na força de soldagem, fez com que aproximadamente 90% dos procedimentos de soldagem fossem consolidados. Mais de 500 soldas foram realizadas em dez meses de operação do dispositivo. Nos experimentos de soldagem, através da avaliação visual das soldas, foi estabelecido que a combinação de parâmetros $C_1 = 19$, 5%, $T_1 = 0$, 5 s, $D = 1$ mm e $F = 2$, 2 N apresentou os melhores resultados para consolidação da junta de solda. No ensaio de flexão estes parâmetros novamente se apresentaram como melhores. Nos

ensaios de tensão de ruptura foi observado que os parâmetros de tratamento térmico possuem grande influência na resistência mecânica da solda, sendo que a combinação de parâmetros T08, C1 = 19, 5%; T 1 = 0, 5s, C2 = 14%; T 2 = 1, 0s, T 3 = 30, 0s; T 4 = 30, 0s apresentou os maiores valores de resistência à ruptura, estes parâmetros também apresentaram as soldas com melhores aspectos de microestrutura. Pode-se definir a zona afetada pelo calor e a região de transição do material de base para o material recristalizado. Nos experimentos de medição da excentricidade da junta de solda conclui-se que a média de desalinhamento das soldas feitas no dispositivo corresponde à 6,36% do diâmetro do fio. No teste de microdureza pode-se definir o perfil de microdureza das soldas, sendo que a zona afetada pelo calor possui uma dureza muito inferior ao material de base, cerca de 300 HV a menos, correspondendo a uma zona de aço recristalizado.

Considerações finais

Concluiu-se com o desenvolvimento deste trabalho que os conceitos de metodologia de projeto desenvolvidos no POSMEC são eficientes no projeto de desenvolvimento de produtos industriais. O conceito inovador do mecanismo de usinagem de ranhuras apresentou eficiência em sua função. Obsevou-se uma elevada sensibilidade da solda em relação aos parâmetros de soldagem, aonde uma variação de apenas 0,5% em um parâmetro de solda foi suficiente para a consolidação ou não consolidação da solda de topo por resistência. Foi notado uma baixa dificuldade de utilização do dispositivo, assim como uma elevada eficiência. O desenvolvimento do dispositivo de soldagem foi de grande importância para a pesquisa no Laboratório de Mecânica de Precisão, sendo que foi solicitado a patente do dispositivo como modelo de utilidade.

Palavras-chave: Metodologia de projeto. Desenvolvimento de produtos industriais. Fio diamantado. Soldagem de topo. Serra de fio contínuo.

ABSTRACT

Diamond Wire Sawing (DWS) is the most promising technology used nowadays to slice silicon (Si) wafers for the electronics and photovoltaic industry. In the DWS, a diamond wire is fed from a supply-spool to a take-up spool, forming a web of multiple strands of wire. The Si ingot is fed against the wire web and sliced into hundreds of wafers by the reciprocating movement of the wire. The reciprocating mode of operation makes it impossible to investigate correlations between input and output parameters of the process, investigations on tool wear are also difficult to perform. Based on the mentioned difficulties found in the reciprocating DWS, in the Laboratory of Precision Engineering (LMP) an experimental wire saw test rig that uses a single looped diamond wire to cut brittle materials was developed. In this way, with a segment of diamond wire of just over one meter in looped shape, operating at constant speed in only one direction, it is possible to observe the wire wear and investigate the influence of the process parameters on the characteristics of the sawed pieces. For the manufacture of looped diamond wire, a resistance-welding device was initially developed in the laboratory. However, the first developed prototypes, despite having achieved their goals, presented several performance problems. In this way, the proposal of the present work is the development of a diamond wire welding device that presented innovative concepts, high-efficiency and ease of operation. Therefore, initially using an industrial product development methodology (PRODIP), the welding device was designed. Then the device was manufactured in the LMP and was tested and used for the accomplishment of several diamond wire welding procedures, providing the laboratory with endless wire saws. Experiments were also carried out to characterize the weld quality, such as visual examination, bend test, rupture strength test, metallography, microhardness and measurement of weld joint eccentricity. Firstly, it was noted the efficiency and importance of using a systematic methodology for the development of industrial products. Through the experiments, welding and heat treatment parameters were found to reach high-quality welds. The microhardness profiles of the welding joints were characterized and the heated affected zone was defined. Through the eccentricity measurement, it has been found that the welds have an average misalignment of only 6,36% of the wire diameter, achieved by constructive factors of the device. Thus, the developed welding device reached its target successfully, so it was filed for patent as utility model.

Keywords: Design methodology. Industrial product development. Diamond wire. Upset welding. Endless wire saw.

LIST OF ABBREVIATIONS

ABNT	<i>Associação Brasileira de Normas Técnicas</i>
ASM	American Society for Metals
ASTM	American Society for Testing and Materials
BM	Base metal
CERMAT	Research Center of Ceramic and Composite Materials
DOE	Design of experiments
DIN	<i>Deutsches Institut für Normung</i>
DWS	Diamond wire sawing
HAZ	Heat-affected zone
HV	Vickers pyramid number
IDHBS	Inner diameter hollow blade saws
ISO	International Organization for Standardization
LABCONF	Metal Forming Laboratory
LABMAT	Materials Laboratory
LMP	Precision Engineering Laboratory
MWSS	Multi-wire slurry sawing
NeDIP	<i>Núcleo de Desenvolvimento Integrado de Produtos</i>
OD	Outside diameter
POSMEC	<i>Programa de Pós Graduação em Engenharia Mecânica</i>
PRODIP	<i>Processo de desenvolvimento integrado de produtos</i>
PV	Photovoltaic
QFD	Quality Function Deployment
RWMA	Resistance Welder Manufacturers Alliance
SEM	Scanning electron microscope
TRIAC	Triode for alternating current
UFSC	<i>Universidade Federal de Santa Catarina</i>
USB	Universal Serial Bus

LIST OF SYMBOLS

v_c	Cutting speed
v_f	Feed speed
R	Amount of resistance in welding
ρ	Material resistivity
A	Cross-section area of conductor
L	Length of conductor
Q	Amount of heat in welding
I	Electric current
t	Time
e	Eccentricity
θ	Angle
X_n	Displacement between the circle centers
L_0	Half length of the welding zone
L_1	Distance between the 1st and 4th indentation

CONTENTS

1 INTRODUCTION	25
1.1 MOTIVATION	27
1.2 WORK OBJECTIVES	27
1.2.1 Main goal	27
1.2.2 Specific goals	27
1.3 WORK DELIMITATIONS	27
1.4 OVERVIEW OF THIS WORK	28
2 LITERATURE REVIEW	29
2.1 WAFERING PROCESS	29
2.2 DIAMOND WIRE	32
2.3 ENDLESS WIRE SAWS	33
2.4 WELDING	36
2.4.1 Resistance welding	36
2.4.1.1 Resistance butt welding	36
2.5 WELD QUALITY	38
2.5.1 Weld evaluation methods	39
3 DEVELOPMENT OF WELDING DEVICE	41
3.1 INFORMATIONAL DESIGN	42
3.1.1 Project issues	43
3.1.2 Research for technical informations	44
3.1.3 Product life cycle and customers	45
3.1.4 Customers needs	46
3.1.5 Customer requeriments	48
3.1.6 Design requeriments	50
3.1.7 Design specifications	51
3.2 CONCEPTUAL DESIGN	53
3.2.1 Overall function	53
3.2.2 Functional structure	53
3.2.3 Morphological matrix	56
3.2.4 Designs evaluation	59
3.2.5 Design generated	60
3.3 PRELIMINARY DESIGN	61
3.3.1 Device layout definition	61
3.3.1.1 Welding system	62
3.3.1.2 Groove machining system	66
4 EXPERIMENTAL METHODOLOGY	73
4.1 WELDING PROCEDURES	75

4.1.1 Groove shaping	75
4.1.1.1 Diamond wire as groove shaping tool	75
4.1.1.2 Groove shaping procedure	75
4.1.2 Wire end preparation	80
4.1.3 Welding method	81
4.2 EXPERIMENTS	83
4.2.1 Welding pre-tests	84
4.2.1.1 Welding pre-tests samples	84
4.2.1.2 Welding pre-tests parameters	84
4.2.2 Welding tests	87
4.2.2.1 Welding test samples	87
4.2.2.2 Welding tests parameters	87
4.2.2.3 Welding test procedures	87
4.2.2.4 Weld visual examination	88
4.2.2.5 Bend test	88
4.2.3 Rupture strength test	89
4.2.3.1 Rupture strength test samples	89
4.2.3.2 Heat cycle parameters	89
4.2.3.3 Rupture strength testing device	90
4.2.4 Weld joint metallography	91
4.2.5 Complementary experiments	91
4.2.5.1 Weld joint eccentricity	91
4.2.5.2 Vickers microhardness	96
5 RESULTS	99
5.1 WELDING DEVICE PERFORMANCE	99
5.2 WELDING TESTS	103
5.2.1 Visual examination	103
5.2.2 Bend test	105
5.3 RUPTURE STRENGTH TEST	107
5.4 METALLOGRAPHIC EXAMINATION	112
5.5 ECCENTRICITY	117
5.6 VICKERS MICROHARDNESS	117
6 SUMMARY AND CONCLUSIONS	123
6.1 SUGGESTION FOR FUTURE WORK	125
Bibliography	127
APPENDIX A – Quality Function Deployment (QFD)	135
APPENDIX B – Welding power supply	141
APPENDIX C – Weld joints metallography	145

1 INTRODUCTION

The shortage of natural resources has led many countries to search for renewable resources as well as develop green technologies. Based on that, governments around the world have established a series of supportive policies to growth new energy industry. Solar Photovoltaic (PV) industry is one of the potential industries that provide clean and renewable energies (JIA; SAN; KOH, 2016). In 2017 close to 99 Gigawatts (*GW*) of PV panels have been installed globally and the total cumulative installed capacity was above 403,3 *GW* at the end of 2017 (IEA, 2018), as presented in Figure 1.

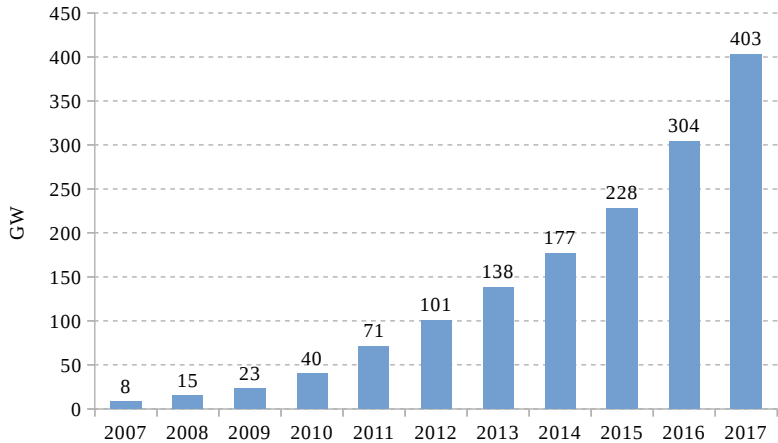


Figure 1: Evolution of cumulative PV installations (*GW*). Adapted from IEA (2018).

However, the cost of electricity generated from solar photovoltaic (PV) system is still higher than conventional sources (e.g., nuclear, coal and gas) due to the high cost of manufacturing the solar panels (ECHEGARAY, 2014).

Photovoltaic solar cells based on crystalline silicon wafer represent more than 94% of the market share today. The multi-wire sawing is the main technology responsible for slicing silicon (Si) ingots into wafers. The cost to produce Si wafers accounts for approximately 30 – 40% of the total solar cell fabrication cost, and the wafering process represents 26% of the wafer cost (MöLLER et al., 2005). Therefore, the multi-wire sawing of silicon is an important subject to be investigated, notably as the industry seeks to reduce the materials and manufacturing costs to increase the economic viability of solar cell technologies.

The two main technologies used nowadays for Si-wafering are multi-wire slurry sawing (MWSS) and diamond wire sawing (DWS). In MWSS, the cut is performed by loose abrasives (silicon carbide) immersed in oil or polyethylene glycol. The slurry is supplied through nozzles over a wire web and carried by the wire into the sawing channel. In DWS, the cut is performed by fixed abrasives (diamond grits) bonded to the wire. The wire motion in DWS is reciprocating (pilgrim-mode), and the wire cutting direction is reversed several times during the cut. The slurry is replaced by coolant fluid, such as water (MÖLLER, 2015), (KNOBLAUCH et al., 2018).

Compared to the MWSS, the DWS process has several advantages, such as productivity two to three times higher, use of water-based cutting fluid that reduces hazardous waste, smaller depth of damage in sliced wafers, reduced kerf loss, stronger wafers leading to longer lifecycle and reducing cost of waste treatment. Thus, DWS was established as a solid technology to meet the demands of society for cleaner and renewable photovoltaic energy (KUMAR; MELKOTE, 2018).

Although wire sawing technology has been widely used in the industry for a long time, research efforts on this complex manufacturing process have been very limited until recent years. The recent boom of crystalline silicon photovoltaic industry significantly promoted research attention in this abrasive manufacturing technology (WU, 2016). Various aspects of wire sawing technology have been investigated, but the reciprocating motion of the diamond wire saws prevented a better investigation of the process.

To overcome the difficulties encountered when investigating DWS using reciprocating machines, it was developed in the Laboratory of Precision Engineering (LMP) an endless wire saw test rig (KNOBLAUCH et al., 2017a). The test rig makes use of industrial diamond wires that are butt-welded in looped shape by an upset welding device that was developed by Knoblauch et al. (2017b). These efforts resulted in a research of great importance for the understanding on wire wear, in which Knoblauch et al. (2018) investigated the wear progression of the diamond grains.

Although the welding device developed in the lab have reached its target, it presents a high failure rate. It has also been noticed that in order to the welds exhibit good integrity, it was necessary for the device operator to have a high knowledge about the process and to have a certain ability to operate the device, thus leading to a dependence of the weld quality on the operator skills.

In this way, it was noticed the need to develop a new welding device that presented high efficiency and reproducibility, and dependence on the operator to obtain high-quality welds.

1.1 MOTIVATION

Welding of diamond wire, although using a widely employed welding concept, is a process that has been tried by few researchers and it is difficult to execute. Since the main work carried out in this area was developed in the LMP, the development of a precise welding equipment that exhibit low failure rate is an opportunity to develop research in topics of diamond wire welding, as well as the establishment of the device as utility model.

1.2 WORK OBJECTIVES

1.2.1 Main goal

The main goal of this work is to develop a device capable of welding diamond wires by the upset welding process with low failure rate and low dependence on operator.

1.2.2 Specific goals

- To apply the knowledge of design methodology developed at POSMEC to structure the design process of the welding device.
- To manufacture a welding device that features innovative concepts.
- To provide advances in research of diamond wire sawing by manufacturing endless diamond wires.
- To present the characteristics of the welded joints of diamond wires.

1.3 WORK DELIMITATIONS

As indicated in previous sections, this work is limited to the development of a diamond wire welding device. However, the development of a welding equipment can be related to several topics, such as improvement in design methodology, welding, materials science and electronics, for example. The characteristics of the welds can also be investigated regarding several topics. Since it is not possible to perform a proper research in several areas in short time, this work is focused on the manufacture of the welding device to supply a laboratory demand for endless wires.

1.4 OVERVIEW OF THIS WORK

This master's dissertation is divided into six chapters, which have been organized in a way to provide the reader with a better understanding of the steps performed in this work.

Chapter 1 introduces the subject of this work, contextualizing the wafering of silicon and the importance of the development of endless wire saws. It is pointed out the main problems observed in the literature and the theme of this study is proposed. Furthermore the research gap, purposes and delimitations of this work are presented.

Chapter 2 discusses the fundamentals of the wire sawing of brittle materials, presents the main research papers that have used endless diamond wire saws and describes the technologies used to manufacture them. In addition, it is discussed the fundamental concepts related to the upset welding process and the main methods of evaluating the quality and integrity of welds performed by this process.

Chapter 3 describes the entire development of the diamond wire welding device. Initially, the design methodology used is contextualized, then each stage of the design methodology is described and applied to the development of the device.

Chapter 4 presents in the first instance the operating procedures of the welding device developed in the previous chapter. Subsequently, the methodology adopted for the experiments and analysis of results is described.

Chapter 5 presents the results obtained by the development of this work. Firstly the results related to the welding device are described, such as its operation. Subsequently the experimental results of the tests performed are discussed.

Chapter 6 is dedicated to the conclusions. It describes the objectives accomplished and the results and advancements achieved. In addition, final considerations and suggestions for future works are presented.

2 LITERATURE REVIEW

2.1 WAFERING PROCESS

The wide utilization of silicon (Si) wafers in photovoltaic solar cell and in microelectronics industries requires parallel processes for the wafer cutting process. Usually, inner diameter hollow blade saws (IDHBS), outside diameter (OD) saws and multi-wire saws are utilized in the silicon wafering. Wire saws possess several advantages over (IDHB and OD) saws. The main advantages are higher productivity, less wafer surface damage, lower kerf loss and the ability to cut ingots of large size and diameter (TEOMETE, 2008), (WU, 2016). Recently, wire saws have been used to cut both brittle and ductile materials, such as sapphire, crystalline silicon, silicon carbide, rare earth magnets, wood, rock, and almost all kinds of ceramics including foam ceramics (CHIKUBA; ISHIDA, 2002),(GE et al., 2004),(TEOMETE, 2008),(TEOMETE, 2011),(WU, 2016).

In Figure 2, a schematic drawing of the multi-wire sawing technology is shown. A single wire is fed from a supply spool through a pulley and tension control unit to the wire guides. Multiple strands of a wire web are formed by winding the wire through 500 – 3000 parallel grooves on the wire guides. The main unit and the slave rollers are responsible for pulling the wire web and holding it tight. Workpiece ingots, glued to the holder, are fed through the web of parallel wires, thereby slicing a hundreds or more wafers simultaneously (KNOBLAUCH et al., 2017b),(WU, 2016).

The machine works based on pilgrim-mode: the wire is set in motion in one direction for several hundred meters, stopped, and then set in motion in the opposite direction for a shorter length (KNOBLAUCH et al., 2017a).

Bidville (2010) notes that the typical silicon ingot size is $125 \times 125 \text{ mm}^2$ or $156 \times 156 \text{ mm}^2$ and has a length of around 300 mm. Several bricks can be sawed together: up to 2 meters of silicon brick length can be cut at the same time in the largest saws. This means that one single cut can produce up to 6000 wafers at a time, assuming that the distance from one wire to the another wire is 300 μm .

The two main technologies used nowadays for Si wafering are multi-wire sawing with slurry (MWSS) and with fixed abrasives (DWS). In the first case, the cutting is achieved by an abrasive slurry which is supplied through nozzles (fluid spray - Figure 2) over the wire web and transported to the sawing channel by the wire. Commercial slurries are based on oil or ethylene glycol and abrasive particles, usually silicon carbide (SiC) (MÖLLER, 2006).

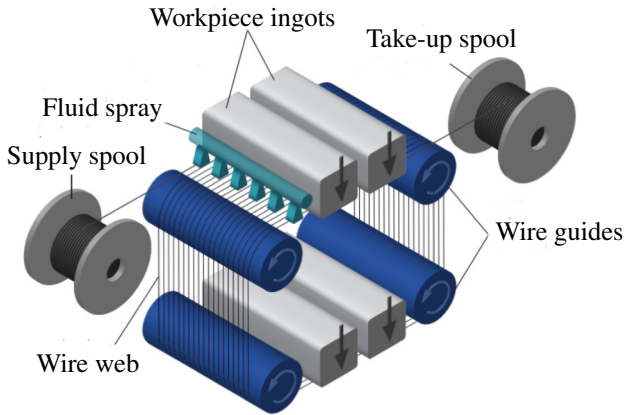


Figure 2: Schematic of multi-wire sawing of ingots into wafers. Adapted from Knoblauch et al. (2017b).

Although these technologies share similar features, the MWSS is fundamentally different from the DWS process regarding material removal mechanism. Material removal in slurry sawing is achieved by the interactions between the SiC particles, the wire and the workpiece. Consequently, the wire is worn and needs to be replaced after each cut. This process is referred to as three-body-wear in tribology (Figure 3 a) (WU, 2016). In this process the conventional cutting speeds are between $10 - 20 \text{ m/s}$, ingot feed rate around $0,3 - 0,5 \text{ mm/min}$ which leads to a total cutting time of $8 - 13$ hours for a standard ingot size, so the process can take up to half the day to run and generates a lot of wastes: the worn steel wire, higher kerf loss, thus more material use, yields larger depth of damage, requiring more post-processing resources. The slurry that contains silicon debris that have to be taken out before the slurry is used again (MÖLLER, 2015)(KUMAR; MELKOTE, 2018).

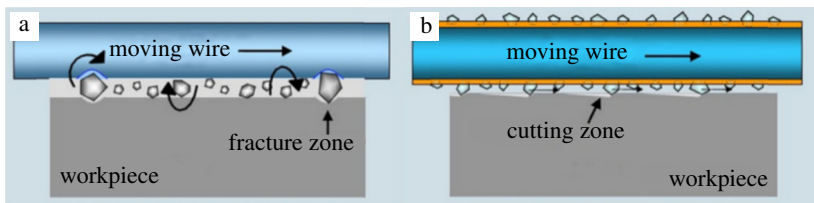


Figure 3: Schematics of the cutting mechanisms: slurry sawing (a), diamond wire sawing (b). Adapted from Wu (2016).

To reduce processing time, to increase productivity, to reduce environmental damage and to machine other harder and more difficult-to-machine materials, diamond impregnated wires, which leads to fixed abrasive machining, have been developed (CLARK et al., 2003).

The multiwire fixed abrasive diamond wire sawing (DWS) technology instead of using SiC grits in slurry as cutting agents, uses a wire impregnated or electroplated with diamond grits that serve as fixed cutting edges, and the abrasive slurry is replaced by a coolant fluid, commonly water. An example of the commercially available diamond wire used in DWS can be seen in Figure 4. As previously mentioned, another difference of the DWS from the MWSS is the material removal mechanism, which can be observed in Figure 3 (b). In DWS the chip is formed through two-body-wear, which involves the direct interaction of the diamond grits with the workpiece material (WU, 2016).

The DWS provides many advantages over the MWSS, like a higher productivity (ingot feed rate can reach $> 1 \text{ mm/min}$), taking cutting time to approximately 2 – 3 hours), an easier recycling of the coolant fluid, a higher possibility of recycling the silicon chip due to the absence of silicon carbide particles, minor wear of the wire and a great potential for the thinner wafer slicing using finer wires (MÖLLER, 2015), (KUMAR; MELKOTE, 2018) . In addition, diamond wire sawing significantly reduces the use of chemicals to clean the wafers after cutting which would cause environmental impacts (YU et al., 2012).

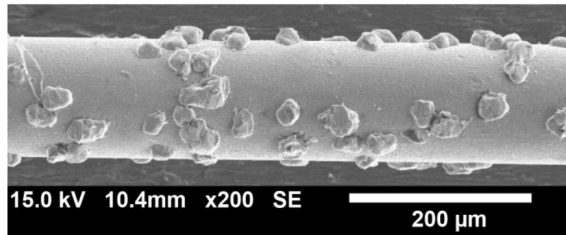


Figure 4: Electroplated diamond wire (WU, 2012).

Due to the mentioned advantages, fixed abrasive wire sawing technology has been widely researched and encouraged in the industry, since the fact of productivity is up to three times greater and have the possibility to recycle the material chip, reaching increasingly thin wafers, with higher quality surface and less material wastage. All these factors have brought greater viability to the manufacturing of photovoltaic solar cells, which promotes cheaper adoption of clean solar energy (KUMAR; MELKOTE, 2018), (KNOBLAUCH, 2019).

2.2 DIAMOND WIRE

The cutting tool used in diamond wire sawing is commonly a steel wire (piano wire) with a surface layer of abrasive grains, laid up by the method of electroplating or resin bonding (WU, 2012). Chiba et al. (2003) notes that resin bonding wire is cheaper to manufacture. More than 10 km of wire can be produced relatively cheaply, but the grains are less strongly bonded to the wire surface. According to Chiba et al. (2003) and Möller (2015), this type of wire does not withstand great cutting forces, they have a lower resistance to wear than electroplated diamond wire tools, and they are extremely difficult to use in multi-wire sawing of hard and large workpieces, which consequently reduces the cutting performance.

In the electroplating technique, the diamond grits are embedded in a nickel-coating layer, which gives a great adhesive strength and high resistance to wear, but at the expense of the higher cost, because the electroplating steps during the manufacturing process are time-consuming. In Figure 5 one can observe a metallography of an electroplated diamond wire used in DWS.

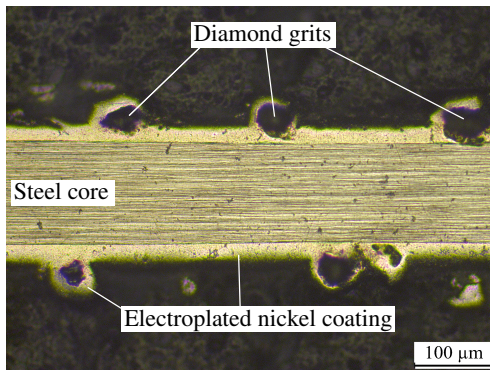


Figure 5: Metallography of the longitudinal cross-section of an electroplated diamond wire.

The steel core of commercially available diamond wires is standardized according to ASTM-A228/A228M-18 (2018): Standard Specification for Steel Wire, Music Spring Quality. This standard specifies cold-drawn steel wire, uniform in mechanical properties, intended especially for the manufacture of springs subjected to high stresses and/or requiring good fatigue properties. Diamond wires can also be made with a stainless steel core, usually AISI 304 austenitic stainless steel, as used in the researches of Sbravati (2014), Tanner (2015) and Götttsching (2017).

2.3 ENDLESS WIRE SAWS

As mentioned earlier, multi-wire sawing machines and even single diamond wire sawing machines, whether for industrial or research applications, make impossible a proper investigation of the cutting process, due to the reciprocating operation mode and the length of wire used.

An efficient way to overcome these challenges and conduct a research for understanding the fundamentals of the cutting process is by using an endless wire saw setup. This saw setup uses an endless (looped) wire that is set in motion to run around two or more guide rollers (pulleys). The workpiece is pushed against the wire, and the motion of the abrasive wire is accountable for the material removal from the workpiece (Figure 6).

Knoblauch et al. (2017a) notes that, the looped wire setup is a way to understand better the process, because it is possible to isolate the cutting speed (v_c) and feed rate (v_f), which can be kept constant during the cut. Moreover, it is even possible to follow the same wire section to investigate the wear progression of a group of abrasive grits after every cut, which would be practically impossible in the case of a spool-to-spool setup, due to the hundreds or even thousands meters of wire.

The concept of endless wire saw for cutting hard materials has been used since the 19th century. In 1888, François Turretini of Geneva in Switzerland, registered the patent US379835A which claims the invention of an endless saw for cutting stones (TURRENTINI, 1888). This technology was restricted to the mining industry for cutting large blocks of ores such as marble. The first report related to low diameter endless wire saws for cutting hard and brittle materials corresponds to a patent invented by HODSEN and HODSEN (2000), which claims a method of manufacture endless wire saw by butt-welding and heat treating, but no experimental results are presented.

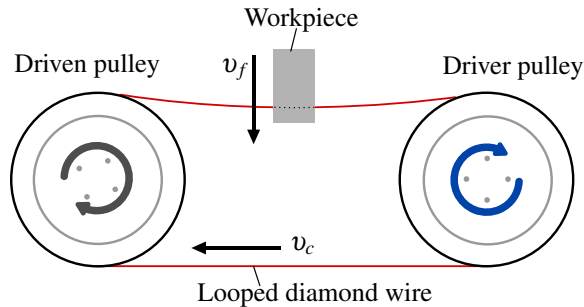


Figure 6: Schematic of endless wire saw setup.

Knoblauch (2019) observed that although the endless wire conception has several advantages, the manufacturing of an endless wire is a critical problem, which is difficult to be done when the wire diameter is lower than $500 \mu m$. Therefore, few works about endless wire sawing have been developed in recent years. In Table 1, one can observe main works in the literature related to the endless wire saw and their respective methods of acquisition or manufacturing the endless wire saws.

Table 1: Endless wire saws referred in literature.

Author	Material cut	$\phi [\mu m]$	Manufacturing method
Hardin (2003)	Wood	300	Commercial butt-welded wire
Meng et al. (2004)	Granite,	500	Commercial butt-welded wire
Meng et al. (2006)	Al_2O_3		
Meng, Ge and Li (2007)	mono-Si		
Ge et al. (2004)	Granite	800	TIG welding
Gao et al. (2008)			
Subbiah et al. (2013)	Mono-Si	140	Commercial looped wire
Sbravati (2014)	no cutting experiment	310	CO_2 laser beam welding
Tanner (2015)	no cutting experiment	310	Angular resistance welding
Göttsching (2017)			
Campos (2016)	no cutting experiment	350	Upset welding
Knoblauch et al. (2017a)	Mono-Si	200	Upset welding
Knoblauch et al. (2017b)		350	
Knoblauch et al. (2018)			

In the first four reported cases (Table 1), the wires were firstly welded in looped-shape without any coating or abrasives, and then coated with diamond grains and cooper and/or nickel layer by electroplating. In the works of Ge et al. (2004) and Gao et al. (2008) were described details about the method of manufacturing and coating the looped wires. The other listed authors used commercial wires or did not specify the manufacturing methods.

It is important to note the diameter of the wire saws used in the reported researches; the only researchers who used endless wire saws with a diameter of less than $500 \mu m$ for machining hard-brittle materials was Subbiah, Saptaji and Zarepour (2013), however, cutting speeds of only $2 m/s$ were achieved. The other works achieved higher cutting speeds (about $20 m/s$), however, using $500 \mu m$ and $800 \mu m$ diameter wires.

In second section of Table 1 are listed the works found in the literature that investigated the development of endless wire saws from diamond wire coming from the wafering industry, these works were developed in the same research group and each contributed to the development of this technology .

Sbravati (2014) developed in his work an equipment capable of positioning the ends of a diamond wire segment forming a butt joint, and through a laser beam welded them. However the welded joints presented large bead size (weld burr) and low strength, breaking when being manipulated.

Tanner (2015) and Götttsching (2017) developed their works using a resistance welding device based on the concept of butt welding with an angular design. However, in their experiments the researchers failed to achieve an adequate alignment of the weld joint due to the design of equipment, forming looped wires of low strength. In the work of Campos (2016), Knoblauch et al. (2017b) and Knoblauch et al. (2017a), a upset welding device was developed. It exhibited capability of welding $350 \mu\text{m}$ and $200 \mu\text{m}$ diameter diamond wires that could be used in a wire saw test rig also developed by them.

An up-to-date work found in the literature that makes use of looped wire concept was done by Knoblauch et al. (2018). The resources developed in the works cited above were used to perform experimental investigations on sawing of silicon, making possible the evaluation and understanding of the wear of single diamond grits, through the concept presented in Figure 7.

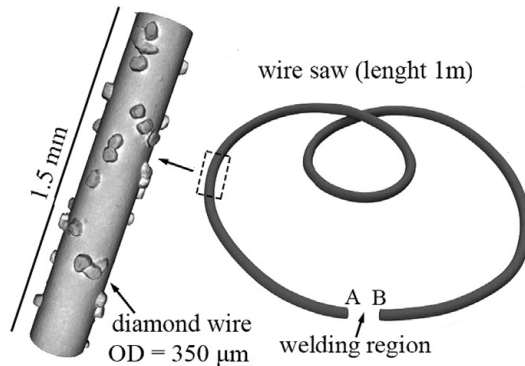


Figure 7: Schematic representation of the twisted looped wire to evaluate the wear of the diamond grits. Adapted from Knoblauch et al. (2018).

In this way, it can be observed that the works that have been most successful in the development of endless wires have used resistance butt-welding technique to join the ends of a segment of diamond wire originated from the wafering industry.

2.4 WELDING

According to DIN-1910-100:2008 (2008), welding is defined as “the permanent joining of components by the application of heat and / or pressure, with or without filler”. The energy required for the process is provided by an external medium. The welding process can occur in three ways: by heating up the material, heating up and applying force or simply applying force.

2.4.1 Resistance welding

Resistance welding is a thermoelectric process in which heat is generated at the interface of the parts to be joined by passing an electric current through the parts for a precisely controlled time and under controlled pressure. The name “resistance welding” assigned to this process is due to the fact that the electrical resistance of the workpiece to be welded is used for the phenomenon of heat generation (LIENERT et al., 2011).

2.4.1.1 Resistance butt welding

One of the simplest and most widely used forms of resistance welding is the upset welding (also called butt-welding), which is usually performed for joining thin workpieces such as rods, tubes or wires. Upset welding is a process which produces coalescence simultaneously over the entire area of two abutting surfaces or progressively along a joint (KEARNS, 1980). As stated by Phillips (1969), an electrical current is passed through the contact area of surfaces until the temperature generated is high enough to allow the forging of a weld between the two workpieces. The heat is generated mainly at the interface between the two workpieces by the flow of current and the contact resistance, in accordance with Joule’s law:

$$Q = I^2 \cdot R \cdot t \quad (2.1)$$

where Q is the amount of heat, I is the electric current flowing through a conductor, R is the amount of electric resistance (Equation ??) present in the conductor, and t is the amount of time that this happens for.

The contact resistance is a function of the nature of the metals to be welded, the contact pressure and the surfaces condition, such as smoothness and cleanliness. This resistance is approximately in inverse proportion to the contact pressure, provided that other factors remain constant. As the temper-

ature of the joint increases, the contact resistance changes, but it finally becomes zero when the weld is formed (PHILLIPS, 1969), (KEARNS, 1980).

The parts interface are softened by the intense heat in this zone because early in the process the joint presents a high electrical resistance, and thus through the application of a load (upsetting force) they are deformed, giving rise to a forged solid state welding (LIENERT et al., 2011).

The usual arrangement for upset welding is shown in Figure 8. One clamping die is stationary and the other is movable to perform the upset. The upsetting force is applied through the movable clamping die or a mechanical backup, or both. The process is done by pressing the workpieces frontally against each other (KEARNS, 1980).

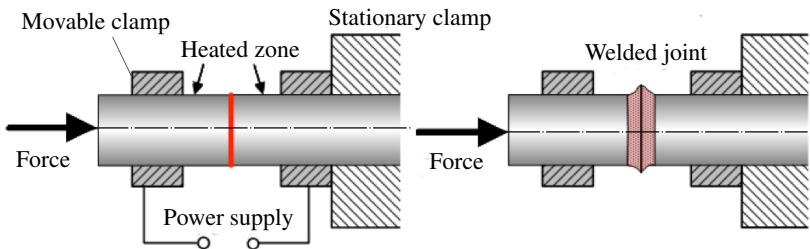


Figure 8: General arrangement of upset welding. Adapted from Campos (2016).

According to Kearns (1980), for uniform heating, the surfaces of the workpiece ends should be flat, comparatively smooth, and perpendicular to the direction of the upsetting force. Before the welding, they should be cleaned to remove any dirt, oil, oxidation, or other materials that will impede welding across the interface.

According to Lienert et al. (2011), the effect of welding conditions, other than the basic parameters of force, current, and time, is generally minimal. The roughness of the surface has a low effect on welding, however the initial contact of the surfaces has an influence on the initial resistance of the joint due to the existing punctual contacts initiating a point heating that will increase the resistance of the joint and thus promote the uniform heating of the cross section. The influence of the surface cleaning and the welding atmosphere will depend on the amount of oxide that may be present in the weld.

Kearns (1980) states that, it is important that the workpiece surfaces are properly aligned in the welding machine so that heat generated on surfaces is uniform. If the parts are misaligned, heating will occur only in the sections

where the contact is obtained and, as the upsetting force is being applied, the parts will tend to slip past each other on the cold metal, as illustrated in Figure 9. This factor should be given careful consideration in the design of the machine, especially when the ratio of the length to the width of the sections is high.

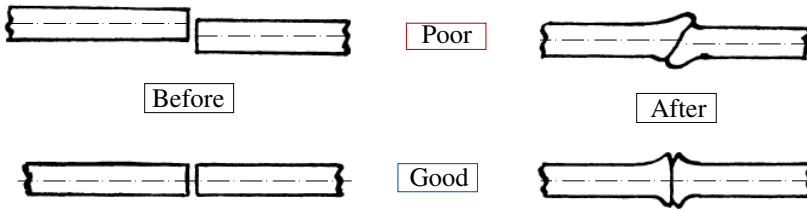


Figure 9: Effect of part alignment on joint geometry. Adapted from Kearns (1980).

According to Kanne (1994) and Lienert et al. (2011), upset welds have a high-quality solid-state metallurgical bond with no melting. The metallurgical structure of the weld zone is that of a hot-worked material with a good diffusion bond and grain growth across the weld interface. This microstructure can result in a higher strength in the weld zone than can be obtained by fusion welds, where properties change significantly due to melting.

As cited by Phillips (1969), when welding carbon steels having more than about 0,30% carbon or hard-drawn steels, post heat treatment of the welded zone may be necessary to normalize the welded section. Postheat treatments are used to provide ductility for subsequent handling of welded wire to permit the weld zone to withstand severe twists and bending faced e.g., in the winding around positioning pulleys.

In Figure 10, one can observe several pieces welded by upset welding. It is important to see and evaluate the appearance of butt-welds because, as it will be reported, the visual evaluation of the weld appearance is an efficient way to evaluate the weld quality.

2.5 WELD QUALITY

Generally, the joints welded by the upset welding technique do not differ much from the base metal in terms of mechanical properties. Since there is no melting during upset welding, the strength of the welds is not decreased to that of the solidificated structures found in fusion welds. The hot working that the weld zone receives during upset welding leads to a microstructure that is often stronger than the base metal, depending upon previous working of the

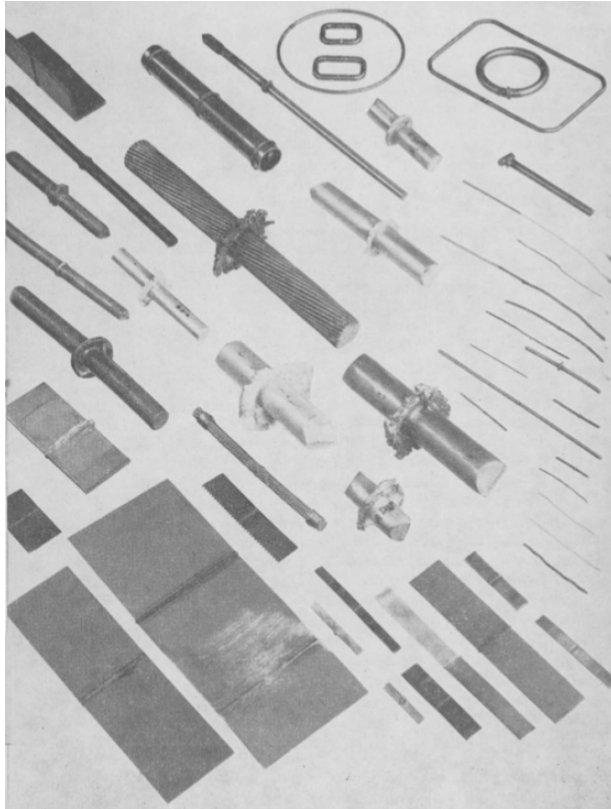


Figure 10: Typical products joined by upset welding (PHILLIPS, 1969).

base metal. In some cases, welds made in wires with proper procedures are difficult to locate after they have passed through a subsequent finishing procedure. In many instances, the welds are then considered part of the continuous wire (KEARNS, 1980),(KANNE, 1994).

2.5.1 Weld evaluation methods

In commercial practice, both destructive and nondestructive tests are employed to ensure maintenance of the quality level in flash and upset welded parts. To evaluate upset welds, several tests can be used; metallographic examination, tension test and bend test are destructive tests intended to evaluate

weld integrity and strength as well. The most common nondestructive tests used to evaluate weld integrity and look for discontinuities are visual, ultrasonic and dye penetrant examination (LIENERT et al., 2011).

When the welded part is used in a critical application, the above procedures are backed by other tests such as magnetic particle, fluorescent penetrant, and radiographic examination (RWMA, 2003).

However, the RWMA (2003) notes that, in this welding process a consistent quality level is maintained after satisfactory welding conditions are established, then the destructive and nondestructive tests commonly used for process control are as follows:

- Visual examination: Visual inspection and examination is the most widely used method of inspecting and qualifying upset welds. As cited by Kearns (1980), each completed weld in the production run should be visually examined for evidences of surface cracks, die burns, misalignment, or other mechanical discontinuities.

Visual examination can also detect the acceptability of weld shape and appearance. However, the visual examination often may not show some defects such as those caused by insufficient heating or related to the metallurgical characteristics of the base metal, because they usually leave no visible effects on the workpiece (LIENERT et al., 2011).

- Metallographic examination: the analysis of metallography of weld and heat-affected zone (HAZ) is performed to examine the microstructural constituents and identify the presence of any metallurgical discontinuities, such as voids, cracks, inclusions and flat spots (KEARNS, 1980).
- Tension test: One way to evaluate the upset welded joints using tension tests is comparing the tensile strength properties to those of the base metal. Mechanical discontinuities are also noted (KEARNS, 1980).
- Bend test: It is the most common method for testing a butt weld. Bend tests are used to force the fracture to occur along the interface for visual examination. If the fracture is through the weld interface and shows complete fusion or occurs outside the weld, the weld quality is considered satisfactory (RWMA, 2003).

3 DEVELOPMENT OF WELDING DEVICE

In this chapter, the methodology used for the design of the diamond wire welding device proposed to be engineered in this work will be presented. Also will be shown the manufacturing and assembly of the welding device.

According to Rozenfeld et al. (2006) the product development consists of a set of activities that seek, from the needs of the market and technological possibilities and constraints, to reach the design specifications of a product and its production process, so that it can be manufactured.

A new product needs a well-structured design that methodically describes all phases of planning and execution, as well as mapping the needs and desires of customers (ROZENFELD et al., 2006). Regarding this, Back et al. (2008) state that it is indispensable to use a systematic methodology in terms of planning, managing, monitoring and controlling the stages of product design.

Therefore, a design methodology is intended to provide the designer with a logical reasoning in the processing of a project, capable of identifying the design problem, leading the actions to find a suitable solution to this problem (PEREIRA, 2004).

Thus, for the development of the diamond wire welding device, a product development methodology known as the PRODIP (*Processo de desenvolvimento integrado de produtos*) model was employed. The PRODIP model proposed by Back et al. (2008) is focused in the development of industrial products and was initially elaborated based on the experience of the NeDIP (*Núcleo de Desenvolvimento Integrado de Produtos*) in the design, manufacturing and testing of prototypes of agricultural machinery. Figure 11 illustrates the PRODIP reference model. It can be observed that this model is divided into three major phases: planning, design process and implementation.

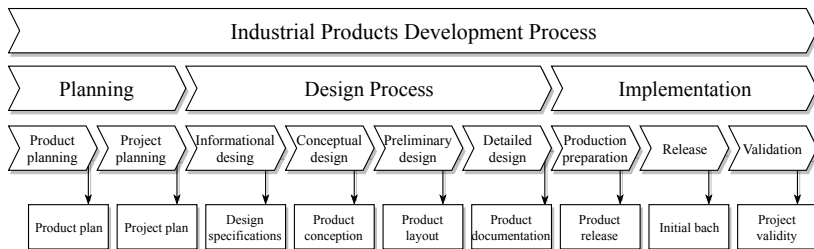


Figure 11: The PRODIP Model: A product design methodology developed at UFSC and proposed by Back et al. (2008).

The Planning phase is responsible for the definition of scope both for product and project. The Design Process phase comprises all activities related to product design, this phase starts with just one idea of a prototype and must end with a product ready to start production. In the Implementation phase the product is ready to be produced and topics of manufacturing, quality control, production and assembly lines are covered. Finally the product is released on the market followed by steps of project validation (BACK et al., 2008).

It can be observed that the PRODIP model comprises a very complete methodology of industrial product development. However, since the objective of this work is the development of an equipment to be used in the laboratory, to provide advances in academic research, the Planning and Implementation phases were not addressed in the methodology developed in this work.

In this way, only the Design Process phase was considered, and it can be observed in more detail in Figure 12. This stage of product development is divided into four major phases. Each phase has outputs that are essential for the progress and development of the project. However, the Detailed Design phase has not been used, because the welding device corresponds to a laboratory prototype and not a commercial industrial product.

The next sub-chapters present each stage applied in the development of the welding device.

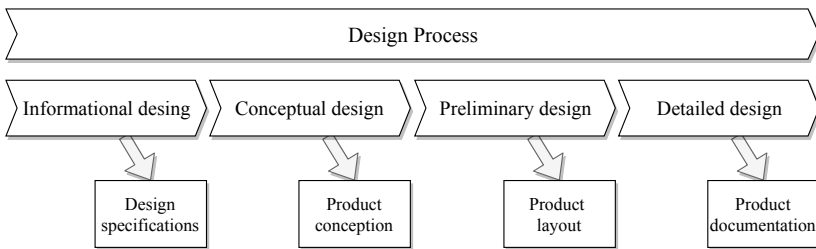


Figure 12: The phases of the Design Process from PRODIP Model. Adapted from Back et al. (2008).

3.1 INFORMATIONAL DESIGN

The informational design phase, according to Back et al. (2008), is the first phase of the design process. In this phase the goal is the establishment of the design specifications, which will guide the technical development of the product.

3.1.1 Project issues

This section summarizes the main technical problems that lead the careful development of the technology of diamond wire welding, in order to provide advances in the research of machining of hard and brittle materials.

To join the ends of a diamond wire segment to thereby form an endless wire, a welding process known as upset welding was chosen. This is a well known process in the industry, commonly used for joining chain links, pipes and steel rods, as previously mentioned. However, the dynamics of this process is limited when working with pieces of very small size. In the case of diamond wire, it is intended to weld steel wires of approximately $350\ \mu\text{m}$ in diameter or smaller. In this way, commercial upset welding machines are not applicable for welding such small parts. In this context, the main problems of the project arise.

It is understood, from literature on welding and from works developed in this area, that for the upset weld to be properly consolidated, it is necessary that:

- The two ends of a diamond wire are positioned and fixed, so that their cross-sections are concentric and coaxial with each other.

However, due to the micrometric diameter of the wire cross-sections, it is necessary that the positioning and alignment of the wire ends, which are fixed in separate sets, be compatible with the wire diameter. That is, if a maximum eccentricity misalignment of 15% of the wire diameter ($350\ \mu\text{m}$) is accepted, it is necessary for the welding device to be able to align the two ends with a maximum eccentricity deviation of only $52,5\ \mu\text{m}$. Therefore, it is necessary that the design takes these dimensions into account and the mechanical construction are accurate.

- A constant linear force must push one wire end against the other, generating a contact pressure between the cross-sections.

This force corresponds to the forging force, also called upsetting force, which is responsible for the deformation and joining of the material when it reaches a softening state caused by the Joule heating. Thus, before and during the passage of the electric current, a constant force is required to be applied to the weld joint in the direction of the longitudinal axis of the wire.

However, due to the small diameter of the diamond wire, it is necessary to apply a constant force with small magnitude, around $1\ \text{N}$ to $5\ \text{N}$. Thus, in order to perform an upsetting force within this range, it is necessary that the mechanical components, which promote the wire

ends movement and exert pressure on the weld joint, are capable of being moved by forces significantly smaller than those necessary for consolidation of the weld joint. If the force required by the components to be moved is greater than the force required to consolidate the welding, too much force will be applied and the weld joint will deform.

- The welded wire must be removed in a looped shape from the welding device.

The device configuration must allow the welded wire to be removed in looped shape after the welding procedure. In this way, there are design limitations that restrict the use of some methods to provide the weld joint alignment.

These are the main problems inherent to the dynamics of the upset welding procedure when working with very small parts. The whole design of the device must be carried out taking into account these issues, in order to overcome them and successfully perform the diamond wire welding.

3.1.2 Research for technical informations

According to Fonseca (2000) the research on technical information must be carried out in three segments:

- Research for information about similar products:

The development of this work is based on the specific demand of the Precision Engineering Laboratory (LMP) to have a diamond wire welding device more efficient and accurate than the current device that the laboratory has. In this way, the only similar product that is known is the one developed by Knoblauch et al. (2017b), and it is currently in the facilities of LMP. It serves as basis for the development of the new device.

Therefore, the technical information and expertise of the designers of the previous device have great value for the development of a new prototype. This information was shared among the lab members, and there are also reports of manufacturing and operation of the previous devices.

- Research for available manufacturing technologies and methods:

The device developed in this work can be characterized as an adaptive product, according to the classification of Jansson model proposed by Condoor et al. (1992) and Fonseca (2000). Thus, the device has a

high degree of technological innovation, but also presents a low configuration complexity. According to Pereira (2004), this type of project involves modifications to satisfy new requirements or improve the performance of an existing project.

In this way, it is intended to use manufacturing technologies that are known by the design team and are available in the laboratory facilities, since more than one project in this research line has already been developed, thus there is a manufacturing know-how learned.

- Research for patents of the product to be designed:

The research was done by patent documents in national and international collections, and was also carried out on search engines. However, no patent registration was found that included a diamond wire welding device or even some resistance welding machine for small diameter wires.

In this way, there was no patent information related to the subject to contribute to the development of the welding device. However, it was observed the opportunity to develop a robust equipment of high efficiency and with innovative concepts that could be patented as a utility model.

3.1.3 Product life cycle and customers

The life cycle is defined by the steps that a product undergoes, from planning to disposal or recycling. Each step of the product life cycle involves different users, and through its identification one can list the needs of each user in order to establish a list of design requirements (BACK et al., 2008).

In order to obtain customers by phase of the product life cycle, which define their needs that will be transformed into user requirements, one must go through the knowledge spiral presented in Figure 13, thus identifying the internal, intermediate and external customers of each phase.

The life cycle for the diamond wire welding device is defined as consisting of the following phases: design, manufacturing, assembly, usage, feature and maintenance. Due to the purpose of this work being the development of a welding device to be used in the laboratory, initially for research purposes, the steps of packaging, storage, transport, trade, recycling and disposal were disregarded.

Customers are not only the direct users of the product, but all the staff involved in the life cycle phases (FARINA, 2010). Thus, it is defined as the customers of the stages of the production sector: the technical employees, en-

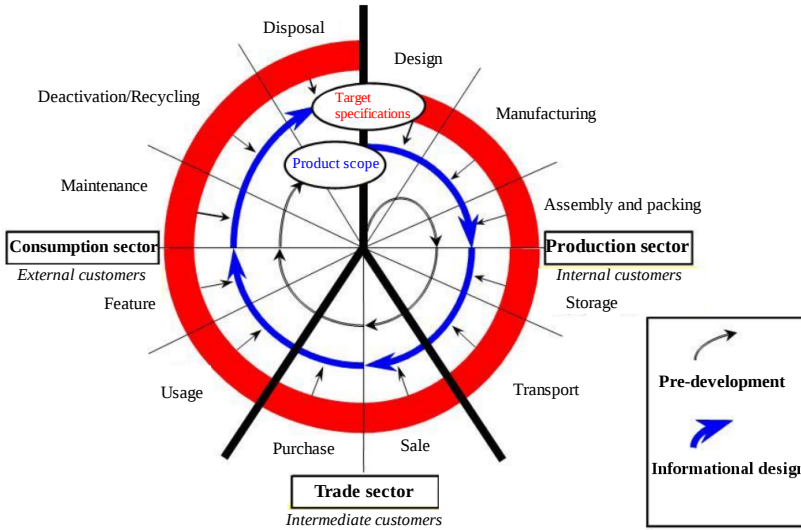


Figure 13: Product life cycle. Adapted from Rozenfeld et al. (2006).

gineers, teachers and researchers of the laboratory. The customers of the consumption sector are identified as being the teachers, engineers, researchers, and lab members who use the device to perform procedures and experiments.

According to Mazute (2014), after the identification of the customers by life cycle phases, there is a need to choose some basic attributes of the product, which are inherent characteristics of the product. The definition of basic attributes supports the next step of this design phase, the obtaining of the customers needs.

Based on similar projects to the one developed in the present work, the basic attributes chosen were: performance, resistance, aesthetics, ergonomics and saving.

3.1.4 Customers needs

In order to identify the needs of the product customers, it is necessary to understand the informations, shown in Table 2, where Fonseca (2000) identifies need, requeriment and specification.

The identification of customers needs was carried out through consultations and interviews with the product users. As product users throughout the life cycle are members of the laboratory and members of the same research

Table 2: Categories of information in the informational design phase (FONSECA, 2000).

Category of information	Meaning
Need	Direct statement of user or customer
User requirement	Need, taken to design language
Design requirement	Measurable requirement, accepted for project
Design specification	Design requirement, conveniently specified

line, the capture of needs occurred directly with these customers.

The information was collected in an engineering language and the repetitions were eliminated. The list of customers needs, sorted by the life cycle phases, is shown in the Table 3.

Table 3: List of customer needs.

Life cycle	Customers needs
Design	01 Welding wires of different diameters
	02 Facilitate the device setup
	03 Ensure alignment to the wire ends
	04 Fix the wire ends to be welded
	05 Resist abrasion in the fixing region
	06 Provide an electric current through the wire
	07 Ensure the correct wire positioning by constructive factors
	08 Make it possible to set the distance between the electrical contacts and the wire ends
	09 Provide continuous force during welding
	10 Enable configuration of the provided force
	11 Enable the clear visualization of the weld joint
	12 Facilitate the viewing of the process and the final result
	13 Easily remove the welded wire after welding
	14 Low failure rate
	15 Resistant
	16 Be fine
	17 Do not have sharp edges
	18 Be made of materials available in the lab
	19 Low cost
	20 Precise manufacturing
	21 Ease to manufacture

Table 3 continued from previous page

Manufacturing	22	Low production cost
	23	Short production time
	24	Use laboratory facilities
Assembly	25	Simple assembly
	26	Easy setup
	27	Simple operation
Usage	28	Easy access settings
	29	Process visualization (by camera)
	30	Enable visual inspection of consumable items
Feature	31	Ensure reproducibility of welding
	32	Robust
	33	Maintain uniformity in weld consolidation
Maintenance	34	Easy maintenance
	35	Easy access materials

Thirty-five needs were identified and listed according to the stage of the life cycle they represent.

3.1.5 Customer requirements

After being grouped, customers needs were transformed into customers requirements, that is, they were turned into short and direct phrases, as suggested by Back et al. (2008). The requirements are indicated with a degree of importance between 1 and 5, established by the main users and developers. The list of customers requirements is shown in Table 4.

Table 4: List of customers requirements.

Life cycle	Customers requirements		
	01	Be able to weld wires of different diameters	4
	02	Be easy to set up	4
	03	Have a mechanism for machining grooves for wire ends	5
	04	Have a groove shaped for wire ends fixing	5
	05	Have an abrasion resistant groove	4
	06	Be able to pass electric current through the wire	5

Table 4 continued from previous page

Design	07	Be able to ensure the correct wire ends positioning by constructive factors	5	
	08	Have a die opening setting	3	
	09	Be able to provide continuous force during welding	4	
	10	Have a way to configure the provided force	5	
	11	Be able to enable the viewing of the weld joint	3	
	12	Have an easy viewing of the welding result	3	
	13	Have an easy way to remove the welded wire	5	
	14	Have good performance	4	
	15	Be resistant	3	
	16	Be fine	2	
	17	Have rounded edges	2	
	18	Be made of materials available in the laboratory	3	
	19	Be economically viable	3	
	20	Be accurate	4	
	Manufacturing	21	Be easy to manufacture	3
		22	Have low manufacturing cost	2
		23	Have short production time	2
		24	Be manufactured in the laboratory	4
Assembly		25	Be easy to assemble	3
		26	Be simple to set up	3
Usage	27	Be simple to operate	5	
	28	Have accessible settings	4	
	29	Be able to position a camera	3	
	30	Have easy visibility of consumable items	3	
Feature	31	Be able to reproduce quality welds	5	
	32	Be robust	5	
	33	Be able to maintain uniformity in weld consolidation	3	
Maintenance	34	Be easy to maintain	3	
	35	Be made of accessible materials	3	

3.1.6 Design requirements

The next step of the informational design phase is to convert customers requirements into design requirements. Design requirements are measurable expressions that indicate how to meet the requirements of project customers (PEREIRA, 2004)

According to Mazute (2014), this conversion constitutes the first physical definition of the product, because it is measurable, this is associated with the definitive characteristics that the product should present. As described by Fonseca (2000) and Mazute (2014), this step is a very important moment for the design process.

The requirements follow goals, which means that the measurable requirement must be maximized or minimized according to its purpose and unit of measurement. Table 5 lists the design requirements, which were obtained by converting the customers requirements. It is important to realize that customers requirements that are not measurable have not been converted and addressed in this step, so only twenty-three requirements have been synthesized.

Table 5: List of design requirements.

Design requirements		
1	Eccentricity of the weld joint	Minimize ↓
2	Hardness of the wire contact region	Maximize ↑
3	Electrode resistivity	Minimize ↓
4	Electrode thermal conductivity	Minimize ↓
5	Electrode mechanical resistance	Maximize ↑
6	Electrode ductility	Maximize ↑
7	Electrical resistivity of the groove	Maximize ↑
8	Device setup time	Minimize ↓
9	Manufacturing cost of device	Minimize ↓
10	Die opening	Minimize ↓
11	Upsetting force	Minimize ↓
12	Static friction of the welding motion	Minimize ↓
13	Device stiffness	Maximize ↑
14	Opacity of materials near to weld joint	Minimize ↓
15	Precision of groove machining system	Maximize ↑
16	Positioning range of the machining syst.	Maximize ↑
17	Dimension of the machining system	Minimize ↓
18	Wire tensioning for machining	Maximize ↑
19	Groove machining path	Maximize ↑

Table 5 continued from previous page

20	Hardness of adjustment and moving parts	Maximize ↑
21	Elastic modulus of adjustment and moving parts	Maximize ↑
22	Hardness of static parts	Maximize ↑
23	Overall dimension of the welding device	Minimize ↓

3.1.7 Design specifications

The output of this methodology phase is the framework of design specifications, taking into account design goals and constraints. The design specifications do not define the solution for the project, as described by Farina (2010), its main function is the generation of subsidies for decision making in the selection of design alternatives.

The list of design specifications is in order of importance for each requirement, starting with the most important to the least significant specification for project development. The hierarchy of design specifications was performed with the help of QFD (Quality Function Deployment) tool, which is contextualized by Fonseca (2000), Back et al. (2008), Mazute (2014) and Pereira (2004) and is described and illustrated in Appendix A. The QFD tool is based on the relationships between customers and design requirements.

Table 6 lists the design specifications for the diamond wire welding device, sorted with their relative weights, with the desired target, its unit of measurement and the risks of not reaching the requirements, causing undesired outputs.

Table 6: List of design specifications.

Description of specifications	Unit	Goal	Risk
Device setup time (8,64)	<i>min</i>	< 5 <i>min</i>	Process to be time consuming, operator to tire physically, difficulty of operation
Manufacturing cost of device (7,61)	<i>R\$</i>	< <i>R\$</i> 100,00	Manufacturing of device is canceled due to short budget
Eccentricity of the weld joint (6,91)	<i>%</i>	< 15% wire diameter	Weld joint no concentric, unconsolidated weld, device does not work
Precision of groove machining system (5,92)	<i>mm</i>	< 0,01 <i>mm</i>	Absence of precision for machining system, misaligned welds

Table 6 continued from previous page

Static friction of the welding motion (4,96)	<i>N</i>	$< 1 N$	Stip-slick behaviour, too much upsetting force, unconsolidated welds
Upsetting force (4,83)	<i>N</i>	$1 < F < 7 N$	Insufficient or too much force, small setup range
Hardness of adjustment and moving parts (4,76)	<i>HV</i>	$> 150 HV$	Backlash and deformation
Die opening (4,73)	<i>mm</i>	$0 < d < 3 mm$	Small setup range
Elastic modulus of parts (4,63)	<i>Gpa</i>	$> 200 Gpa$	Backlash and deformation
Device stiffness (4,60)	-	Maximum possible	Deform during operation, loss of concentricity
Opacity of materials near to weld joint (4,24)	-	-	Absence of visibility
Electrical resistivity of the wire slot (4,13)	ρ	$> 1 \times 10^{14} Ohm.cm$ not conductive	Electrical current leakage
Overall dimension of device (3,74)	<i>mm</i>	$< 400 \times 300 mm$	Space obstruction
Electrode ductility (3,59)	<i>HV</i>	$< \text{wire harness}$	Absence of physical and electrical contact
Hardness of the wire contact region (3,38)	<i>Mohs</i>	$> 9 Mohs$ max. possible	Loss of concentricity, deformation of the groove
Hardness of static parts (3,38)	<i>HV</i>	around 75 HV	Absence of device stiffness, backlashes
Dimension of the machining system (3,20)	<i>mm</i>	$< 400 \times 150 mm$	Difficulty of assembly, usage and maintenance
Electrode resistivity (3,17)	ρ	around 2×10^{-8} excellent conductor	Sparking, unconsolidated welds
Wire tensioning for machining (2,94)	<i>N</i>	$0 < F < 50 N$	Low machining force, do not shape the groove properly
Positioning range of the machining system (2,94)	<i>mm</i>	$> \text{wire fixing part}$	Do not shape the groove properly
Electrode mechanical resistance (2,76)	<i>GPa</i>	Resist wire fixing	Break the groove during the wire fixing
Groove machining path (2,63)	<i>mm</i>	$> \text{wire fixing part}$	Shape irregular groove
Electrode thermal conductivity (2,29)	<i>KmC</i>	Poor conductor	Conduct excess heat

In the next steps, design specifications should be used as the basis for the product to meet the desired characteristics and avoid the risks that may occur. In this way, it is essential that the most important items in Table 6 be considered key points for the product development, such as the device setup time, the manufacturing cost of device, the eccentricity of the weld joint, and other significant items according to Table 6.

3.2 CONCEPTUAL DESIGN

The first task performed in this step is the definition of the overall function of device. Subsequently a functional structure is defined to fulfill the overall function.

By selecting a suitable functional structure, the device design begins to be developed. By combining possible solution principles, some solutions for the product are generated. The method of combining solution principles is called the morphological matrix, which is disseminated by authors such as Pahl et al. (2007) and Back et al. (2008).

At the end of this phase, conceptual solutions for the proposed problem are presented, the solutions with the greatest potentiality to be developed in the preliminary design phase are evaluated.

3.2.1 Overall function

According to Pereira (2004), the establishment of the overall function must be made from the design specifications, establishing a relationship between the system function, other technical systems and the environment; presenting the inputs and outputs of energy, materials and signals that pass through the system.

In this way, the overall function of the device was established from the design specifications, by the knowledge of the research group in the development of the previous devices and due to the study of the work developed by Knoblauch et al. (2017b). The overall function is represented in a flow diagram of lines, which represent the inputs and outputs of energy, material and process signals.

In Figure 14 the diagram representing the overall function of the welding device can be seen. In the center of the diagram is the main function of device, that is, the welding of diamond wire.

3.2.2 Functional structure

As suggested by Mazute (2014) and Pereira (2004), the overall function of the product must be deployed in subfunctions. In this way, the main function of the device was deployed in six subfunctions. Figure 15 shows the functional structure of the diamond wire welding device.

Each subfunction shown in Figure 15 also has internal partial functions necessary to achieve the purpose of the subfunctions. In this way, a

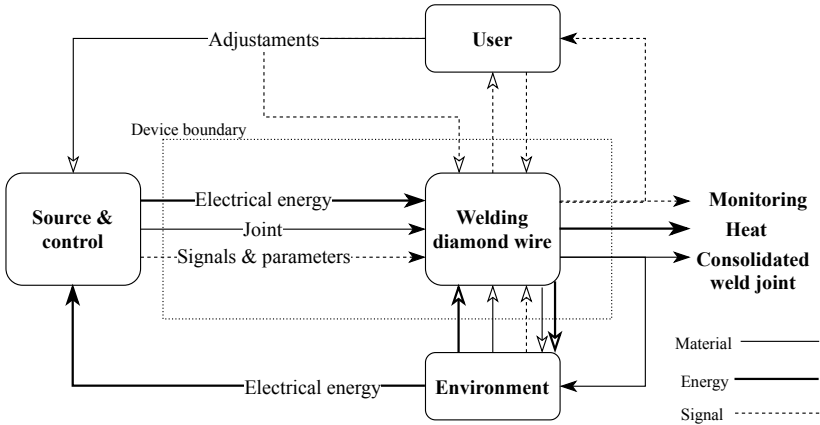


Figure 14: Overall function of diamond wire welding device.

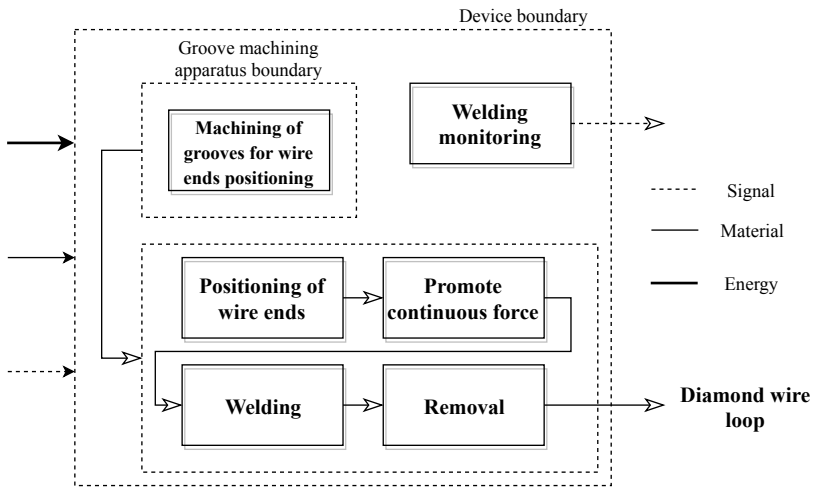


Figure 15: Deployment of subfunctions of the diamond wire welding device.

complete functional structure for the device is established, contemplating the main purpose of the device and the design requirements.

In Figure 16 a diagram showing the complete functional structure of the welding device can be seen. As before, the partial functions were established through the knowledge of the designers respecting the design requirements and specifications.

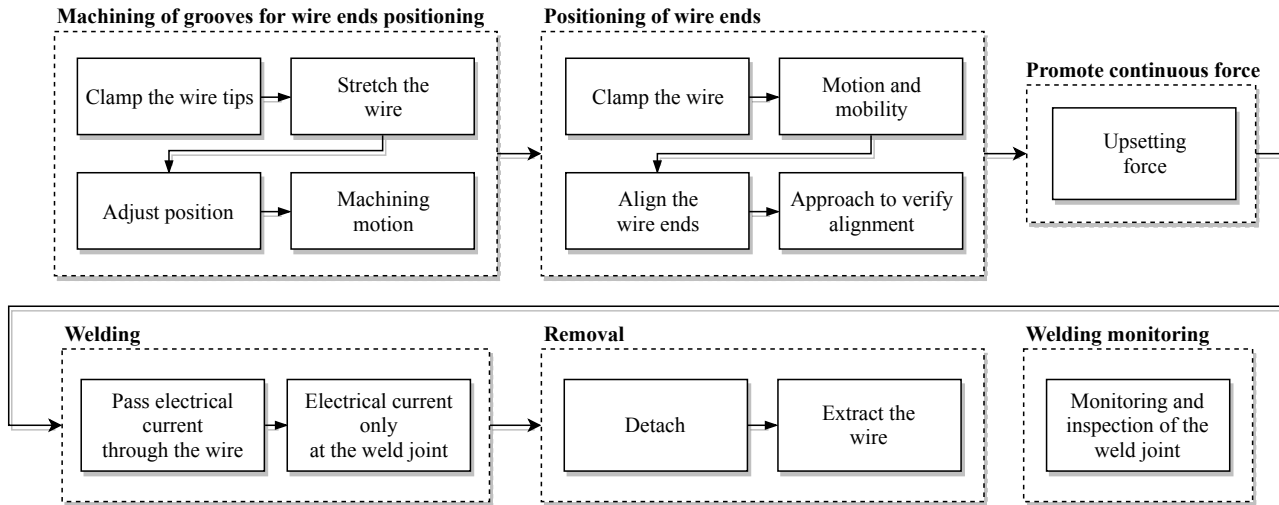


Figure 16: Complete deployment of subfunctions of the diamond wire welding device.

3.2.3 Morphological matrix

Mazute (2014) describes that for the subfunctions of the established functional structure, one must find solution principles that will later be combined and materialized, leading to a basic solution to the problems.

Back et al. (2008) cites that the project team must obtain several alternative solutions to the problem, in order to select the best and most innovative product design. For this, the systematic method of the morphological matrix is used.

The morphological matrix can be observed in Table 5, in the left column the subfunctions of the functional structure are described, the following columns represents the proposed solutions for each function, through which five different designs were formed.

To fill the morphological matrix with the principles of solutions, the project team was consulted and intuitively the solutions were proposed. The solutions for each subfunction were arranged, so that there were no replications of solutions for different device designs.

Table 7: List of functions of the functional structure of the welding device.

Functions	Design 1	Design 2	Design 3	Design 4	Design 5	
Machining of grooves for wire ends positioning						
Clamp the wire tips (both sides)	Screws + plates	Screws + plates	Magnetic	Quick-closing devices (chest)	Clamp	
	Screws + plates	V groove	U groove	Quick-closing devices (chest)	Clamp	
Stretch the wire	Spring	Spring	Spring	Actuator	Manually + fixation	
Adjust position	Screw	Micrometric spindle	Differential screw	Differential screw	Manually	
Machining motion	Manually	Manually	Stepper motor	Servo motor	Servo motor	
Positioning of wire ends						
Clamp the wires	Quick-closing devices (chest)	Screws + plates	Quick-closing devices (chest)	Belt + buckle	Pressure clamp	
Motion and mobility	Linear guide	Linear bearings	Linear guide	Spindle	Spindle	
Align the wire ends	Horizontal displacement	By construction ¹	By construction ¹	By construction ¹	Screw	Guideway
	Height	By construction ¹	By construction ¹	By construction ¹	By construction ¹	Guideway
	Angulation	By construction ¹	By construction ¹	By construction ¹	By construction ¹	Stud
Approach to verify alignment	Manually	Manually	Automated	Crank handle	Automated	
Promote continuous force						

¹Achieved by machining grooves.

Table 7 continued from previous page

Upsetting force	Spring	Spring	Electric actuator	Manually	Electric actuator
Welding					
Pass electrical current through the wire	Electrical connector	Electrical connector	Electrical connector	Electrical connector	Electrical connector
Electrical current only at the weld joint	Insulating groove	Insulating groove	Insulating welding device	Insulating ink	Insulating welding device
Welding monitoring					
Monitoring and inspection	Naked eye	USB microscope	Thermal camera	Camera	Naked eye
Removal					
Detach	Quick-closing devices (chest)	Screws + plates	Quick-closing devices (chest)	Belt + buckle	Pressure clamp
Extract the wire	Manually	Manually	Manually	Manually	Tweezers

3.2.4 Designs evaluation

To evaluate the designs formed in the morphological matrix, Rozenfeld et al. (2006) suggests that the Decision Matrix Method be applied. The main objective of this activity is to choose, among the designs formed previously, the best of these concepts, which will be transformed into the final prototype.

In this method, one of the conceptions generated is chosen as a reference, and all other conceptions are compared with the reference. For each function, it is indicated whether the design is “better than” (+), “equal to” (=) or “worse than” (-) the reference design.

The five generated designs were added to the decision matrix (Table 8), design #1 was chosen as a reference because it presented the most basic technology. Taking into account the relative weight (Rw) of each evaluation criterion, from the QFD method, each proposed solution for device functions has been evaluated according to customer requirements and design specifications. Thus, it is possible at the end of the Decision Matrix to observe which is the most appropriate design to be developed.

Table 8: Decision matrix.

Design requeriments	Rw	Design				
		1	2	3	4	5
Device setup time	8,64	=	+	+	+	+
Manufacturing cost of device	7,61	-	-	-	-	=
Eccentricity of the weld joint	6,91	=	+	-	-	-
Precision of groove machining system	5,92	+	+	+	+	-
Static friction of the welding motion	4,96	+	=	+	+	+
Upsetting force	4,83	=	+	-	-	+
Hardness of adjustment and moving parts	4,76	=	=	=	=	=
Die opening	4,73	=	=	=	=	=
Elastic modulus of adjustment and moving parts	4,63	=	=	=	=	=
Device rigidity	4,60	=	=	-	-	-
Opacity of materias near to weld joint	4,24	=	=	=	=	=
Electrical resistivity of the groove	4,13	=	-	=	=	-
Overall dimension of the welding device	3,74	=	=	=	=	-

Table 8 continued from previous page

Electrode ductility	3,59	=	=	=	=
Hardness of the wire contact region	3,38	=	=	-	=
Hardness of static parts	3,38	=	=	-	-
Dimension of the machining system	3,20	+	-	-	=
Electrode resistivity	3,17	=	=	=	=
Wire tensioning for machining	2,94	=	=	-	-
Positioning range of the machining system	2,94	+	-	-	+
Electrode mechanical resistance	2,76	=	=	=	=
Groove machining path	2,63	=	=	-	-
Electrode thermal conductivity	2,29	=	=	=	=
Amount +	+	17,0	26,3	19,5	21,3
Amount -	-	7,6	17,8	42,4	34,2
Result		9,4	8,4	-22,9	-12,8
Ranking		1°	2°	4°	3°

As can be seen in Table 8, the design #2 presented the highest numerical value, thus corresponding to the best combination of solutions for the development of the device according to the project priorities.

3.2.5 Design generated

According to Mazute (2014) after evaluating the best design solution for the product, it is necessary to present the design in more detail, so that decisions can be made with higher security. Thus, the design must be presented in sketches, capable of being evaluated.

In this way, several sketches were initially designed by hand to represent the solutions of the proposed design. Through discussions and evaluation of some materials available in the lab, the first design of the device was developed in Autodesk Inventor software. Figure 17 shows the sketch of the proposed design.

It is important to note that the sketch presented in Figure 17 does not represent the final version of the product, but it is a design that meets all the design requirements. This is the last step of the conceptual design phase, so this design will be improved in the next step of the methodology.

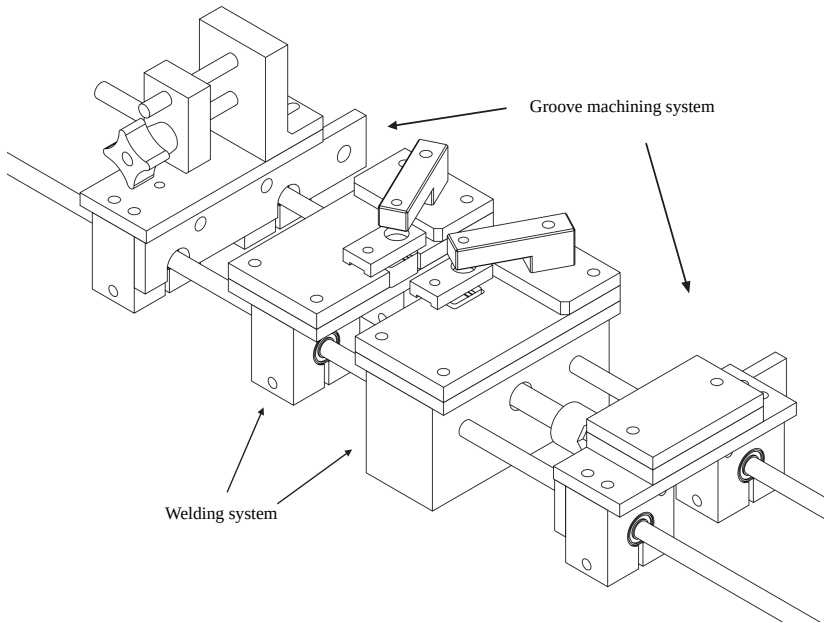


Figure 17: First concept generated of the diamond wire welding device.

3.3 PRELIMINARY DESIGN

In this phase, the conceptual solution is developed in terms of layout, arrangement, shapes, geometry, materials and manufacturing processes. According to the reference methodology, the development of the prototype may occur at this stage.

3.3.1 Device layout definition

To define the preliminary layout of the welding device, the first step was to identify and classify the parts in components, assemblies and systems. With these definitions it is easier to work on each part's characteristics and mainly understand the design.

3.3.1.1 Welding system

As mentioned earlier in section 3.2.5, several sketches of device layouts have been developed until the sketch of Figure 17 was defined. In this way, that layout clearly represents the idea of the operation and the main components of the welding device.

Another sketch of the initial design of device is shown in Figure 18. The welding device is basically divided into two systems, one being responsible for the machining of a groove for the positioning of the weld joint, and the other one is the responsible for welding.

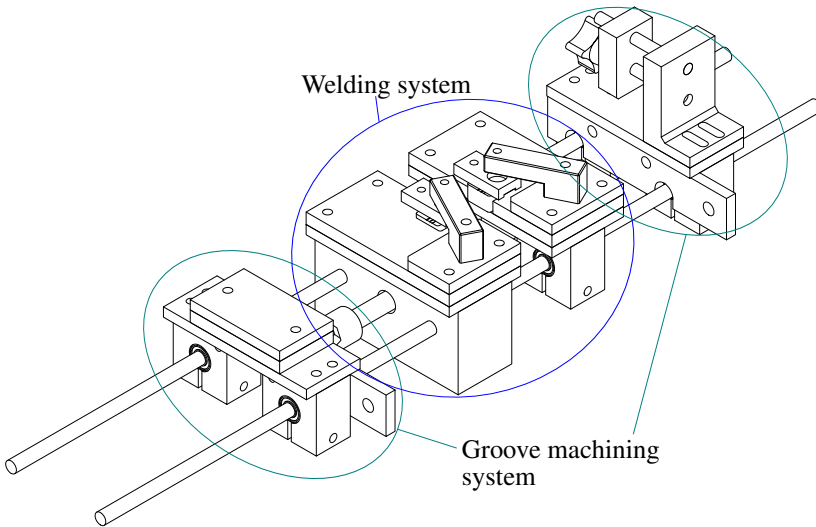


Figure 18: Groove machining and welding systems.

The welding system consists of two assemblies, similar to industrial upset welding machines, in which there is a fixed assembly and a movable assembly that together perform the movement and the upsetting force on the weld joint. In this way, two assemblies, one fixed and one movable, were designed for the diamond wire welding system. In Figure 19, the welding system can be observed in detail.

The fixed assembly consists of a set of parts, and the large central block (1) serves as the basis for the rest of the device. This block will be fixed on a machine tool table, made of cast iron, in order to keep the device fixed on a work table. On top of the central block there are two plates of similar

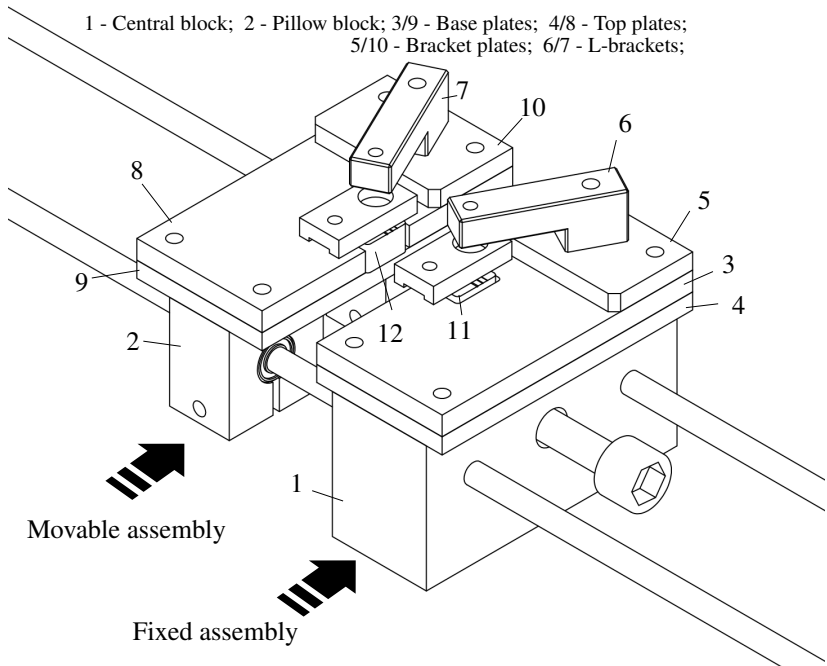


Figure 19: Welding system in detail.

size, the top plate (3, 8) has an inlet for positioning the grooved inserts (11, 12), on which a groove will be shaped to fit the diamond wire ends to form the weld joint. The bottom plate (4, 9) serves as the base for the insert.

The smaller plates with the bevelled corners (5, 10) forms the basis for the L-shaped bracket (6, 7), which is responsible for the positioning of the electrical contact (electrode) on the top of the diamond wire. The electrode is responsible for transmitting electric current from the welding source to the diamond wire ends. The L-brackets (6, 7) allow the adjustment of the height and distance from the electrodes to the welding joint. In Figure 20 it can be seen in more detail the region where the wire ends are fixed and the weld joint is formed.

The electrode (12) is a rectangular plate in which there are a threaded bore (minor hole) to be clamped an electrical terminal and a circular inlet to accommodate a bearing. In the bearing, one end of a bolt will be fixed, the bolt is threaded in the L-brackets (6, 7) and is used to adjust the height of the electrodes and the pressure on the wire ends. By moving the part (6) in the indicated axis of rotation, the distance from the electrode to the weld joint

can also be adjusted. A ceramic insert (11) was chosen as the support for the diamond wire. In these inserts will be shaped grooves with a diamond wire, to create a fit with the size and shape of the diamond wire itself to be welded.

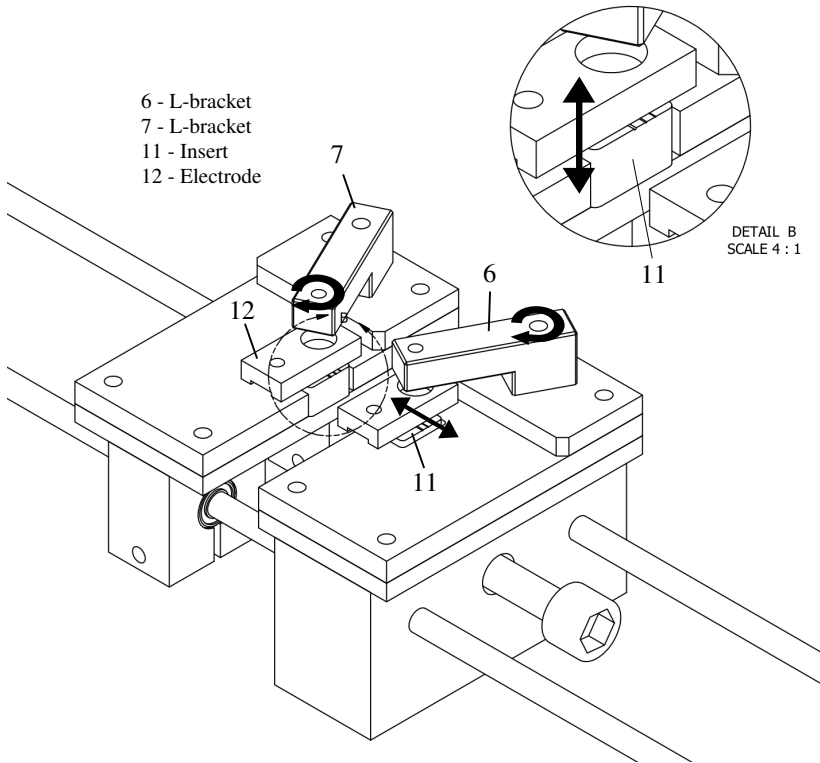


Figure 20: Detailing of fixing region of wire ends.

In Figure 21 it can be seen in more detail the region where the weld joint is formed by the union of the ends of a single diamond wire segment.

The ends of the diamond wire segment are positioned on ceramic inserts, inside the grooves. The electric contact presses the wire to stay in position, then the upsetting force is applied. The movement and force required for the welding procedure are performed by the movable assembly.

The movable assembly is very similar to the fixed one, the plates (8, 9), the smaller plate (10), the L-bracket (7), the electrical contact (12) and the insert (11) are components equal as the fixed assembly (Figure 19), only geometrically mirrored. However, instead of a single block (1), there is a set

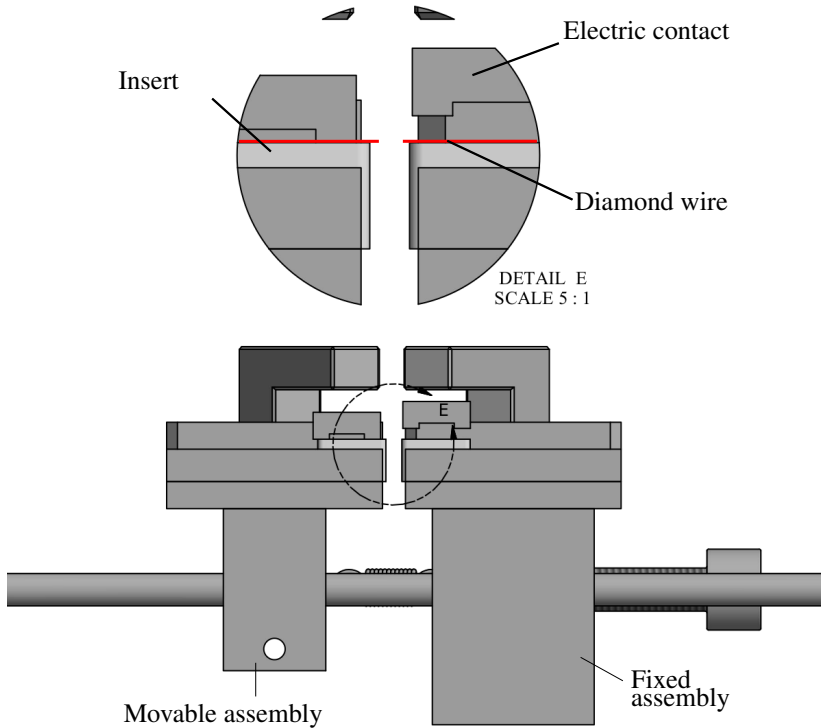


Figure 21: Welding zone in detail.

of components that enables the movement of this movable assembly over the cylindrical linear guideways. This set of components consists of two blocks (2) and two linear ball bearings (13), each bearing is attached to a block. This type of component is known as pillow block, and can be seen in Figure 22.

As shown in section 3.2.4, the spring is the ideal component to perform the movement of the movable assembly and consequently the upsetting force required to perform the welding. A tension spring has been chosen, so that it must pull the movable assembly towards the fixed assembly, in the direction of the longitudinal axis of the welding joint. A spring tension adjustment system must also be designed.

These are components of great importance for the device operation. Its positioning, design and dimensioning must be done carefully, because as seen earlier, one of the main problems faced in diamond wire welding is the execution of low, smooth and constant upsetting forces, avoiding the stip-slick

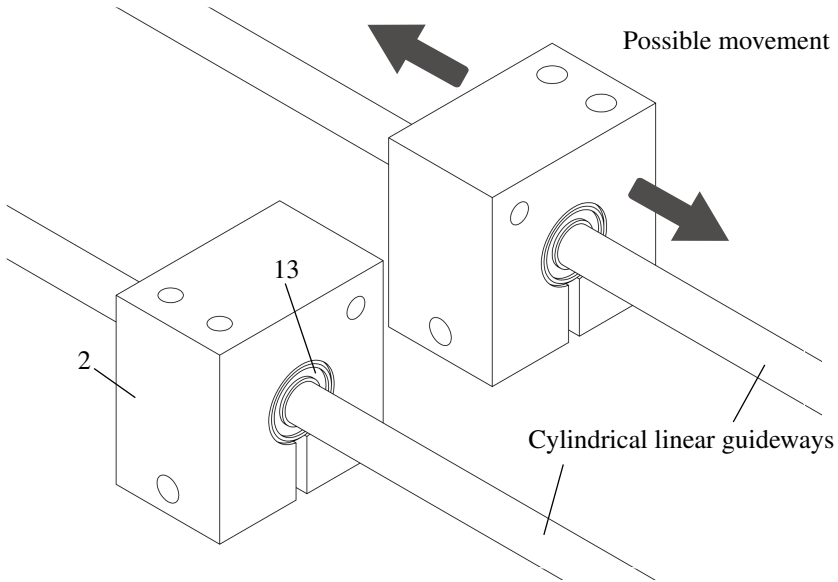


Figure 22: Pillow blocks.

behavior, which is detrimental to weld consolidation.

In this way, it was determined that the tension spring should be at the same height as the cylindrical guideways and the linear bearings, to perform a linear movement and decrease the moment on the linear bearings. The positioning of the spring and bolt designed to adjust the spring tension can be seen in Figure 23. The spring attachment was not designed in this sketch, because the spring has not yet been sized and chosen.

Therefore, the welding device was defined as having two distinct systems, the welding system and the groove machining system. The welding system consists of two assembly, one movable and one fixed, which together perform the welding procedure through the functionality of its components and assemblies.

3.3.1.2 Groove machining system

This system is designed to meet one of the key customer requirements: “have a groove machining mechanism”. As mentioned before, one of the main aspects in upset welding of small diameter workpieces is the formation of a concentric weld joint. Thus, it has been defined that the diamond wire

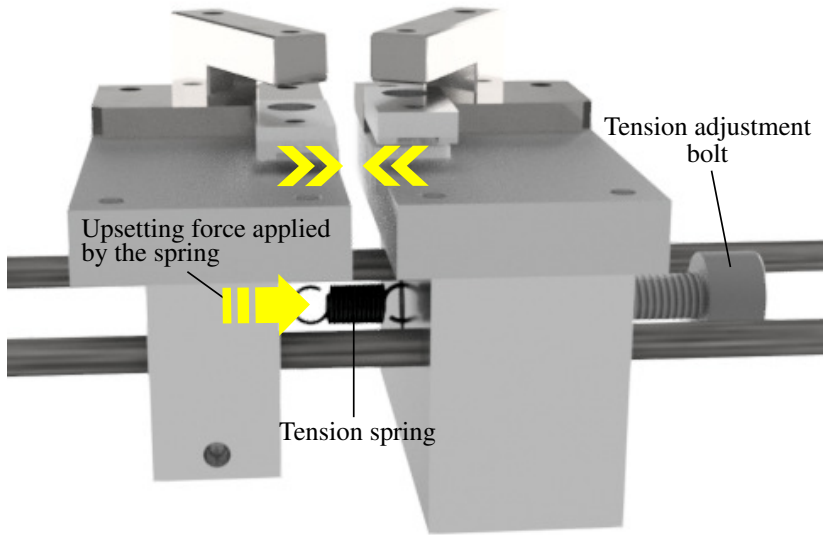


Figure 23: Spring positioning and tension adjustment.

welding device should have a mechanism capable of making itself a fitting for the wire ends in exactly the same shape and diameter of the diamond wire that would be welded. In addition, the axis of the fit must be in exactly the same direction as the weld is performed, i.e. the position of the longitudinal axis of the weld joint must be parallel to the axis of movement of the upsetting force.

Thus, it was defined that a groove machining mechanism, that uses a diamond wire as shaping tool would be an appropriate solution to manufacture a fit for the ends of the wire to be welded. To develop this proposed solution, it was known that in order to perform the welding movement and the upsetting force, a relative movement between two sets was necessary. Thus, a linear motion pattern should be possible in the device. For the execution of a linear movement in machine tools, Stoeterau (2004) states that linear guides are components with rectilinear pattern of movement and generally restricted in one degree of freedom.

In this way, it was chosen to work with cylindrical linear guideways, since they are the most common forms of linear guides, and with recirculating ball bearing, because they are components that present smoothness of movement and absence of the stick-slip behavior (STOETERAU, 2004).

Therefore, it was initially designed cylindrical linear guideways of great length for the device, in order to solve the problem of groove machin-

ing. By having long linear guides to conduct the welding movement, the same guides could be used to perform the groove machining motion. Thus, if the wire used for machining is aligned parallel with the guides, consequently the groove would be shaped parallel to the guideways' axes.

Thus, by construction, the wire ends would be positioned with its longitudinal axis parallel to the axis of movement of the upsetting force. In this way, the looped wire must have a aligned weld joint, solving one of the biggest problems of diamond wire welding. In Figure 24 it can be seen an illustration of this solution.

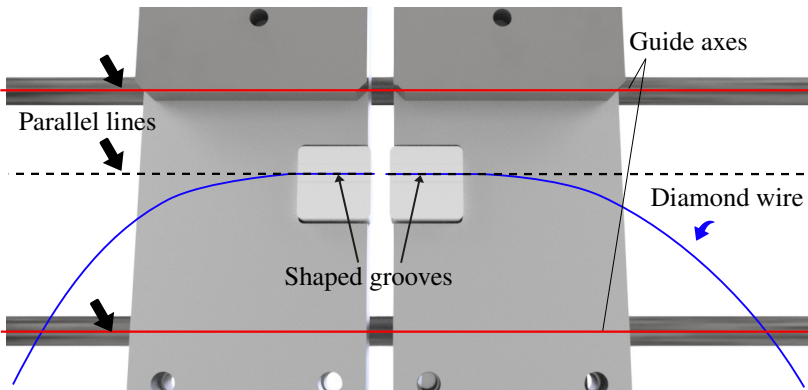


Figure 24: Grooves position relative to guide axes.

In Figure 24 the red lines represent the direction in which the movable assembly of the welding system is moved, the dashed black line represents the direction of the shaped grooves. If the longitudinal axes of the linear guideways are parallel to the longitudinal axes of the grooves, the welding joint should be concentric, but deviations and backlashes in the components may compromise the weld joint alignment.

Therefore, from the proposed solution, the assemblies that form the groove machining system were designed. A diamond wire segment is fixed between the assemblies, one being responsible for fine positioning adjustment of one wire end, and another responsible for coarse positioning adjustment of the other wire end, as can be seen in more detail in Figure 25.

In Figure 25 the diamond wire used to groove shaping is represented in blue color, this wire has its ends attached to the two assemblies. In the coarse adjustment assembly, the wire end is clamped between two plates in a random position, but it is estimated that the wire would be above the ceramic insert. The other wire end is attached to the fine adjustment assembly, and its position is adjusted by a mechanism composed of a spring and adjusting screw. Thus,

by using the adjusting screw with a thin pitch, accurate positioning of the wire can be achieved, so that it is aligned and parallel to the pillow blocks movement and thus the groove is shaped aligned.

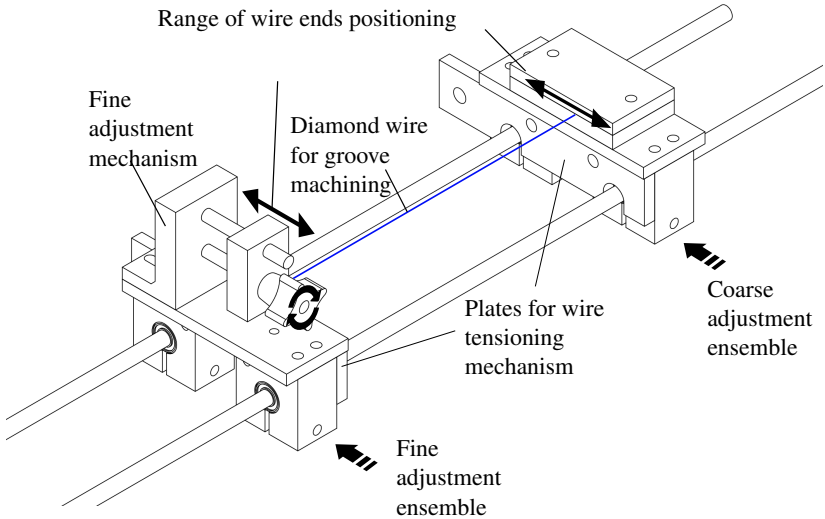


Figure 25: Groove machining system.

In Figure 25 it can be seen two plates fixed in front of each assembly. These plates were designed so that between them a tensioning mechanism, like a spring, could be placed to push the assemblies in opposite directions to tension the diamond wire and also to keep the two assemblies coupled.

In Figure 26 it can be seen an illustration of the groove machining system and a representation of how the groove shaping is performed. Slight inclinations in the diamond wire can be observed because it is attached approximately 1 mm below the height of the insert that will be machined, the red arrows represent the tensioning on the wire that will be applied by a mechanism responsible for holding the assemblies coupled.

Once the diamond wire is tensioned, by manually performing an alternating motion of the groove machining system, the diamond grains of the wire will remove small amounts of material from the ceramic insert. By performing this process repeatedly, a groove will be formed in the shape of the wire. The viewing of the diamond wire position and the monitoring of the groove shaping will be done through a USB microscope connected to a computer. By the use of the microscope, one can control the alignment of the wire with the guide axis by using the adjusting screw.

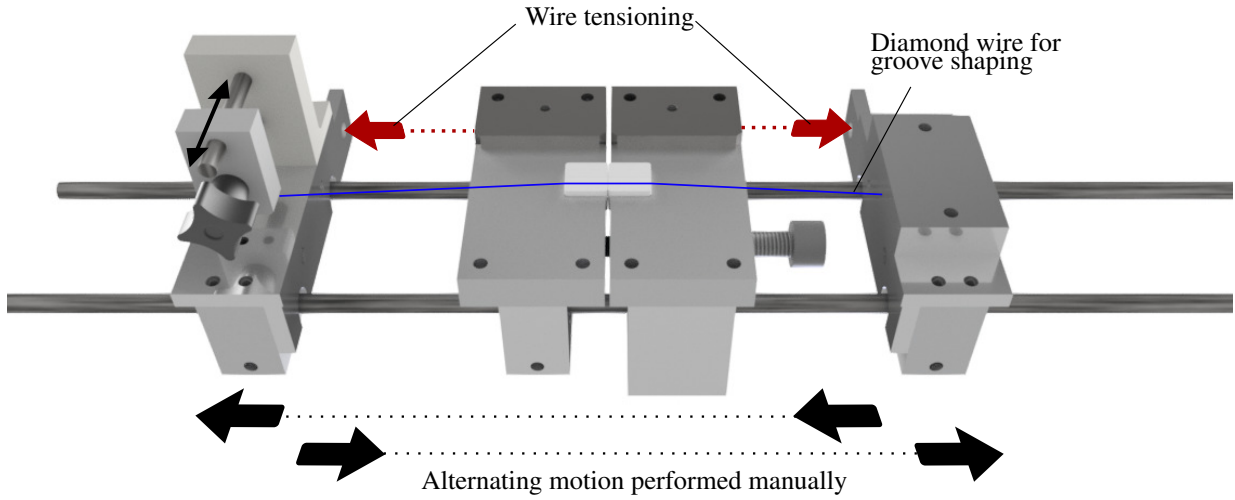


Figure 26: Groove machining operation.

After the complete design of the groove machining system, it was possible to assemble in a 3D drawing software the diamond wire welding device and visualize how the device would look after its final assembly. An illustration of the final assembly of the welding device can be seen in Figure 27.

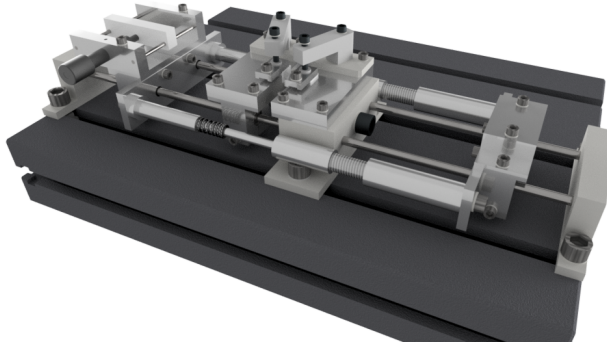


Figure 27: Welding device assembled in 3D drawing software.

The device components were manufactured and the welding device was assembled, a tensile spring which perform a force of approximately 5 N with a displacement of 10 mm was chosen, and a tension adjustment system and the attachment points of the spring were manufactured. After this process, the welding device (Figure 28) was ready to perform the first test procedures.

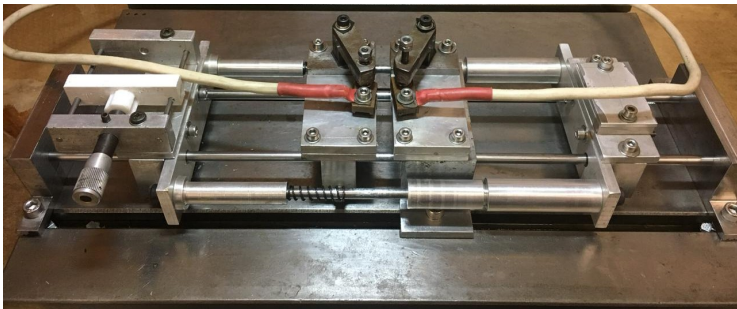


Figure 28: Diamond wire welding device.

4 EXPERIMENTAL METHODOLOGY

The purpose of this chapter is to present the experimental procedures used to perform welding experiments, to validate the development of the welding device and to present the characteristics of the welds performed in the device.

The experiments are divided into:

- **Welding parameters definition:** It is the standard procedures for using the welding device, which are necessary for the accomplishment of diamond wire welding experiments.
- **Welded joint qualification:** It is the experimental procedures carried out to find the appropriate welding parameters to achieve a high quality weld. For this, tests of mechanical strength and visual examination of weld joints were carried out. After these tests, the welding parameters were determined and the device was used to weld diamond wires in looped shape for several machining experiments.

In this experiments' section, the experimental procedures for the characterization of the eccentricity and microhardness profile of the welded joints are also discussed.

Figure 29 shows a flowchart summarizing the performed activities at this stage of the work.

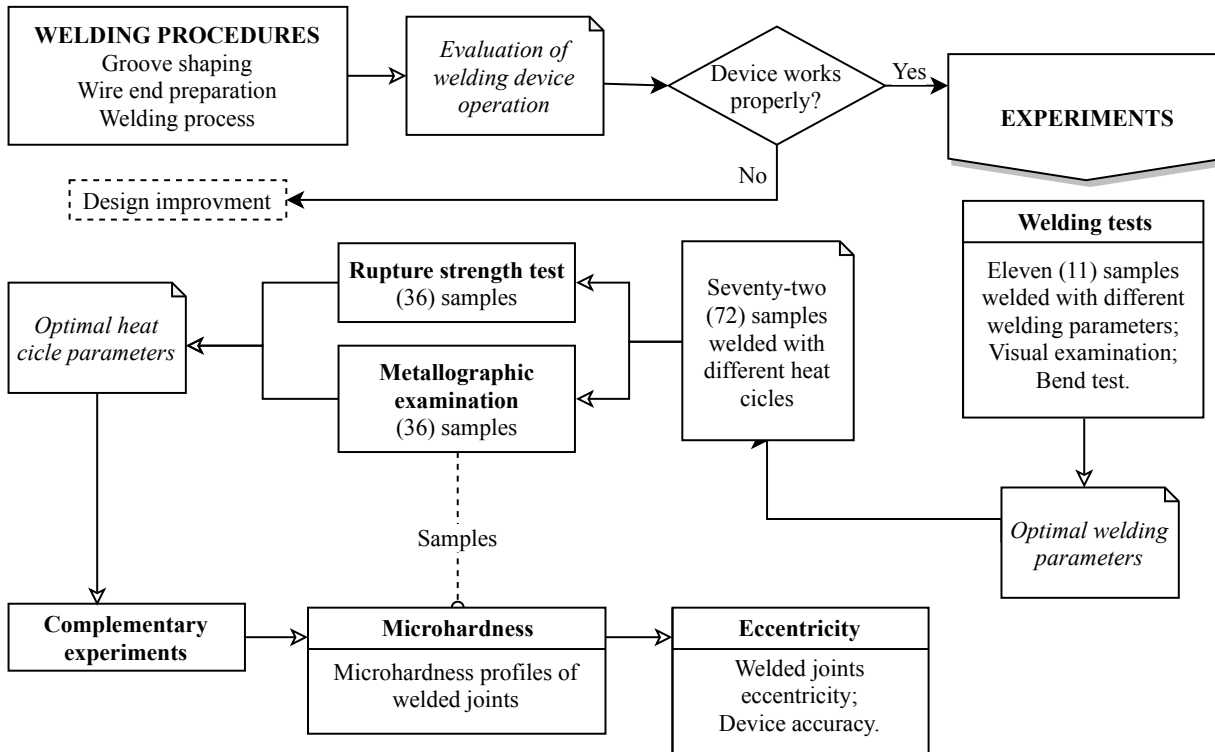


Figure 29: Experimental methodology flowchart.

4.1 WELDING PROCEDURES

In this section, the procedures necessary to conduct diamond wire welding experiments on the developed device will be described. Firstly, it will be described how the groove shaping is performed. Subsequently, it will be described how the ends of a diamond wire segment are prepared to be welded. And finally, it will be described how a welding procedure is performed.

4.1.1 Groove shaping

4.1.1.1 Diamond wire as groove shaping tool

For machining the aluminum oxide (Al_2O_3) inserts to shape a groove, a diamond wire of $350\ \mu m$ outer diameter is used, supplied by Norton Saint-Gobain. This is the same type of wire that is used in welding experiments. For the groove machining procedures a segment of diamond wire approximately $300\ mm$ was used.

4.1.1.2 Groove shaping procedure

Firstly, some components of the welding device are disassembled, such as the L-brackets together with the electrical contacts, remaining the welding device with exposed aluminum oxide inserts.

The diamond wire segment is then clamped between the plates of the coarse adjustment assembly, in an approximate position where it would be on the inserts and aligned with the linear guideways. Then, the other end of the wire segment is fixed on the movable block of the fine adjustment assembly. As can be seen in Figure 30 (b). Thereafter, the wire is tensioned through the tensioning mechanism, whereby the two central components of the mechanism are rotated at the same time to push the movable assemblies away from each other, in order to get the groove-shaping wire tensioned.

In Figure 30 (a) it can be seen how the wire segment is fixed in the machining system. In Figure 30 (b) it can be seen that due to rotation of the central component of the tensioning mechanism, the spring is pressed and thus the wire is tensioned.

The correct positioning of the diamond wire segment in relation to the direction of the groove machining movement is one of the most impor-

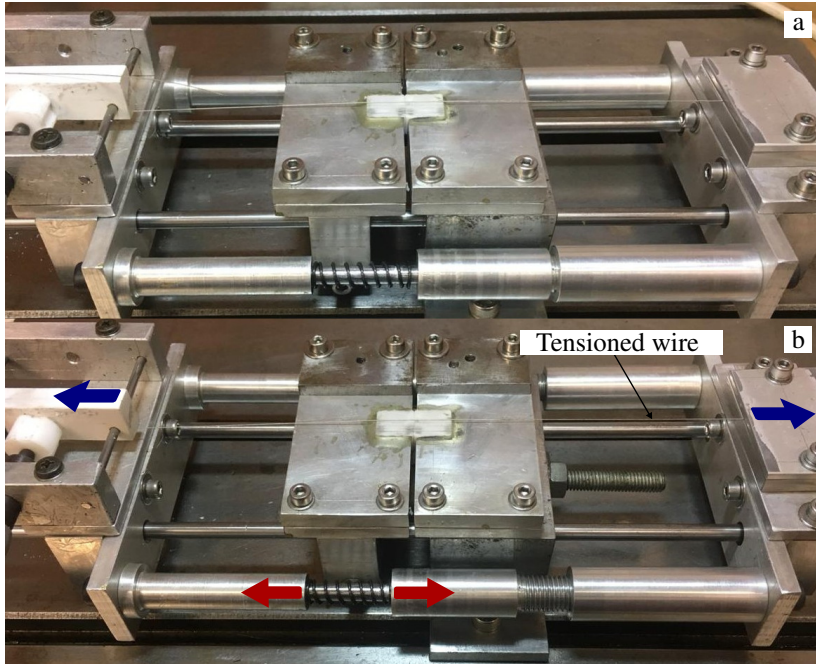


Figure 30: Tensioning of the wire segment for the groove shaping procedure.

tant activities in the use of the developed welding device. It is through the correct positioning of the diamond wire that the groove is shaped in a path aligned with the upset movement, which consequently contributes to setting up a well-aligned weld joint.

In order to correctly adjust the position of the diamond wire segment that performs the groove shaping, a microscope is required to facilitate the visualization of the wire alignment and positioning. A portable microscope (USB Dino-Lite 200x magnification) was used to assist the fine positioning of the wire and the monitoring of the groove machining process (DINO-LITE, 2014). In Figure 31 it can be seen how the portable microscope is positioned over the machining region of the groove. In Figure 32 it can be seen how the microscope image is projected on the computer screen.

At this point, the wire is tensioned and put in direct contact with the aluminum oxide insert, so if the machining system is moved, the diamond grains will begin to grind the insert. Therefore, to adjust the position of the wire without the machining process begins, a piece of adhesive tape is placed between the wire and the insert. In this way, there is no interaction between



Figure 31: Microscope positioning over the inserts.

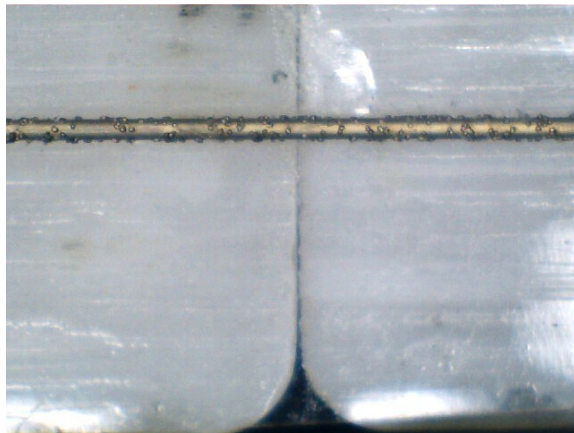


Figure 32: Microscope image projection.

the wire and the insert, and the alignment of the wire can be adjusted.

To adjust the wire position and alignment, the machining system is moved slowly in alternating directions. In this way, it is observed if the wire is moving at some point in a transverse direction to its axis. An imaginary line or some reference point in the image, projected by the microscope, can be used to check for a displacement in the transverse direction to the movement of the wire axis.

Figure 33 shows an illustration of the wire alignment. The red line represents the wire axis and the yellow line is a reference line, perpendicular to the face of the insert and aligned to the upsetting movement direction. In Figure 33 (a) the wire is stationary in a random position and there is a distance a_1 between the wire and the reference line, when moving the system up to the middle of the possible path (Figure 33 b), it can be observed that there is a transverse displacement of the wire in relation to the yellow line, leading to a new distance b_1 , which is different from a_1 , when moving the system to the end of the path (Figure 33 c), the transverse displacement increases ($c_1 \neq b_1$). This indicates that the wire is misaligned in relation to the direction of the linear guides (upsetting movement).

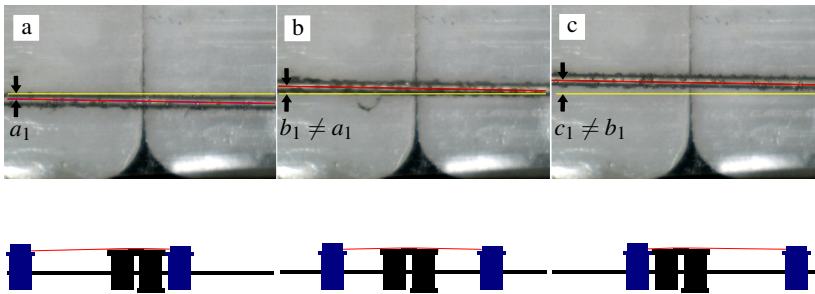


Figure 33: Incorrect alignment of the diamond wire a) in a initial random position b) at middle of the path c) at end of the path.

By rotating the micrometric adjuster, the position of the wire is modified according to the established reference. If moving the machining system in alternating directions there is no movement of the wire in some direction transverse to its longitudinal axis and to the reference line ($a_1 \approx b_1 \approx c_1$), it is concluded that the wire is aligned with the movement provided by the linear guideways.

In Figure 34, it can be observed the same wire used in Figure 33, but now with its position corrected through the micrometric adjuster. In Figure 34 (a) the wire was positioned according to the reference line (yellow line). It can be seen in Figures 34 (b and c) that when moving the machining system, the wire does not move transversely, thus concluding that it is aligned.

In this way, the groove shaping can be started. In order for the groove to be shaped with equal depth throughout the insert, the diamond wire is pressed slightly against the insert with a small block of aluminum. The machining region is wetted with water so that the aluminum oxide chip is carried by the water and the groove is kept clean, facilitating the visualization of the shaping process.

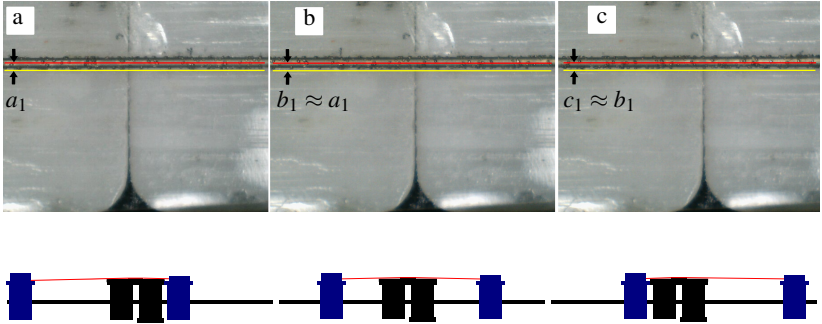


Figure 34: Correct alignment of the groove-shaping diamond wire.

Therefore, by performing the reciprocating movement of the groove machining system for about 10 minutes, a shaped groove having a depth approximately equal to half the diameter of the diamond wire is obtained.

In Figures 34, an illustration of the shaped grooves can be seen. The image was obtained by the Dino-Lite portable microscope.

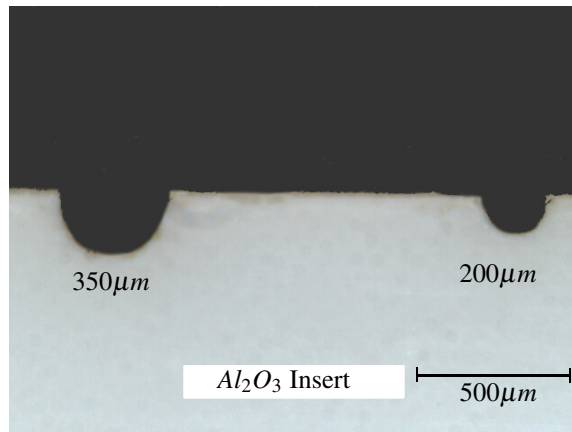


Figure 35: Shaped grooves.

After the shaping of the grooves have been performed properly, initial welding experiments could be performed.

4.1.2 Wire end preparation

Phillips (1969) notes that for some upset welding applications, the surfaces to be welded need to be machined to provide clean, parallel and comparatively smooth abutting surfaces. In this way, the ends of the samples were machined by sanding to form a cross section perpendicular to the axis of the wire segment. To perform this procedure, the end of the wire is fixed between two aluminum oxide inserts, in one of the inserts there is a slot of diameter slightly larger than the wire and perpendicular to the base of the insert, so the wire is pressed between the two inserts remaining perpendicular to the insert base.

In a metallographic grinding machine, available in LMP, using silicon carbide metallographic sandpaper with particle size 600, this set is pressed against the sandpaper and water is used as fluid. Therefore, only the end of the wire that protrudes out of the inserts is ground, thus forming a cross section.

In Figure 36 it can be seen an end of $350\ \mu\text{m}$ diameter diamond wire, after the grinding process, these image was taken under a scanning electron microscope (SEM) model TM-3030 HITACHI, available at CERMAT-LMP and under an optical microscope LEICA available at LABMAT.

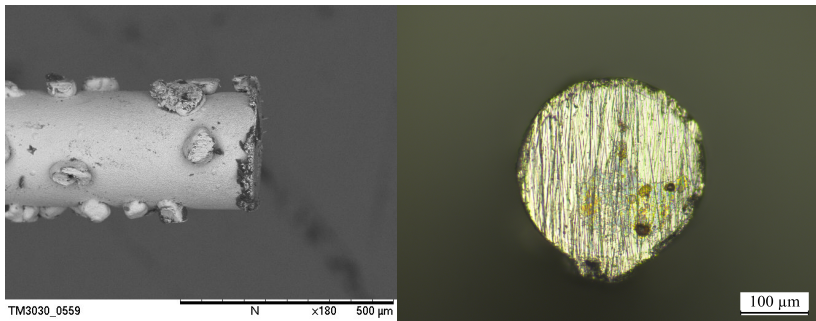


Figure 36: Wire end prepared using a metallographic grinding machine.

Samples of diamond wire have a curvature due to being wound on a spool, thus prior to welding experiments, the sanded ends are cleaned with ethyl alcohol to remove sanding sludge and are manually unbended, so that the radius of curvature of the wire do not impair the alignment of the weld joint.

4.1.3 Welding method

As it has been previously contextualized, the upset welding is a resistance welding process wherein coalescence is produced simultaneously over the entire area of abutting surfaces by the heat obtained from the resistance to electric current through the area of contact of those surfaces (PHILLIPS, 1969).

The surfaces to be welded should line up properly in the welding machine so that the heat generated is the same over the entire contact area. In this way, it will be described how the resistance upset welding procedure is performed in the device developed in this work, following the concepts of resistance upset welding process.

The basic welding procedures are the same for experiments using 25 mm-long and 1,4 m-long wire segments. Firstly, one wire end is positioned in a groove, corresponding to its diameter, in a position where the end protrudes approximately 3 mm out of the Al_2O_3 insert. Then, the wire is lightly pressed with the electrical contact. This procedure is repeated with the other wire end.

The next step is to adjust the distance of the cross sections of the wires ends protruding from each inserts. Phillips (1969) and Kearns (1980) established the name of the space between electrical contacts, or electrodes (clamping jaws), as die opening. In this way, before the welding process there is an initial die opening and after the welding, there is a final die opening. That is, in this step the die opening is adjusted through the individual adjustment of protrusion length of each wire end.

Auxiliary components, here called as calipers, are used to make this adjustment, these components are small aluminum blocks that have recesses of 0,3 mm, 0,4 mm, 0,5 mm and 1 mm. The base of the block is abutted into the insert and the wire end is pushed through the recess region, so the protrusion of the wire out of the insert has a dimension equal to the recess height. When using a block with a recess of 0,4 mm in the two ends, it is achieved a die opening of 0,8 mm.

In Figure 37 (a) one can observe how the die opening adjustment component is abutted against the wire end. In Figure 37 (b) the wire end is pushed into the groove. In Figure 37 (c) it can be seen the die opening caliper. In Figure 38 it can be observed a drawing illustrating the process of die opening adjustment.

It is important to mention that in previous works that carried out resistance welding of diamond wires, as per Campos (2016) and Knoblauch et al. (2017b), it was observed that the electrodes should be slightly further away from the wire end than the inserts. That is, the die opening between the Al_2O_3 inserts is smaller than the die opening between the electrodes. This

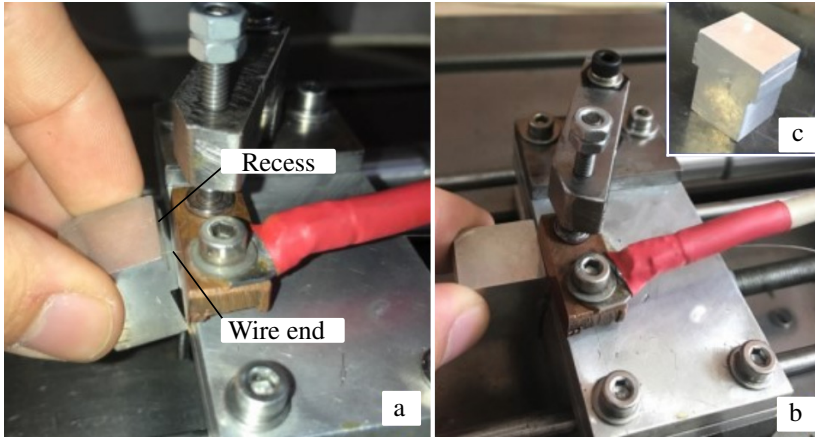


Figure 37: Die opening adjustment a) part abutted on the wire end b) wire end pushed into the groove c) die opening caliper.

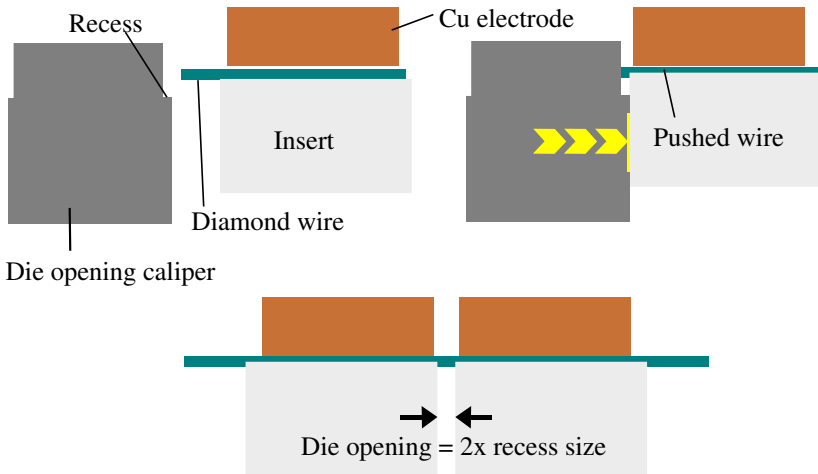


Figure 38: Drawing of die opening adjustment.

factor, according to the authors mentioned, contributed to weld consolidation.

After the die opening has been adjusted, the bolts that regulate the pressure of the electric contacts on the diamond wire ends are tightened, ensuring that the wire ends will not be moved during the welding process.

The movable assembly of the welding system is then approached to

fixed one, the wire ends are abutted slightly, and the alignment of the weld joint is checked. A magnifying glass is used to aid in the alignment checking, the portable microscope can also be used.

Thereafter, the spring having an end attached to the movable assembly is hitched to the tension adjustment bolt. The desired force for the welding process (upsetting force) is adjusted by the bolt, where a millimetric scale assists in the adjustment of the upsetting force, since the elastic constant of the spring is known. In Figure 39, it can be seen the spring position and how it is hitched to the tension adjustment bolt.



Figure 39: Spring position.

Thus, after these steps have been performed, the weld joint formed by the diamond wire ends, no matter if it is an experiment sample or a loop-shaped wire, is ready to receive the electric current coming from the welding source, so that the resistance upset welding takes place.

4.2 EXPERIMENTS

In this section, the experiments that were carried out to validate the welding device will be described. In addition, the experiments carried out to characterize, evaluate and improve the welds performed on the developed device will be presented.

Firstly, welding experiments were performed to find the best combination of welding parameters responsible for proper weld consolidation. Later on, to evaluate the influence of the heat cycle parameters on the weld, rupture strength tests and metallographic characterization were performed. Then, additional experiments were carried out to evaluate the eccentricity of the weld joint and to characterize the microhardness profile of the welds.

4.2.1 Welding pre-tests

In order to evaluate if the diamond wire welding device was able to perform welding procedures and experiments, some previous welding tests were carried out. It was also intended to evaluate if the welding parameters established by Campos (2016) would be adequate to perform welds on the new developed device.

4.2.1.1 Welding pre-tests samples

For an experiment where the purpose is to evaluate the weld joint consolidation, there was no need to weld a wire in looped shape. So small segments of diamond wire were. The wire has a cold drawn steel core standardized according to ASTM-A228/A228M-18 (2018).

For the welding pre-tests, diamond wire samples of $50\text{ mm} \pm 5\text{ mm}$ in length and $350\text{ }\mu\text{m}$ in diameter were used. The samples were cut with a cutting pliers, and their two ends were prepared for the welding process by the procedure described in section 4.1.2.

4.2.1.2 Welding pre-tests parameters

In this work, a welding power supply that was previously developed during the work of Knoblauch et al. (2017b) and Campos (2016) was used. This welding source is responsible for providing energy for the resistance welding process and heat cycle.

In summary, the main parameters of the resistance upset welding process performed in this work can be divided into two groups:

- Welding parameters: Initial current (C_1), initial current application time (T_1) or initial time, upsetting force (F) and die opening (D).
- Heat cycle parameters: Secondary current (C_2) and times of application and decrease of secondary current (T_2 , T_3 and T_4); T_2 is the time to reduce the current from C_1 to C_2 ; T_3 is the application time of current C_2 , and T_4 is the reduction time of current from C_2 to zero.

Details of the welding source and the graphical representation of welding and heat cycle parameters can be seen in Appendix B.

It is important to note that current values (C_n) are set in the welding power supply as a percentage value $C_n[\%]$ of the maximum power available

by the electrical circuit. This is done because the current in which the welding stages occurs is not a controlled variable. The true value of the current is determined by the behavior of the weld joint in relation to the power applied by the power supply in terms of $C_n[\%]$, but the value of the electrical resistance of each weld joint is variable. Besides, after the start of welding, the electrical resistance of the weld joint also varies with temperature. To know the true values of the process variables it would require a monitoring system of the energy provided by the welding source.

Thus, due to the unfeasibility of monitoring the welding electrical variables, the welding parameters are described in terms of percentage of the total current that the welding source can provide. However, it is estimated that $C_{n(RMS)} = 20\%$ corresponds to approximately 25 A and $C_{n(RMS)} = 16\%$ to 20 A, at $U_{(RMS)} = 0,7 V$ (KNOBLAUCH et al., 2017b).

It was observed in the work of Knoblauch et al. (2017b), Campos (2016) and Tanner (2015), that the welding parameters (C_1 , T_1 , F , and D) were the only ones responsible for the consolidation of the weld joint. Since the heat cycle parameters did not significantly influence the weld consolidation. Thus, in this stage of welding pre-tests, only the variation of the welding parameters (C_1 , T_1 , F , and D) is performed.

Campos (2016) observed that a initial current value (C_1) of approximately 19% – 20% applied for a time (T_1) of 1 s with a die opening (D) of 1 mm and an upsetting force (F) of 5 N – 6 N, formed a combination of optimal parameters for the consolidation of a suitable weld joint for 350 μm wire. This combination of parameters can be observed in Table 9.

Table 9: The best set of welding input parameters for a successful weld established by Campos (2016).

Welding parameters			
C_1	T_1	Die op. (D)	Force (F)
19 – 20%	1,0 s	1 mm	5 – 6 N

In this way, some initial welding tests were performed in order to evaluate if the welding parameters established by Campos (2016) (Table 9) would also be ideal for welds performed in the new welding device. However, after several tests it was observed that these parameters (Table 9) were not applicable to weld diamond wires in the device developed in this work.

By visually evaluating the welds and with the aid of the portable microscope, it was observed some factors that made it impossible to consolidate successfully the welds. Initially it was noticed that the welded joints were buckled. It was also observed a fragility of the welds and uneven weld burr. Phillips (1969) describes that buckled weld joints and uneven weld burrs are

problems caused by excessive upsetting force, excessive welding time and steel of high carbon content.

In this way, it was concluded that the upsetting force of 5 N was very high and that too much heat was being supplied for a long time to the weld joint.

An important point to note is the difference in upsetting force performed by the device developed in this work compared to the previous devices. In the work of Knoblauch et al. (2017b) and Campos (2016), the upsetting force was performed by a compression spring, the minimum force for moving the movable welding assembly was 2,5 N and the ideal upsetting force established by Campos (2016) was 5 N . Thus, in the device developed in the present work there was no evident minimum force limitation, the movement and the upsetting force are significantly smoother, thus increasing the range and the sensitivity of upsetting forces that could be ideal for the weld joint consolidation.

Therefore, due to the welding results using the parameters established by Campos (2016) (Table 9), and due to the differences between the welding devices, the welding parameters described in Table 10 were established for welding pre-tests in order to find the range or the combination of welding parameters that would reduce the observed problems and enable the next welding experiments and procedures to reach welds with higher rupture strength and quality.

Table 10: Pre-tests welding parameters.

Welding parameters			
C_1	T_1	Die Op. (D)	Force (F)
14%	0,4s;0,5s;0,6s;1,0s	0,4mm;1mm	2N;3N;4N;5N
15%	0,4s;0,5s;0,6s;1,0s	0,4mm;1mm	2N;3N;4N;5N
16%	0,4s;0,5s;0,6s;1,0s	0,4mm;1mm	2N;3N;4N;5N
17%	0,4s;0,5s;0,6s;1,0s	0,4mm;1mm	2N;3N;4N;5N
18%	0,4s;0,5s;0,6s;1,0s	0,4mm;1mm	2N;3N;4N;5N
19%	0,4s;0,5s;0,6s;1,0s	0,4mm;1mm	2N;3N;4N;5N
20%	0,4s;0,5s;0,6s;1,0s	0,4mm;1mm	2N;3N;4N;5N

Thus, approximately one hundred sixty welding procedures were performed with the combinations of parameters presented in Table 10 on 50 mm \pm 5 mm long samples. Each sample was observed during the welding process. Afterwards, the welding the samples were evaluated visually and were manually bent and tensioned for strength evaluation.

In these experiments, it was concluded that upsetting force (F) between 2,0 N – 2,5 N , die opening (D) of 1 mm, initial time (T_1) of 0,5 s and

initial current (C_1) between 17% – 20% would be an adequate combination of parameters for the welding tests. All other ranges of welding parameters resulted in unconsolidated welds.

With this range of parameters, the major defects previously observed such as burning of the weld joint, buckle, and irregular burr formation were slightly decreased. However, there were no solid welds yet with high strength.

4.2.2 Welding tests

The welding tests were carried out with the goal of finding the ideal combination of welding parameters that would consolidate a uniform, aligned and strong weld joint.

4.2.2.1 Welding test samples

For welding tests, diamond wire samples of $50\text{ mm} \pm 5\text{ mm}$ long and $350\text{ }\mu\text{m}$ in diameter were used. Each sample had its two ends prepared by the procedures described in section 4.1.2, so when cutting a sample in the middle, there were two cross sections, representing one welding experiment.

4.2.2.2 Welding tests parameters

In Table 11, it can be observed that for the welding experiments, only the current C_1 was varied among the welding parameters, because the other parameters have been already evaluated in the initial test stage 4.2.1.

In this step, it was intended to find the ideal value of C_1 for the consolidation of the weld joint, since it is the main welding parameter along with its application time T_1 , which in this experiment was kept fixed due to the observations made in the pre-tests.

Table 11 also lists the heat cycle parameters (C_2 , T_2 , T_3 and T_4) used in these experiments, it is worth mentioning that these were the same heat cycle parameters used previously in the pre-tests.

4.2.2.3 Welding test procedures

Eleven samples were welded using the parameters described in Table 11. The procedures previously described in sections 4.1.2 and 4.1.3 were used

Table 11: List of parameters used in the welding experiments.

Welding parameters								
	C_1	C_2	T_1	T_2	T_3	T_4	Die Op. (D)	Force (F)
PT1	17,0%	14,0%	0,5s	1,0s	30,0s	30,0s	1mm	2,2N
PT2	17,5%	14,0%	0,5s	1,0s	30,0s	30,0s	1mm	2,2N
PT3	18,0%	14,0%	0,5s	1,0s	30,0s	30,0s	1mm	2,2N
PT4	18,5%	14,0%	0,5s	1,0s	30,0s	30,0s	1mm	2,2N
PT5	19,0%	14,0%	0,5s	1,0s	30,0s	30,0s	1mm	2,2N
PT6	19,5%	14,0%	0,5s	1,0s	30,0s	30,0s	1mm	2,2N
PT7	20,0%	14,0%	0,5s	1,0s	30,0s	30,0s	1mm	2,2N
PT8	20,5%	14,0%	0,5s	1,0s	30,0s	30,0s	1mm	2,2N
PT9	21,0%	14,0%	0,5s	1,0s	30,0s	30,0s	1mm	2,2N
PT10	21,5%	14,0%	0,5s	1,0s	30,0s	30,0s	1mm	2,2N
PT11	22,0%	14,0%	0,5s	1,0s	30,0s	30,0s	1mm	2,2N

to perform the welding experiments.

4.2.2.4 Weld visual examination

For the visual examination of the welded joints, the samples were taken under the optical microscope LEICA, available in the Materials Laboratory (LABMAT). In order to visualize the samples in the microscope, it was necessary to use an auxiliary mounting to fix the samples and to be able to position them.

4.2.2.5 Bend test

Phillips (1969) describes that the most common method for testing upset welds in wires is to clamp the welded sample in a vise e.g., and bend the sample back and forth until a fracture occurs. Kanne (1994) also cites bend test as a simple indication of weld strength.

Thus, in order to evaluate the quality and mechanical strength of the welds, after the visual examination the samples were bent manually, and the behavior of the welded joints was observed.

4.2.3 Rupture strength test

In order to evaluate the quality of the diamond wire welds performed in the device developed in this work, and to evaluate the influence of heat cycle parameters on mechanical strength of the welds, rupture strength tests were performed.

As this test is not standardized, due to the innovative character of this work, the test results will express the maximum load that each welded joint withstand before breaking, rather than the resultant stress-strain relationship in standardized tensile tests.

The results are expressed as engineering stress (σ) in *MPa*, this unit is defined by the F/A ratio, where F is the instantaneous load applied in a perpendicular direction to the section of the sample, in N unit. A represents the cross-sectional area of sample before any load is applied. As the rupture occurs away from the weld joint in a region of diameter equal to the nominal diameter of the wire, and since the area of the weld joint is unknown, the variable “ A ” corresponds to the nominal diameter of the diamond wire.

4.2.3.1 Rupture strength test samples

Since the diamond wires used for the sawing experiments are welded in loop shape, it was determined that the rupture strength tests would be performed on looped wires.

Thus, for the rupture strength test, samples of diamond wire 600 *mm* long and 350 μm diameter welded in loop shape were used.

4.2.3.2 Heat cycle parameters

In order to evaluate the influence of the heat cycle parameters on the rupture strength of the welds, the parameters described in Table 12 were used to weld the samples. The procedures previously described in sections 4.1.2 and 4.1.3 were used to perform the welds.

Three samples of each set of parameters described in Table 12 were welded, corresponding to thirty-six samples for rupture strength tests.

Table 12: Welding and heat cycle parameters used in the experiments.

Welding parameters								
	C_1	C_2	T_1	T_2	T_3	T_4	Die op. (D)	Force (F)
T01	19,5%	15,0%	0,5s	0,2s	30,0s	30,0s	1mm	2,2N
T02	19,5%	15,0%	0,5s	1,0s	30,0s	30,0s	1mm	2,2N
T03	19,5%	15,0%	0,5s	30,0s	30,0s	30,0s	1mm	2,2N
T04	19,5%	14,0%	0,5s	0,2s	30,0s	30,0s	1mm	2,2N
T05	19,5%	14,0%	0,5s	1,0s	30,0s	30,0s	1mm	2,2N
T06	19,5%	14,0%	0,5s	30,0s	30,0s	30,0s	1mm	2,2N
T07	19,5%	13,0%	0,5s	0,2s	30,0s	30,0s	1mm	2,2N
T08	19,5%	13,0%	0,5s	1,0s	30,0s	30,0s	1mm	2,2N
T09	19,5%	13,0%	0,5s	30,0s	30,0s	30,0s	1mm	2,2N
T10	19,5%	12,0%	0,5s	0,2s	30,0s	30,0s	1mm	2,2N
T11	19,5%	12,0%	0,5s	1,0s	30,0s	30,0s	1mm	2,2N
T12	19,5%	12,0%	0,5s	30,0s	30,0s	30,0s	1mm	2,2N

4.2.3.3 Rupture strength testing device

In order to carry out the rupture strength experiments, a rupture strength testing device for looped diamond wires was developed in the facilities of Precision Engineering Laboratory, partially developed by Renz, Völker and Miller (2017), and by the present work's author.

In Figure 40, a photograph of the developed rupture strength testing device can be seen. In the work of Bühlmann (2018) it can be obtained details about the software and data acquisition system used in this equipment.

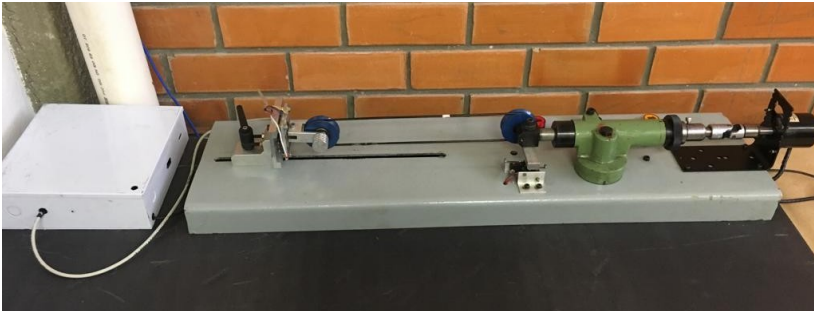


Figure 40: Rupture strength testing device for welded diamond wires.

Samples of diamond wire welded in loop shape are placed around two pulleys, a motor drives one of the pulleys, and through the load cell the force being applied to the looped wire is measured. In this way, due to the cali-

bration method used, the value of the tensioning force on one section of the looped wire is recorded, so it is known what force was necessary to break the weld joint.

The experiments were carried out on the same day and period, keeping the temperature of the environment constant and taking into account the conditions of the electric grid.

4.2.4 Weld joint metallography

In order to characterize and visually evaluate the influence of heat cycle parameters on weld quality, metallography of welded joints were performed. For the metallographic experiments, diamond wire samples of 30 mm length and 350 μm diameter were welded with the welding and heat cycle parameters described in Table 12, also used for welding the samples for rupture strength tests. Three samples of each combination of parameters presented in Table 12 were welded, corresponding to thirty-six samples for the metallographic experiments.

The samples were embedded in bakelite moulds, in a model EFD40 hot mouting press machine of FORTEL manufacturer. Later on, they were ground, polished and etched at Metal Forming Laboratory (LABCONF) facilities. For visual examination of the samples, they were taken under the LEICA optical microscope, available in the Materials Laboratory (LABMAT).

4.2.5 Complementary experiments

4.2.5.1 Weld joint eccentricity

As mentioned above, if the wire ends were positioned misaligned, a portion of material would not heat up and consequently the weld would deform and not consolidate. However, there are welds that consolidate but are slightly misaligned, which is detrimental to the use of this welded wire in sawing experiments. Thus, in order to verify the capability of the welding device to perform aligned welds and to measure the misalignment of the welds, a set of experiments was performed to evaluate the eccentricity of the weld joints.

According to the Collins English Dictionary by Guha (2016), eccentricity can be defined as “not having the same center, as the two circles one inside the other” or “not having the axis exactly in the center; off-center”.

Thus, it is considered that a weld joint that was formed by two trans-

verse sections, corresponds to two overlapped circumferences. If the weld joint is completely aligned, the eccentricity between the centers of the two circumferences corresponds to zero. However, if the weld joint is misaligned, there will be a positive value of eccentricity between the centers of the two circumferences.

Considering that the longitudinal axes of the two wire ends are parallel and that the two ends have the same diameter, the centers of the circumferences, corresponding to the cross sections of the wire ends, can be determined by the position of the longitudinal axes.

Thus, to evaluate the eccentricity of the weld joints, a measurement method was developed in which the maximum distance between the longitudinal axes of the welded diamond wire ends can be measured. By establishing one of the axes as the reference line, the distance between the longitudinal axes is measured and the eccentricity is determined.

For this experiment, ten samples of diamond wire 50 mm long and 350 μm in diameter were welded. The samples were welded with the best set of welding parameters that will be presented in chapter 5. The welding of the samples was performed according to the procedures described in sections 4.1.2 and 4.1.3.

The method developed to measure eccentricity consists of viewing the welded joint in two positions out-of-phase by a 90° rotation. In Figure 41 an illustration of the method used to measure the eccentricity of the welded joints can be seen. A rotatory wire holder developed by Knoblauch (2019) is used as auxiliary support, it allows to fix a segment of welded diamond wire and rotate it on its own longitudinal axis, which is illustrated in Figure 41.

Therefore, the welded diamond wire segment is fixed inside the cylindrical part, so this part is released in a random position on the "V" groove of auxiliary mounting. Then, this set is positioned under the optical microscope and the focus of the image is adjusted. Subsequently, a photography of the welded joint with 200x magnification is taken. Thereafter, the cylindrical part is rotated 90°, and a further photography is taken.

In Figure 42, two pictures taken of a welded joint can be seen, the first picture (Figure 42 a) was taken in a random position and the second one (Figure 42 b) rotated by 90° with respect to the first one.

This procedure was performed for ten welded samples. The images were analyzed in ImageJ® software three times for each of the ten samples. The mean and standard deviation of the measurements of each sample were calculated. It was not considered pixel errors of the image because it was estimated that the two wire ends had the same diameter, so the minimum, maximum and average eccentricity was calculated considering the standard deviation of all the measurements of the ten samples.

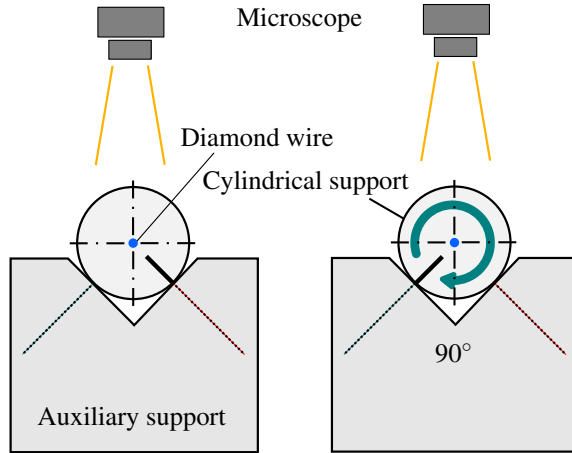


Figure 41: Illustration of eccentricity measurement method.

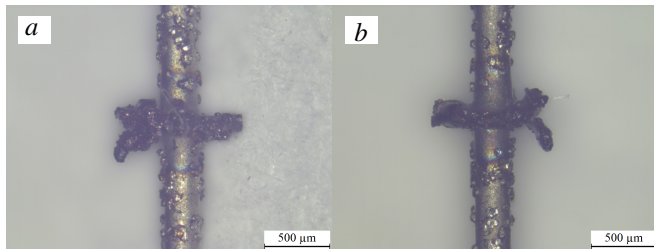


Figure 42: Pictures of welded joint taken in two positions out-of-phase by a 90° rotation.

In Figure 43, it can be seen an illustration of how this method was developed. A misaligned welded joint is represented in the figure. The wire end in the red color was established as a reference, the X_n values are positive when it is to the right of the end in blue. Positive rotation direction was set counterclockwise and eccentricity is represented by the symbol (e).

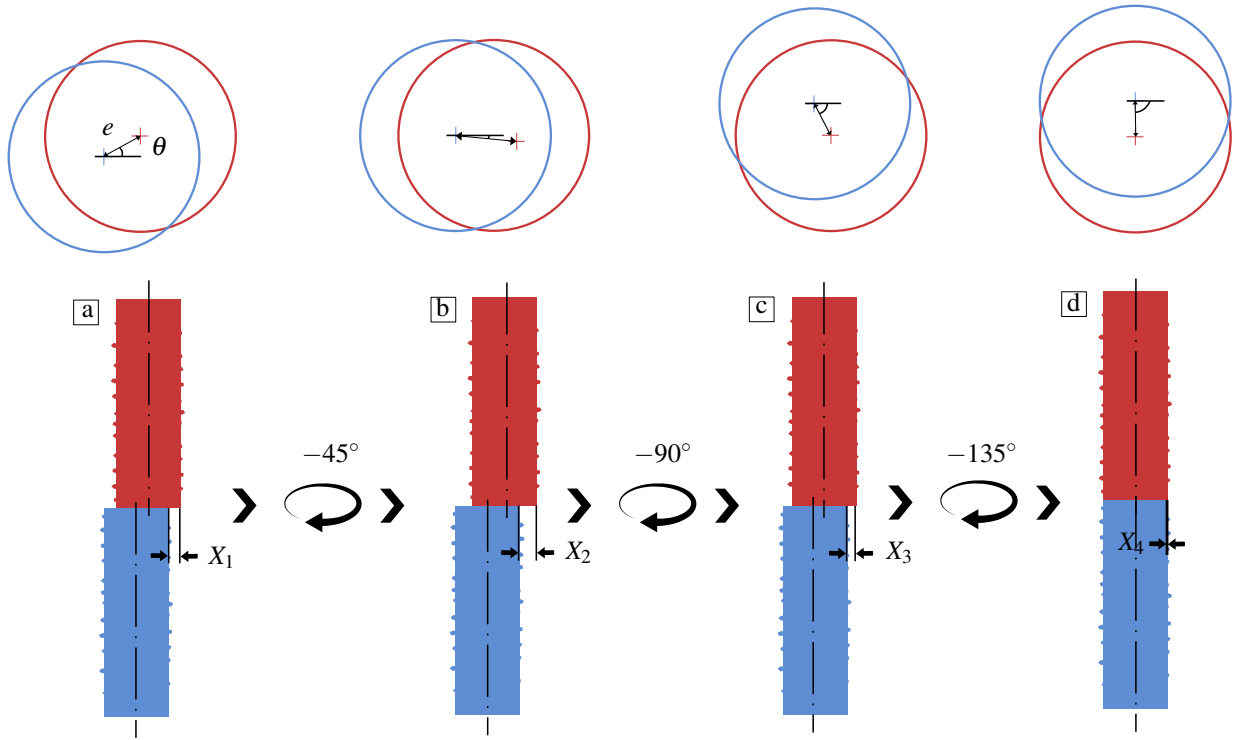


Figure 43: Method used for the equation of eccentricity.

In Figure 43 (a), the welded wire is in a random position, it can be seen that there is a displacement X_1 between the circle centers. The value of this displacement X_1 corresponds to:

$$X_1 = e \cdot \cos(\theta) \quad (4.1)$$

After rotating this welded wire at 45° , it can be seen that there is a new displacement X_2 , so it can be defined X_2 as:

$$X_2 = e \cdot \cos(\theta + 45^\circ) \quad (4.2)$$

By rotating the wire again at 45° , the welded joint shown in 43 (c) is rotated 90° from the starting position. In this way, it can be defined X_3 as:

$$X_3 = e \cdot \cos(\theta + 90^\circ) \quad (4.3)$$

As before, after a further rotation of 45° , the displacement X_4 can be defined as:

$$X_4 = e \cdot \cos(\theta + 135^\circ) \quad (4.4)$$

The expression of X_3 can be rewritten as:

$$X_3 = -e \cdot \sin(\theta) \quad (4.5)$$

In this way, the eccentricity can be calculated by:

$$e^2 = (e \cdot \cos(\theta))^2 + (-e \cdot \sin(\theta))^2 \quad (4.6)$$

Thus, eccentricity is defined as:

$$e^2 = X_1^2 + X_3^2 \quad (4.7)$$

Therefore, to calculate the eccentricity of the welded joint it is required two out-of-phase images in a 90° rotation.

In Figure 44, an illustration of this method can be seen. In position (A) the wire is apparently aligned when viewed from above, however when rotating the wire by 90° the greatest deviation of the weld joint is achieved.

Thus, it can be concluded that the method and the Equation 4.7 are valid for any position in which the wire is observed.

The X_n displacements of pictures were measured in ImageJ[®] based on the scale embedded in the image by the software of the LEICA optical microscope under which the pictures of the weld joints were taken.

The mean and standard deviation of the measurements were calculated, and thus the average eccentricity of the welds, performed in the welding

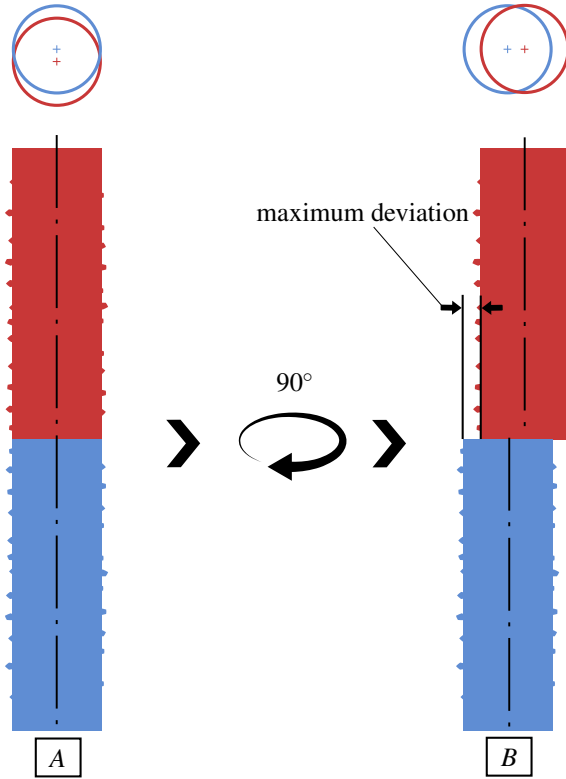


Figure 44: Illustration of eccentricity viewing.

device developed in this work, was determined through Equation 4.7.

It is important to note that these experiments were performed after a long period of welding device usage, to represent the capability of the device to perform aligned welds even after several welding procedures have been performed previously.

4.2.5.2 Vickers microhardness

Vickers microhardness tests were performed using the equipment model HMV-2TADW from SHIMADZU, available in the Metal Forming Laboratory (LABCONF). This equipment has a square base pyramidal indenter with face angles of 136° , as determined by standard ASTM-E92-17 (2017).

After the metallographic examination experiment, the three samples of each combination of welding parameters (Table 12) were taken to the Vickers microhardness tester. In order to characterize the microhardness profile of the welded joints and verify the influence of the heat cycle parameters on the microhardness of the welded wires, the indentations were performed along the length of the weld joint, as illustrated in Figure 45.

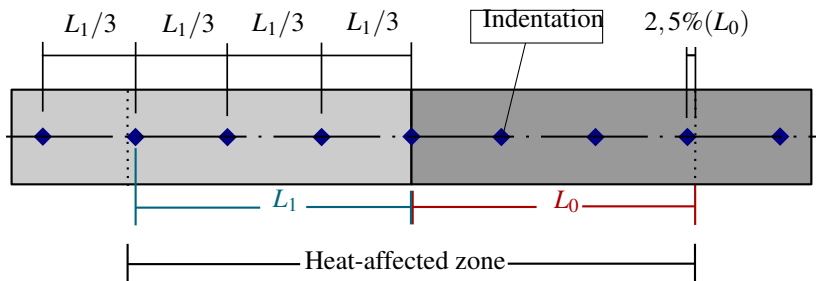


Figure 45: Location of microhardness indentations.

Some welds have different lengths, due to the manual adjustment of the die opening, so it was determined that the distance between the indentations would correspond to 32,5% of half the length (L_0) of the heat affected zone.

In order to identify the value of the Vickers microhardness of the diamond wire in its natural state, without having undergone the welding process, the metallographic preparation of three samples of diamond wire was performed, subsequently each sample was indented six times along its length.

According to ASTM-E92-17 (2017), the distance between indentations must be equal to or greater than 2,5 times the diagonal of the indentation, to avoid interaction with new indentations and possible microcracks resulting from previous indentations. The tests were performed using the HV 0,2 scale, which insert a load of approximately 1,961 N for 10,0 s (standard estimated time: 10,0 s to 15,0 s).

5 RESULTS

The purpose of this chapter is to present the experimental results of this work and its contributions. Firstly, the operation and performance of the welding device are evaluated. Afterwards, the experimental results of evaluation and characterization tests of the welds are presented.

5.1 WELDING DEVICE PERFORMANCE

In Section 4.1 it was described the procedures required for conducting diamond wire welding experiments on the welding device developed in this work. Firstly, the groove shaping procedures were performed, in these procedures it was observed that the developed groove shaping system was able to perform its required function successfully. The groove shaping process proved to be easy to do and was carried out in a controlled manner, without any unexpected behavior. Shaped grooves in Al_2O_3 insert can be seen in Figure 46.

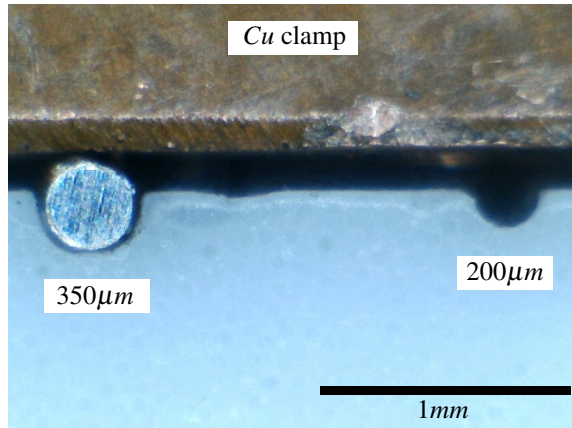


Figure 46: Grooves shaped in Al_2O_3 insert by developed the groove shaping system.

However, it has been realized the need to lightly press the diamond wire against the inserts during the groove shaping, if the wire is moved freely, the groove would be deeper at the edges of the inserts, thereby shaping misaligned grooves. However, by lightly pressing the diamond wire with an aluminum plate, the grooves were shaped evenly.

In Figure 47, there are two different inserts used for fixing diamond wire ends for welding. These inserts were used in the work of Knoblauch et al. (2017b), Campos (2016) and Tanner (2015). It can be noted that there is a difference between the grooves of each insert, and also in relation to the insert shown in Figure 46.

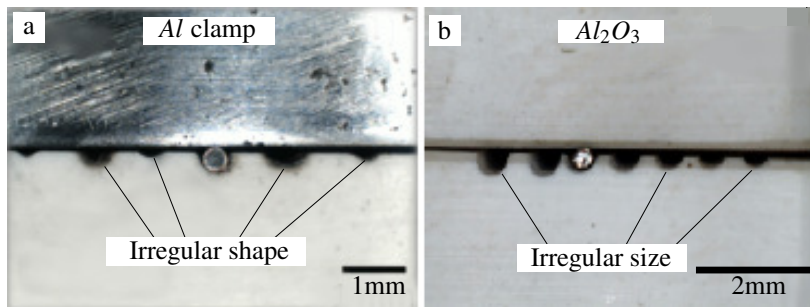


Figure 47: Grooves made in aluminum oxide inserts a) by wire b) by diamond grinding disc. Adapted from Campos (2016).

In Figure 47 (a) the grooves of the insert were shaped with the diamond wire itself, but manually made, resulting in grooves of irregular shapes and sizes. In Figure 47 (b) the grooves were shaped with a small diamond grinding disc on a milling machine, resulting in grooves with irregular size and depth.

In Figure 46, it can be seen that the two grooves have a more circular shape than the other ones shown in Figure 47, so the wire is better fitted and prevents its movement during the welding. The need for the device operator to adjust the wire position to achieve weld alignment is also overcome, reducing the setup time of the welding device.

Also, it should be noted that the groove shaping processes used for shaping and machining the grooves shown in Figure 47 are difficult to be executed. In the first case shown in Figure 47 (a), it takes more than one person to tensioning the diamond wire, press it against the inserts and move it alternately. In this process, the wire does not follow a limited path and there is no way to ensure alignment of the groove with regard to subsequent welding movement. In the second case, shown in Figure 47 (b), it is necessary to position the complete device on a milling machine, then an abrasive disk is installed, the position of the components is adjusted and the machining process is performed.

Thus, using the groove shaping system developed in conjunction with the welding device, grooves aligned and closest to the shape and diameter of

the diamond wire can be achieved, than by other processes previously used.

In the initial stage of welding procedures (Section 4.1), in subsequent welding experiments (Section 4.2) and in welding procedures to manufacture looped diamond wires, the behavior and performance of the welding device (Figure 48) was observed. Through annotations, it was possible to monitor the amount of consolidated welds that the device was able to manufacture in certain time periods.

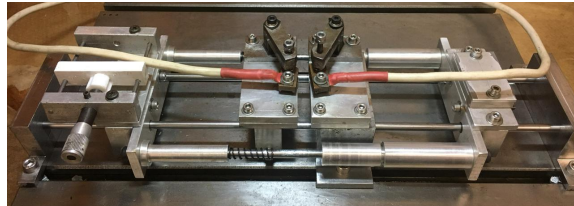


Figure 48: Diamond wire welding device.

Firstly, it was observed that the accomplishment of a welding procedure was easier to perform in the device developed in this work, than in the previous devices developed in the laboratory. This is mainly due to the grooves in which the wire is positioned, which ensures the alignment of the weld joint by construction, overcoming the need for the operator to visualize the weld joint and adjust it manually.

The correct choice and dimensioning of the materials for the components of fixing and position adjustment of the wire ends, were also factors that contributed to reduce the difficulty of carrying out welding procedures. The L-brackets made of ABNT 1045 steel and larger in size than the ones used in previous devices, have contributed to a greater regularity of the die opening dimension and distance from the electric contact to the edge of the inserts.

The use of electric contacts made of copper also contributed to the consolidation of the welds and consequently the efficiency of the welding device, since in the previous welding devices electrical contacts made of aluminum were used, which could form a layer of aluminum oxide on its surface. According to Lytvynov (2019), aluminum oxide exhibits electrical resistivity of up to $2,9 \times 10^9 \text{ Ohm.cm}$, causing an electrical isolation between the electrode and the diamond wire, making it impossible to weld.

The use of a tensile spring to perform the upsetting force was also a factor that contributed to improve the device weld success rate. In the previous welding device used by Campos (2016) and Knoblauch et al. (2017b), the upsetting force was performed by a compression spring, which deformed laterally upon being pressed, in addition to being oversized due to the need

for the upsetting force to be greater than the pre-load of the linear guides, in this case the stick-slip behavior occurred frequently, and when the welding movable carriage would move, the upsetting force was too high for welding.

In this way, the use of a tensile spring together with linear cylindrical guideways and linear bearings without pre-load, contributed significantly to the performance of the welding device. The stick-slip behavior has not been noted in the welding motion, and one can work with considerably smaller upsetting forces than previously used in other devices.

These were the main factors that contributed to the performance of the welding device developed in this work. Compared to previously devices available in the laboratory, it was realised that the welding setup time was shortened, the device operation difficulty was also reduced, the influence of the operator on the welding process was also reduced, and the reproducibility of the diamond wire welding was increased.

In Table 13, a summary of the amount of welds made in the diamond wire welding device can be observed. The amount of welds are approximate values based on lab annotations.

Table 13: Amount of welds made in the developed welding device.

Mouth	March	April	May	June	July	Total
Amount	30	100	60	50	20	
Applic.	Tests; Experiments;	Experiments; Machining of Mono-Si;	Experiments; Machining of Mono-Si;	Experiments;	Experiments;	
Mouth	August	September	October	November	December	Total
Amount	30	120	40	40	30	520
Applic.	Machining of NdFeB;	Experiments; Machining of NdFeB;	Experiments;	Machining of NdFeB, Ceramics,	Machining of NdFeB, SmCo;	

It can be seen that, more than five hundred welding procedures were carried out during approximately ten months. Over this time, it was observed some factors, such as the grooves wear, thus needing the shaping of new grooves when wear has become detrimental. It was also noted the appearance of clearances in linear bearings due to excessive use of the equipment, however not compromising the weld success rate. Besides that, approximately 95% of welds were consolidated.

In this way, the main achievement of the development of the diamond wire welding device was the amount of consolidated welds that were made for experimental research on DWS at the LMP. In addition, dozens of looped diamond wires welded by this device were sent to the Institute of Machine Tools and Manufacturing (IWF) at the Swiss Federal Institute of Technology (ETH) to be successfully used to cut mono-Si on an endless wire saw test rig.

5.2 WELDING TESTS

5.2.1 Visual examination

According to Phillips (1969), visual examination is the most widely used method of inspecting resistance butt welds. The author also mentions that in some cases it is necessary to evaluate the weld after removing the upset material, because this material tends to hide weld defects. However, as it can be seen in the following figures, it is possible to visually notice significant differences between the welds, not requiring the removal of the upset material.

In Figures 49, 50, 51 and 52, one can see the images of welded joints of diamond wires, referring to the experiments described in section 4.2.2.

In Figure 49 (a) the wire was welded with an initial current value $C_1 = 17\%$. It can be seen that there was no upset material, that is, the wire ends did not soften to the point of deformation enough to join them. It is also visible that the joint misaligned and one of the ends slightly warped. In this case, there was not enough power for the welding to occur, as the upsetting force is constant, the wire warped when it was warmed.

In Figure 49 (b), a behaviour similar to the weld of Figure 49 (a) can be observed. However, in this case the initial current value was slightly higher. Thus, there was not enough power for the welding, but the energy supplied was enough for the wire ends to warp more.

The weld performed with a current value $C_1 = 18\%$ is shown in Figure 49 (c), it can be observed that the contact region between the cross sections has a slight portion of upset material, but still not enough power to consolidate the welding.

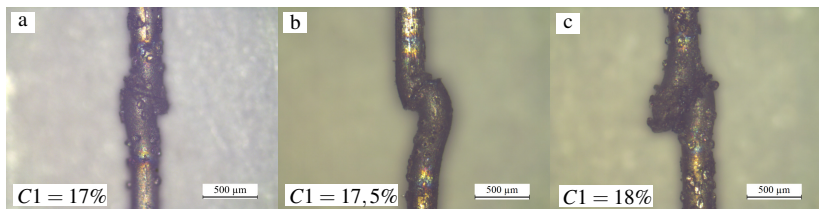


Figure 49: Welds performed with parameters a) PT1, b) PT2 and c) PT3 (Table 11).

In Figure 50 (a) one can see a weld performed with $C_1 = 18,5\%$. An appearance similar to that previously one seen in Figure 49 (c) is identified, there is a small amount of softened material at the interface of the wire ends,

however as there was not enough power for the welding, the wire ends overlapped.

Reaching the value of $C_1 = 19\%$, it can be seen in Figure 50 (b) that there is a portion of upset material at the interface between the wire ends. This sample shows less misalignment and more straight ends than previous ones, confirming that the lack of power in the previous welds, was one of the factors that made the wire ends warp during welding.

Using a current value $C_1 = 19,5\%$, the welded joint shown in Figure 50 (c) was obtained. One can observe a large amount of upset material at the weld joint, the wire ends are straight and there is no evident misalignment, like those seen in the previous welds. Thus, indicating that this value of $C_1 = 19,5\%$ could be close to the appropriate C_1 value for weld consolidation.

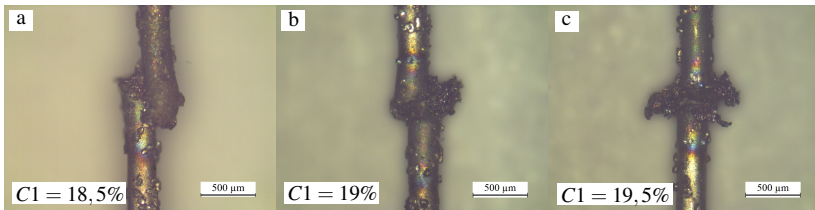


Figure 50: Welds performed with parameters a) PT4, b) PT5 and c) PT6 (Table 11).

The appearance of the weld shown in Figure 50 (c) is similar to the welds illustrated in the Figure 10, which Phillips (1969) cites as examples of upset butt welds. This sample also resembles to the appearance of upset welds presented in the literature by Brunst (1952) and Fahrenbach (1939). In the works developed by Knoblauch et al. (2017b) and Campos (2016) the welds considered as ideal had similar aspects, but with less significantly upset material.

Increasing the current value to $C_1 = 20\%$, the weld shown in Figure 51 (a) was obtained, it may be noted that the weld burr is not uniform around the wire. Welding the samples with $C_1 = 20,5\%$ and $C_1 = 21\%$, the welded joints presented in Figure 51 (b) and (c), respectively, were obtained. In these welds it may also be noted that the upset material is not uniform around the wire, it is concentrated on one side only, as if it had flowed out in one direction.

Reaching the current value $C_1 = 21,5\%$ it can be seen in Figure 52 (a) that the weld was not consolidated, presenting a darkened appearance as if it had been burned. In Figure 52 (b) one can see the weld performed with current value $C_1 = 21,5\%$, which although it shows weld burr, is also darkened and ruptured during the welding procedure. Thus, it is concluded that these welds were carried out with too much power.

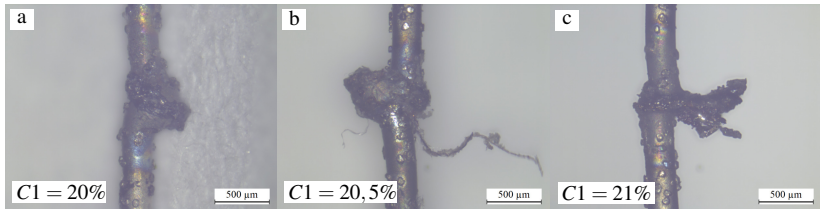


Figure 51: Welds performed with parameters a) PT7, b) PT8 and c) PT9 (Table 11).

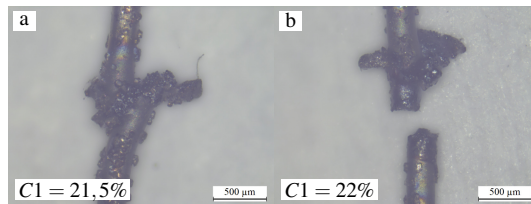


Figure 52: Welds performed with parameters a) PT10, b) PT11 (Table 11).

Thus, in this visual evaluation step, $C_1 = 19,5\%$, $T_1 = 0,5 s$, $D = 1 mm$ and $F = 2,2 N$ was considered the most suitable set of parameters for the welding consolidation of $350 \mu m$ diameter diamond wires.

5.2.2 Bend test

Table 14 summarizes the results of the bend test performed with the samples welded and examined in the previous step. As this experiment is a destructive test, the samples were tested only once and their behavior was observed.

The welds performed with the welding parameters PT1 ($C_1 = 17\%$), PT2 ($C_1 = 17,5\%$), PT3 ($C_1 = 18\%$) and PT4 ($C_1 = 18,5\%$) broke when they were bent. The wire ends detached at the interface by which they were joined, with a small bend movement these four samples easily broke. Thus, it is believed that in these welds there was no solid material joining, due to the low power during welding.

The sample welded with the current value $C_1 = 19\%$ behaved differently from the previous tested welds. Although in the visual examination it can be seen that this weld is unconsolidated and not aligned (Figure 50 b), when bent it behaved ductile. In this case, the weld did not break, the wire bent in a region next to the weld joint, approximately $0,5 mm$ away from the

Table 14: Results of the bend test.

Bend test		
	C_1	Outcome
PT1	17,0%	Broke close to the weld joint
PT2	17,5%	Broke close to the weld joint
PT3	18,0%	Broke close to the weld joint
PT4	18,5%	Broke close to the weld joint
PT5	19,0%	Bent close to the weld joint
PT6	19,5%	Bent close to the weld joint
PT7	20,0%	Broke close to the weld joint
PT8	20,5%	Broke close to the weld joint
PT9	21,0%	Welding broken in handling
PT10	21,5%	Welding broken in handling
PT11	22,0%	Unconsolidated weld

welded joint interface. This was a behavior expected for a good weld. However, the wire remained bent, demonstrating that the weld region has a small range of elastic deformation compared to the base wire.

The sample welded with the current value $C_1 = 19,5\%$ exhibited the best visual characteristics evaluated previously (Figure 50 c) and also behaved properly in this test. Similar to the previous weld, this sample did not break when it was bent, only deformed in a region close to the welded joint, approximately 0,5 mm apart.

The two samples welded with parameters PT7 ($C_1 = 20,0\%$) and PT8 ($C_1 = 20,5\%$), broke when they were bent. However, since there was a joining between these wire ends, the rupture occurred close to the weld joint.

The two samples welded with parameters PT9 ($C_1 = 21\%$) and PT10 ($C_1 = 21,5\%$), broke in handling, before the bend test could have been carried out. Thus, too much power in welding made the welded joints fragile. As it can be seen in Figure 52 (b), the weld performed with current value $C_1 = 22\%$ broke during welding due to excessive welding power.

Although Phillips (1969) and other authors of resistance welding literature mention that if in the bend test the workpiece breaks out of the weld joint, it means that the weld joint consolidated. However, the authors cite that in the bend test the workpiece is usually bent several times until the fracture occurs, and thus its behavior is observed. In the experiments carried out in this step, the diamond wire broke close the weld joint with only one bending movement, this behavior is not expected for a good quality weld.

Thus, after welding pre-tests, visual inspection and bend test experiments, it was determined that $C_1 = 19,5\%$, $T_1 = 0,5 s$, $D = 1 mm$ and

$F = 2,2 N$ are the most suitable parameters for consolidation of the weld joint of $350 \mu m$ diameter diamond wires.

In Figure 53, an image obtained by scanning electron microscopy of a weld, performed with the parameters described above, can be seen.

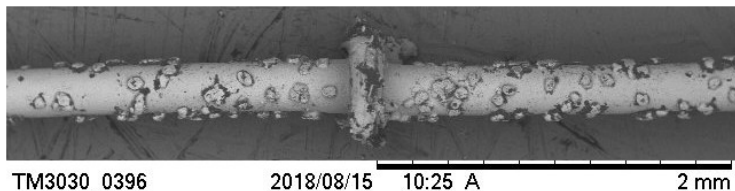


Figure 53: Diamond wire welded with PT6 welding parameters.

5.3 RUPTURE STRENGTH TEST

In Figure 54, a graph representing the overall result of the rupture strength test experiments can be seen. The experiments were carried out with the samples of diamond wire welded in looped shape, in order to verify the quality of welded joints and to observe the influence of the heat cycle parameters on the rupture strength of the welds.

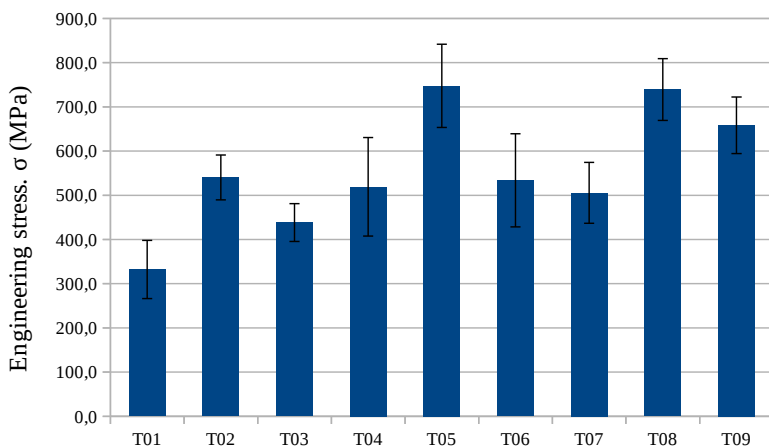


Figure 54: Rupture strength of diamond wire welds with different heat cycle parameters.

As previously mentioned, the graphs of results represent the average rupture strength of the weld joints done, corresponding to the engineering stress (σ). It can be observed initially, that the highest rupture strength values were obtained when welding the wires with the parameters $T05$ and $T08$.

The welds performed with the parameters $T05$ and $T08$ broke at an average tensile load of $747,6 \text{ MPa}$ and $739,3 \text{ MPa}$ respectively. These welds have very similar heat cycle parameters, only the value of current C_2 is different, where $C_2 = 14\%$ for $T05$ and $C_2 = 13\%$ for $T08$. In this way, it can be observed that the $T08$ heat cycle is performed with less energy than in $T05$, so there is a greater difference between C_1 and C_2 in parameters $T08$, corresponding to a faster cooling than in $T05$.

However, as the difference between the mean values of rupture strength between these parameters is very small and are within the range of the standard deviation, it can not be concluded which of these parameters results in a weld with higher rupture strength.

In the graph of Figure 54 it can also be seen that the welded joint that exhibited the lowest rupture load was welded with the combination of parameters $T01$, where the current value $C_2 = 15\%$ and time $T_2 = 0,2 \text{ s}$. The mean value of engineering stress (σ) of the $T01$ samples corresponds to $332,0 \text{ MPa}$.

It can also be seen, from the above graph, that the samples welded with $T09$ parameters can also be considered as welds having higher rupture strength, because although the mean engineering stress value corresponds to $658,3 \text{ MPa}$, its standard deviation is within the range of $T05$ and $T08$ standard deviations. However, the highest (σ) value measured in the experiments was $904,5 \text{ MPa}$, corresponding to a sample welded with the parameters $T05$.

The welds performed with the parameters $T10$, $T11$ and $T12$ did not present sufficient strength to be tested, these welds were performed with the current value $C_2 = 12\%$. Thus, it was concluded that few energy was supplied for the heat cycle and the welding was very fragile due to fast cooling.

To facilitate the understanding of the rupture strength tests, graphs were generated representing the results of each welding parameters group that have the same value of C_2 with different times T_2 , there are also graphs relating results of welds performed with the same time T_2 , but with different values of current C_2 . In the graph shown in Figure 55, one can see the result of the rupture strength test of the samples welded with $T_2 = 0,2 \text{ s}$. It can be observed that among the welds performed with the shortest time T_2 , the samples $T01$ ($C_2 = 15\%$) are the less strong. Among the samples welded with parameters $T04$ and $T07$, no differences in rupture strength can be observed.

In the graph that can be seen in Figure 56, a behavior similar to that seen previously is observed. These welds were performed with $T_2 = 1,0 \text{ s}$.

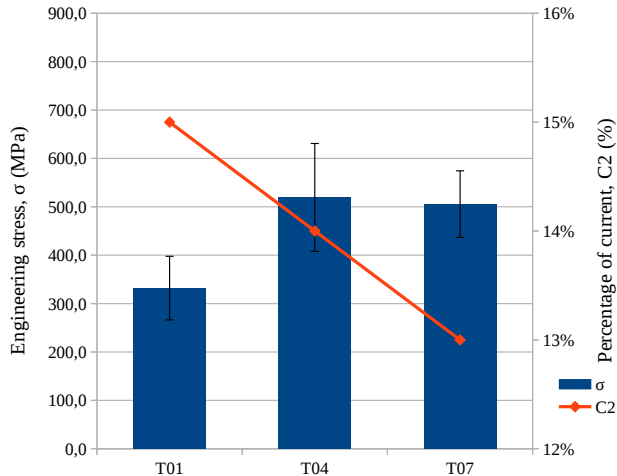


Figure 55: Rupture strength of welds performed with $T_2 = 0,2 s$.

This group of samples exhibits the highest values of rupture strength. The samples welded with parameters $T02$ ($C_2 = 15\%$) resulted in the lowest engineering stress values, as well as in the previous group. Again, no significant difference was observed between the second and third parameters ($T05$ and $T08$) presented in the graph.

In the third graph of this type of relationship (Figure 57), are presented the rupture strength of the welds performed with $T_2 = 30 s$, which turns out to be the longest heat cycle (T_2) time. It can be seen that samples $T03$ ($C_2 = 15\%$) exhibited the lowest rupture strength among those of their group, as well as in the two previous results with $C_2 = 15\%$. However, in this group one can see a larger difference between the welds performed with $C_2 = 14\%$ and $C_2 = 13\%$, where the samples $T09$ ($C_2 = 13\%$) reached the higher loads. However, this group of parameters exhibits lower rupture strengths than welds made with $T_2 = 1,0 s$.

Thus, it was observed that regardless time T_2 , a current value $C_2 = 15\%$ corresponds to a low rupture strength weld. It was also observed that the difference of 14% and 13% of current C_2 between the short time heat cycles ($0,2s$ and $1,0s$) is not influential in the rupture strength, however when the time of the heat cycle is long ($T_2 = 30 s$) there is difference in rupture strength between welds performed with $C_2 = 14\%$ and $C_2 = 13\%$. Thus, when the C_2 current is at a high plateau (15%), the heat cycle is not performed at the correct temperature to result in a weld of high rupture strength, regardless of

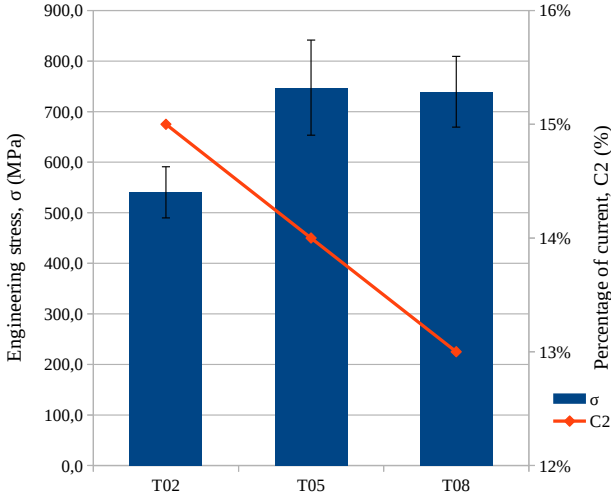


Figure 56: Rupture strength of welds performed with $T_2 = 1$ s.

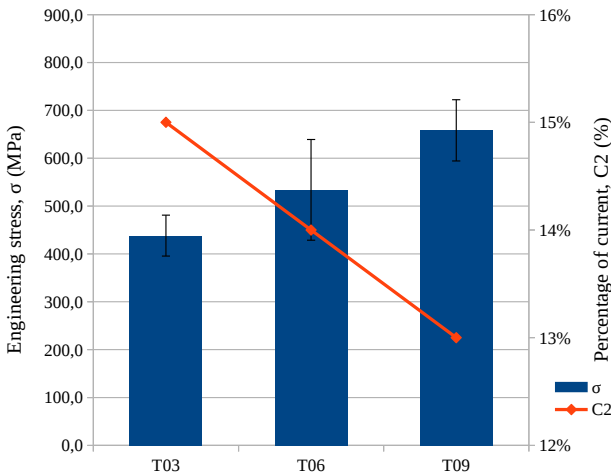


Figure 57: Rupture strength of welds performed with $T_2 = 30$ s.

slope of the cooling curve. Therefore, the longer the cooling time, the more sensitive the weld is to the value of the current C_2 , *i.e.*, the temperature of the heat cycle.

The results of the groups of welds made with the same values of cur-

rent C_2 but with different times T_2 will be presented in Figures 58, 59 and 60.

In Figure 58 one can observe the result of the rupture strength test of the samples welded with the parameters $T01$, $T02$ and $T03$, in which $C_2 = 15\%$. It can be seen that the highest values of rupture strength were achieved by the welds performed with parameters $T02$ ($T_2 = 1,0$ s), and the lowest value by $T01$ ($T_2 = 0,2$ s). By increasing the time T_2 from $0,2$ s to $1,0$ s, the rupture strength of the welded joints increased considerably, with $T_2 = 1,0$ s a value of engineering stress $\sigma = 540,3$ MPa was obtained, while with $T_2 = 0,2$ s was $\sigma = 332,0$ MPa. By considerably increasing the time T_2 from $1,0$ s to $30,0$ s the rupture strength was reduced. This group of samples welded with $C_2 = 15\%$ showed the lowest values of rupture strength among the other ones, a factor that can also be observed in the graph of Figure 54.

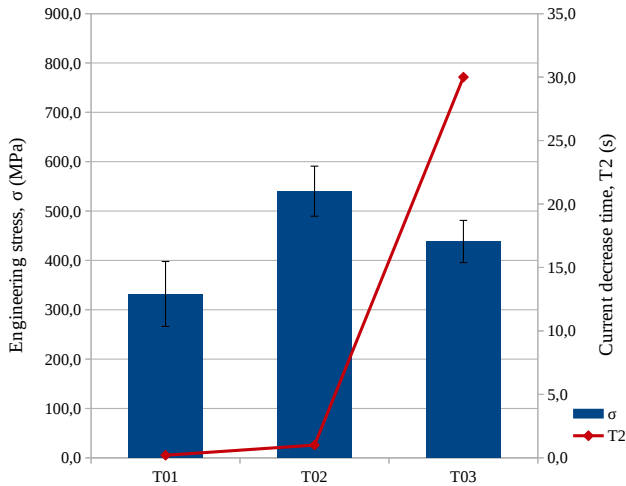


Figure 58: Rupture strength of welds performed with $C_2 = 15\%$.

In Figure 59 one can see the graph of rupture strength test results of samples welded with $C_2 = 14\%$. The behavior of this group is the same as previously seen in samples welded with $C_2 = 15\%$. In these welds, by slightly increasing the time T_2 from $0,2$ s to $1,0$ s there was a significant increase in the rupture strength, which corresponds to $519,3$ MPa for $T04$ and $747,6$ MPa for $T05$. Again, by increasing the cooling time to $T_2 = 30$ s one has a decrease of the rupture strength in relation to the welds performed with $T_2 = 1,0$ s.

In the graph shown in Figure 60, it can be observed the same behavior

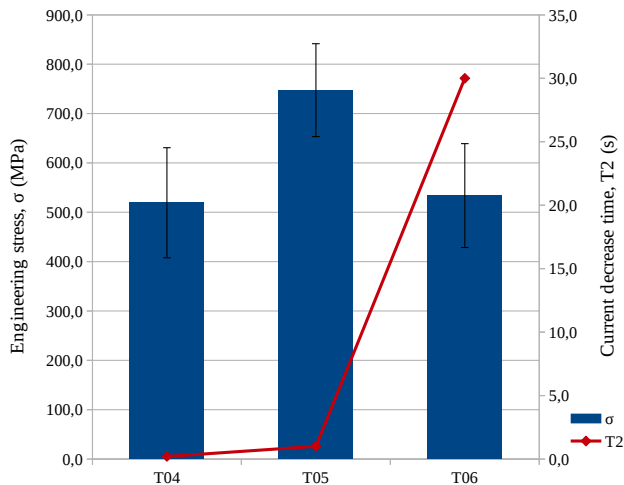


Figure 59: Rupture strength of welds performed with $C_2 = 14\%$.

seen in the previous results. The welds performed with the shortest heat cycle time ($T_2 = 0,2 s$) exhibit the lowest engineering stress values, and when the time T_2 was increased to $1,0 s$, higher rupture strength values were obtained. By increasing the heat cycle time T_2 to $30 s$, the rupture strength was reduced.

It is important to note the high sensitivity in rupture strength of the welded joints with regard to the variation of the heat cycle time T_2 , that is, in the slope of the cooling curve. It can be observed in the three graphs presented before, that the welds performed with $T_2 = 1 s$ exhibited the highest rupture strength and the welds performed with $T_2 = 0,2 s$ were the least strong.

5.4 METALLOGRAPHIC EXAMINATION

In order to observe the metallographic characteristics of the welded joints and to evaluate the influence of different heat cycle parameters on weld quality, the metallographic examination was performed. The metallography described in this section is also appended (Appendix C), for better visualization.

In Figure 61 one can see images obtained by optical microscopy of three welds performed with different current C_2 values and same time $T_2 = 30 s$. Between the three welds presented in Figure 61 no significant differences could be noticed. However, it can be observed in these welds that there

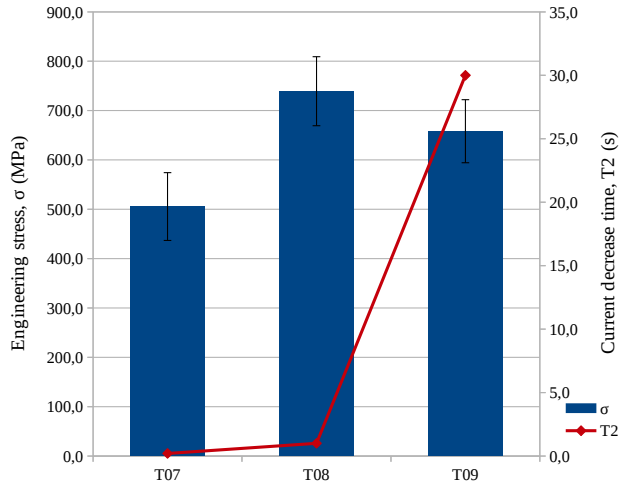


Figure 60: Rupture strength of welds performed with $C_2 = 13\%$.

is a difference in the grains size in the middle of the weld in relation to the grains size at the ends, close to the base metal material. This difference can be the factor that contributes to the decrease of the rupture strength in relation to the welds performed with $T_2 = 1 s$, because the larger grains in the central region, resulting from a slow cooling in the heat cycle ($T_2 = 30 s$), reduce the total area of grain contours that would hinder the movement of disagreements, as pointed out by Callister (2001).

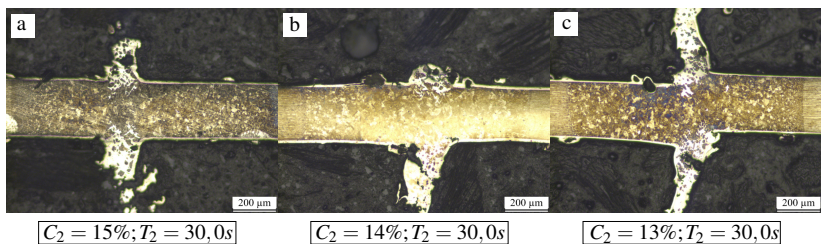


Figure 61: Welds performed with parameters a) T_03 , b) T_06 and c) T_09 (Table 12).

In Figure 62, one can see two metallographies of welds made with $T_2 = 0,2 s$. It can be seen from Figure 62 (a) that there is not such a large difference between the grains size of the central region of the weld relative to the ends. This is believed to occur due to a faster cooling during the heat

cycle ($T_2 = 0,2 s$).

The white layers that can be seen in Figure 62 are metallographic imperfections that occur in the nital etching of steels containing a very thin dispersion of martensite particles in a ferrite matrix, as described in Voort (1985). It can be seen that the weld performed with the $T07$ parameters (Figure 62 b) has a larger region of white layer, than the weld performed with $T04$ parameters (Figure 62 a), because the $T07$ parameters has a lower current value C_2 , consequently a faster cooling, resulting in smaller grains, which is more difficult to be revealed by metallographic etching, thus forming the white layers.

In Figure 61 it can be seen that there are no white layers as seen in Figure 62, it is believed that due to the cooling during the heat cycle of samples $T03$, $T06$ and $T09$ occur more slowly, there is no formation of such a refined microstructure. It is important to note that this fact was repeated for the other metallography performed with these welding parameters.

Thus, it is believed that welds made with $T_2 = 0,2 s$ have a brittle weld joint due to the very thin grain structure resulting from rapid cooling during the heat cycle. The other welds made with $T_2 = 0,2 s$ ($T09$) showed an intense white layer zone and the samples broke during the metallographic preparation, as they were really brittle.

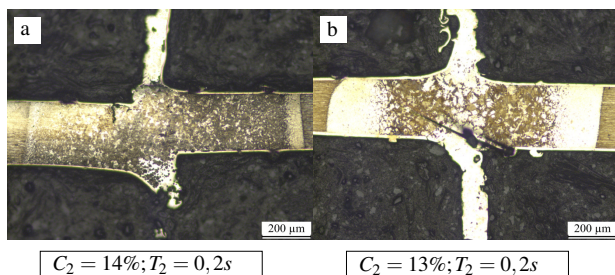


Figure 62: Welds performed with parameters a) $T04$ and b) $T07$ (Table 12).

In Figure 63, one can see two metallography of welds done with $T_2 = 1,0 s$, being $T05$ (Figure 63 a) and $T08$ (Figure 63 b). It was previously observed that these two welding parameters resulted in welded joints with the highest values of rupture strength. However, all samples welded with $T08$ parameters presented the characteristic that can be seen in Figure 63 (b), large white layers, thin grain structure, and fracture due to a brittle region. The welding was repeated with $T08$ parameters and the metallographic experiments were carried out several times, however the characteristics of the samples were the same.

It can be observed that the set of parameters $T08$ has a lower current C_2

value and consequently the heat cycle is performed at lower temperatures than with $T05$, so the welds performed with $T08$ are less ductile than those made with $T05$ parameters. Thereby, it is believed that the observed breakages are due to the movement of the welded joint during the metallographic grinding. It can also be seen that the weld performed with $T05$ parameters has a more uniform structure than the other ones discussed.

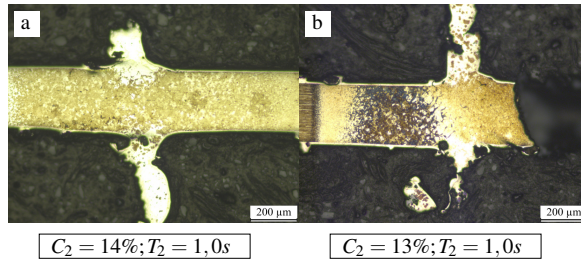


Figure 63: Welds performed with parameters a) $T05$ and b) $T08$ (Table 12).

Thus, through the results of rupture strength experiments and metallographic examination, it was concluded that the welds performed with the combination of parameters $T05$ has the high highest strength and quality characteristics among the other welds analyzed. In Figure 64 one can see in more detail the metallography of a weld made with the parameters $T05$. It can be noticed a greater uniformity in grain size in whole weld, in relation to the other welds discussed before. Also, a more uniform geometrical aspect is observed than the other welds, which can mean that even the parameters T_2 and C_2 could influence the alignment of the weld joint.

In Figure 65, a metallography of the weld performed with the $T05$ parameters is presented and some characteristics are highlighted. The region defined by abbreviation BM corresponds to the base metal, which is the diamond wire in its natural state of cold drawn steel. The HAZ defines the region of the wire that had its structure modified due to the welding heat, which is the heat-affected zone. There is a thin layer of nickel in the contour of the whole welded wire, and in the central region of the weld this layer is expelled outward forming the weld burr.

In Figure 65 one can clearly see the difference between the microstructures of the HAZ and the base material. The diamond wire used in this work has a cold drawn steel core, as cited by Schindler et al. (2009) due to the wire drawing process, the grains acquire a preferred orientation or texture, as the gradual stretching of the grains occurs in the direction of principal deformation. In this way, one can observe the stretched grains aspect of the BM microstructure.

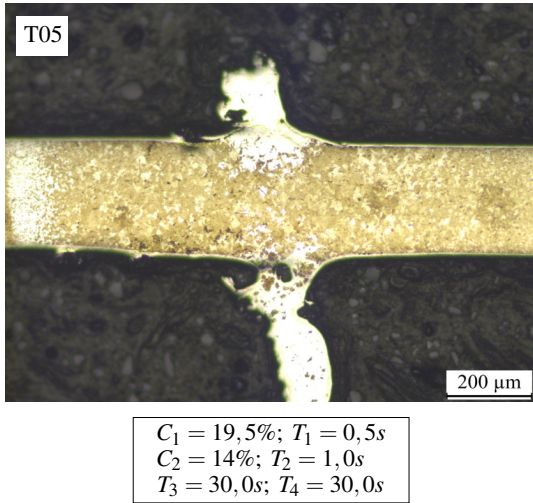


Figure 64: Metallography of welded joint performed with T05 parameters combination.

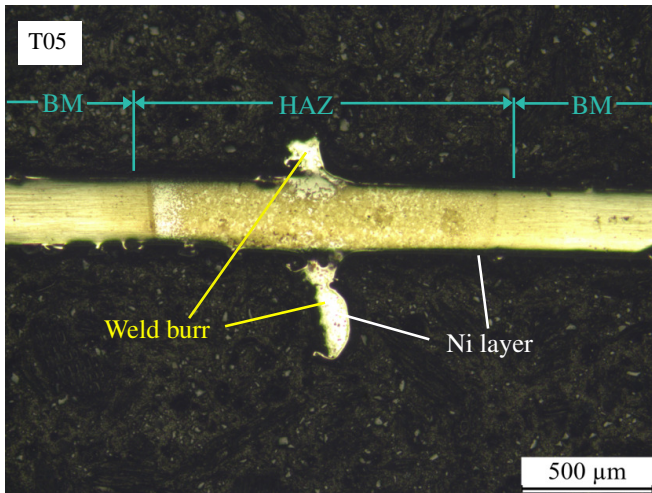


Figure 65: Metallography of welded joint.

The characteristic of HAZ microstructure is similar to recrystallized structures of cold-worked metals, as could be noted in Callister (2001); Raji and Oluwole (2013) and Zidani et al. (2006). As cited by Halberg (2011)

recrystallization is a thermally activated process, consisting of the generation of strain-free grains during the annealing of cold-worked metals. Thus, it is defined that the HAZ microstructure corresponds to a recrystallized grain structure.

5.5 ECCENTRICITY

As described before, one of the major challenges in upset welding of diamond wires is to achieve aligned weld joints, since the upset welding process depends heavily on the weld joint alignment to occur properly. As this work was developed mainly with the aim of increasing the alignment of the weld joints through constructive factors of the welding device, in the eccentricity experiments it was measured the misalignment of the welded joints made in the developed device.

Table 13 below shows the main results of the experiment by measuring the welded joints eccentricity. Firstly, it is possible to observe the minimal and maximal eccentricity values found, corresponding to $2,07 \mu m$ and $45,64 \mu m$ respectively. In the third column one can see these values corresponding to the percentage of the welded wire diameter.

It can be seen that the mean eccentricity of the ten welds was $22,37 \mu m$, which corresponds to $6,36\%$ of the wire diameter. It is interesting to note that all measured welds have been adequately consolidated. In this way, it can be noticed that the welding device is able to perform welds with slight misalignments that do not compromise the performance of the welding process.

Table 15: Eccentricity of welded joints of $350 \mu m$ diamond wire.

Weld joint eccentricity		
Measures	μm	% of wire diameter
e (min)	$2,07 \mu m$	$0,59\%$
e (max)	$45,64 \mu m$	$12,97\%$
e (mean)	$22,37 \mu m$	$6,36\%$
σ (st. dev.)	$13,10 \mu m$	$3,72\%$

5.6 VICKERS MICROHARDNESS

In order to characterize the welded joints of diamond wires, vickers microhardness profile measurements were carried out. In Figure 66, a graph representing the microhardness profile of a welded joint done with the T05

parameters combination, previously defined as the most suitable for optimum weld, can be seen. In the horizontal axis are defined the indentations and in the vertical axis, the vickers microhardness values.

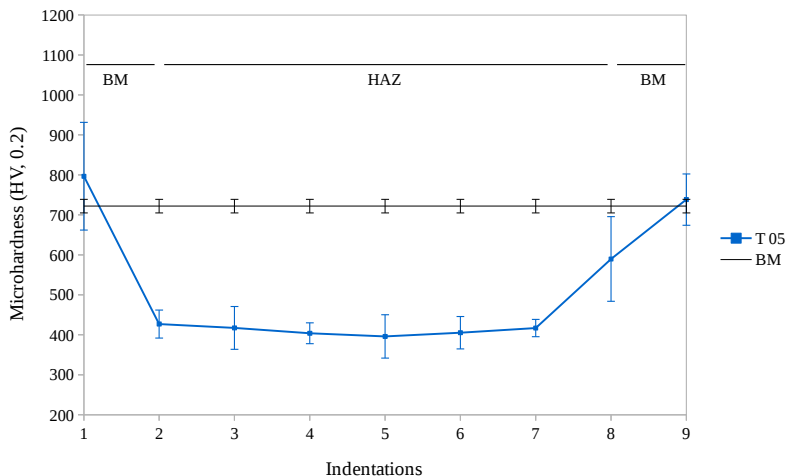


Figure 66: Microhardness profile of the weld done with *T05* parameters.

It is interesting to relate the microhardness profile of Figure 66 with the metallography shown in Figure 65 to observe each region and its respective hardness. The base material exhibits a high microhardness value, around $722HV$. On the other hand, the weld zone exhibits a significantly lower hardness, average $430HV$. The hardness of the wire BM is higher than of HAZ on account of the hardness earned by the cold-drawing of the wire core, also due to the thermally recrystallized microstructure.

It can be seen in metallography (Figure 65) that there is a marked change in the microstructure, which reflects a marked change in microhardness, a fact also demonstrated in flash upset welds by RWMA (2003).

Some indentations measured apart from the microstructure transition and white layers, showed microhardness values different from those of the base material, so the HAZ (Figure 65) was defined slightly larger than the recrystallized structure zone.

It can also be observed in the microhardness profile of Figure 66 that the indentations #2 and #8 are theoretically mirrored, however they have different microhardness values. This fact can be justified by observing Figure 65, where one can see a white layer in one side of the weld, and on the other side there is no white layer representing a thin structure, thus corresponding

to regions with different hardness. This can occur due to imperfections in the power supply for welding joint, from the welding source, electrical contacts, lead wires and electrodes. It may also be due to uneven setting of die opening. However, a large standard deviation is observed in indentation #8, which may represent that this fact does not occur frequently.

In Figure 67 are plotted three microhardness profiles of welds done with the same time $T_2 = 30\text{ s}$ and different current C_2 values, where $T03$ ($C_2 = 15\%$), $T06$ ($C_2 = 14\%$) and $T09$ ($C_2 = 13\%$). A similar behavior can be seen between these profiles, which differ slightly from the microhardness profile shown in Figure 66. It is noted that the indentations #2 and #8, that correspond to the last within the HAZ, have the lowest microhardness values.

Due to the long time $T_2 = 30\text{ s}$, there is a slow cooling in this region which is in contact with the copper electrode and the insert (indentations #2 and #8), the hardness in the center (indentation #5) is slightly higher due to the more intense heat at the weld joint interface. In the resistance welding manuals published by RWMA (2003), similar behaviors are observed in microhardness profiles of flash upset welds, so in this zone that it is should expect a fracture to occur during a strength test.

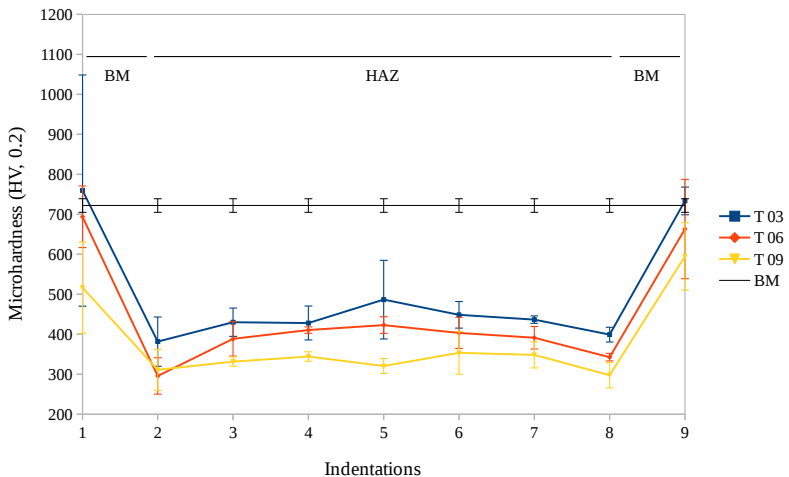


Figure 67: Microhardness profiles of welds done with $T_2 = 30\text{ s}$.

In Figure 68, three microhardness profiles of welds done with the same current value $C_2 = 14\%$ and different times T_2 can be seen. As the welding performed with $T06$ parameters has a significantly longer heat cycle time than the other welds, it is possible to note the difference in microhardness profiles,

especially in the microstructure transition region (indentations #2 and #8), where this weld has the lowest hardness.

In the weld done with $T04$ parameters, in which the time $T_2 = 0,2 s$ is really short, a higher hardness can be noticed in the microstructure transition region, due to a faster cooling. It could be observed in the microstructure shown in Figure 62 (a), that in the structure transition region there is a white layer, which represents a thin grain structure, corresponding to a high hardness zone than the rest of the weld.

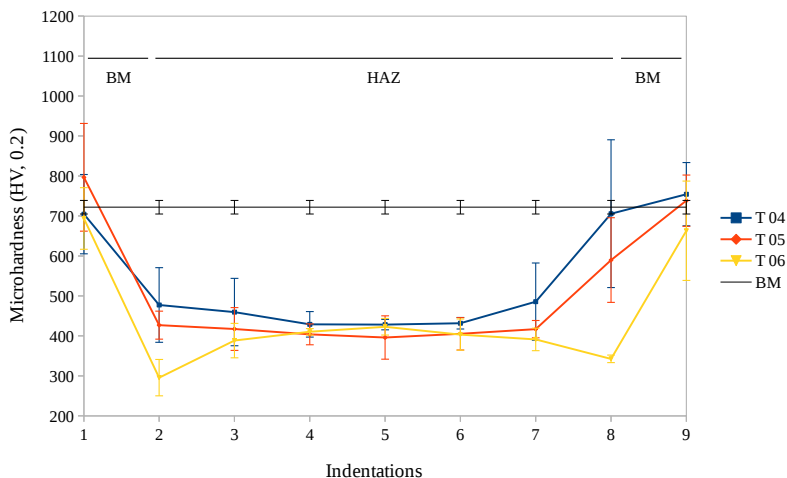


Figure 68: Microhardness profiles of welds done with $C_2 = 14\%$.

In Figure 69, one can see the microhardness profiles of welds done with same time $T_2 = 0,2 s$ and different currents C_2 . It can be observed that the weld done with $T07$ parameters, that has less energy during the heat cycle ($C_2 = 13\%$) exhibit in general high hardness values in relation to the other welds, because the lower current C_2 value represents a higher cooling rate during the heat cycle, leading to a higher hardness structure.

It is noticed that the region most susceptible to microstructural changes, throughout the different heat cycles, corresponds to the region of indentations #2 and #8, which is this the microstructure transition zone, that is positioned close to the copper electrode and next to the remaining unheated wire.

In this way, it was observed that metallurgical problems are not present in great degree in the welds performed in the experiments. It was noted that significant structural and hardness changes took place, since the heat in the upset welding is located between the dies, and since the greatest portion of

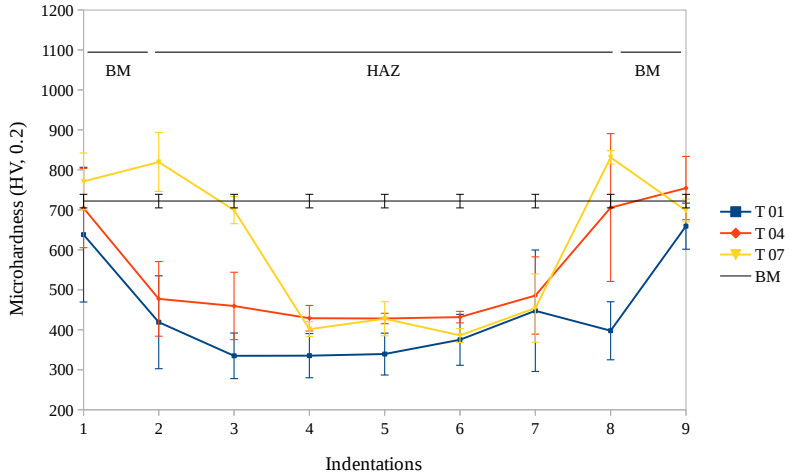


Figure 69: Microhardness profiles of welds done with $T_2 = 0, 2s$.

heat is generated at the wire ends interface, there are successive metallurgical changes in the finished weld, progressing from the highly heated structure in the center of the welded joint through the heat-affected zone to the undisturbed base metal.

6 SUMMARY AND CONCLUSIONS

The purpose of this chapter is to present the general conclusions of the work and, finally, the recommendations for future works.

The main goal of this master's thesis was the development of a device capable of welding industrial diamond wires in looped shape by the upset welding process. In order to reach this objective, an industrial product design methodology was established to assist in the design process of the welding device. The PRODIP methodology, as well as other design methodology concepts developed by UFSC researchers, proved to be adequate for structuring the design process of the device, since it was highly efficient in the organization of information and in the search for solutions to problems. The systematic development of the device based on the principles of solutions found, has made the device meet the main customers requirements, thus accomplishing its proposed function. Thus, in addition to having contributed significantly to the development of this work, the concepts of design methodology used and described serve as a basis for other researchers to develop their projects in a systematic way.

After the final assembly of the welding device, the operation of the groove machining system was initially tested. It was observed that the system worked properly according to expectations, shaping aligned and even grooves. The diamond wire fits snugly into the shaped grooves and there was no considerable gap between the wire and groove, so the wire ends did not move inside the groove, eliminating the need for the operator to manually adjust the alignment of the wire ends, now achieved by construction, thus reducing the setup time and difficulty of device operation, contributing to its efficiency. Being this an innovative concept, which had been established as a customer requirement becoming a design specification.

After the grooves were properly shaped, the first welding procedures could be performed. Initially, the welding pre-tests were carried out to evaluate if the parameters previously established as ideal would also be adequate for the new welding device, however these parameters did not result in consolidated welds. This was mainly due to the mechanical differences between the devices, because in the new device the sensitivity and range of upsetting force are higher. Thus, after hundreds of tests, a range of parameters could be found which could result in consolidated weld joints.

Subsequently, after welding tests, in which the combination of ideal parameters for weld joint consolidation was found, the device was used for several welding experiments and for the manufacturing of hundreds of endless wires. A high success rate of the device was observed, around 95% of

the welds performed were successfully consolidated. It was also noticed a low difficulty to use the device, since several users performed welding procedures properly. In relation to the previous device, the setup time was also reduced, contributing to the supply of laboratory demand for endless wire saws. Several sawing experiments of hard-brittle materials such as silicon, ceramic, porcelain, NdFeB and NiCrBSi, could be performed in the LMP using the endless diamond wires manufactured on the welding device.

It is important to highlight that the main factors that contributed to the development of a high-accurate welding device, such as the design and choice of materials as well as the innovative concepts, were established and processed in the product development methodology stages.

In the welding experiments, the high sensitivity of the weld joint in relation to the welding parameters was noted, in which a variation of only 0,5% of the welding current C_1 was sufficient to achieve a uniform weld joint. It was observed that visual examination was an effective procedure on evaluation of weld quality.

In the bend test it was observed that only the welds that formed a welding burr similar to those defined for butt-welds, that is, had the interface material softened and bonded, showed ductility when bent.

For rupture strength test, a rupture strength testing device for looped wires was initially developed by students from the partner university HTW Berlin, which was improved and put into operation during this work. It was observed the correct operation of the rupture strength testing device supplying the need for this work, now the equipment is available in the laboratory to carry out experiments in future works. In the rupture strength test, the welding parameters which resulted in welds of higher rupture strength, were found. It was concluded that a long heat cycle time did not result in high-strength welds, because it was observed that welds performed with the current decrease time $T_2 = 30\text{ s}$ resulted in regions of low hardness in the microstructure transition, these regions is preferred for fractures to occur.

In the metallographic examination, it was observed that the welds that exhibited the best results in the rupture strength test presented higher microstructure uniformity. It was also possible to observe the characteristics of a welded joint of diamond wire, in which the HAZ and the recrystallized grain structure were defined.

In the eccentricity analysis, it was observed that the average misalignment of the welded joints corresponds to only 3,36% of the wire diameter. Even in the most misaligned welds, the welding was consolidated. It was also concluded that the developed eccentricity measurement method was adequate for the experiment.

In the microhardness experiments it was possible to define the mi-

crohardness profile of diamond wire welds. It was also possible to evaluate some hardness characteristics related to visual aspects of microstructure. It was concluded that the weld done with the parameters *T05*, which exhibited the best results in the previous tests, was also the parameter that presented a profile of microhardness uniform and similar to the described in the literature for butt-welds.

Thus, the results obtained confirmed that the development of the diamond wire welding device met the key customers requirements and provided the Precision Engineering Laboratory with an opportunity for advancement in the diamond wire sawing research. The welding device was also used for the development of graduation work and laboratory internships. Finally, a patent application was requested for the grant of a patent for the diamond wire welding device as utility model in which a set of claims were stated.

6.1 SUGGESTION FOR FUTURE WORK

Here are some suggestions for future work:

- To develop a design of experiments (DOE) to describe and evaluate the most influential welding parameters on weld consolidation and quality, aiming to find the range of welding parameters that allow welding of 200 μm and 120 μm diameter diamond wires.
- To develop a method, electronic circuit or experiment capable of monitoring the actual values of electric variables during the welding process, in order to correlate them with the welds characteristics.
- To develop an experiment in which the upset welding is performed in a controlled and inert atmosphere with a gas such as argon, and observe the effects of the atmosphere on the welds characteristics.
- To develop a torsion test machine for welded diamond wires, to perform experiments with different heat cycle parameters and correlate them with the results of torsion tests.
- To perform sawing experiments, evaluating the influence of weld joint misalignment on the strength and performance of the endless wires during the cutting process.

BIBLIOGRAPHY

ASTM-A228/A228M-18. *Standard Specification for Steel Wire, Music Spring Quality*. ASTM International, West Conshohocken, PA, 2018.

ASTM-E92-17. *Standard Test Methods for Vickers Hardness and Knoop Hardness of Metallic Materials*. ASTM International, West Conshohocken, PA, 2017.

BACK, N.; OGLIARI, A.; DIAS, A.; SILVA, J. C. da. *Projeto Integrado de Produtos: Planejamento, Concepção e Modelagem*. Barueri, SP: Manole, 2008.

BIDVILLE, A. *Wafer sawing process: from microscopic phenomena to macroscopic properties*. Tese (Doutorado) — Université de Neuchâtel, 2010.

BRUNST, W. *Das elektrische Widerstandsschweißen*. Berlin: Springer-Verlag Berlin Heidelberg, 1952.

BÜHLMANN, J. *Development of a high sensitive load cell to measure the wire tension of an endless wire saw*. Semester Thesis - Universidade Federal de Santa Catarina, 2018.

CALLISTER, W. D. *Fundamental of Materials Science and Engineering*. Hoboken, NJ: John Wiley and Sons, Inc., 2001.

CAMPOS, J. E. S. de. *Development of a method for welding Diamond wire Into loop shape*. Trabalho de conclusão de curso - Universidade Federal de Santa Catarina, 2016.

CHIBA, Y.; TANI, Y.; ENOMOTO, T.; SATO, H. Development of a high-speed manufacturing method for electroplated diamond wire tools. *CIRP Annals*, v. 52, n. 1, p. 281 – 284, 2003.

CHIKUBA, M.; ISHIDA, H. Sumimoto Special Metals Co., Ltd, *Method for cutting rare earth alloy, method for manufacturing rare earth alloy plates and method for manufacturing rare earth alloy magnets using wire saw, and voice coil motor*. US patent, US 6,381,830 B1, 2002.

CLARK, W. L.; SHIH, A. J.; HARDIN, C. W.; LEMASTER, R. L.; MCSPADDEN, S. B. Fixed abrasive diamond wire machining - part i: process monitoring and wire tension force. *International Journal of Machine Tools & Manufacture*, 2003.

CONDOOR, S.; SHANKAR, S. R.; BROCK, H. R.; BURGER, C. P.; JANSSON, D. G. A cognitive framework for the design process. *American Society of Mechanical Engineers, Design Engineering Division (Design Theory and Methodology)*, 1992.

DIN-1910-100:2008. *Welding and allied process - vocabulary - part 100: metal welding process with additions to din en 14610:2005*. German Institute for Standardisation (Deutsches Institut für Normung), 2008.

DINO-LITE. *Microscópio Digital Dino-Lite AM7013MZT*. 2014. <<http://www.dinolite.com.br/dino-lite-am7013mzt>>. Acessado em 05/10/2018.

ECHEGARAY, F. Understanding stakeholder's views and support for solar energy in brazil. *Journal of Cleaner Production*, v. 63, n. 1, p. 125 – 133, 2014.

FAHRENBACH, W. *Widerstandsschweißen*. Berlin: Springer-Verlag Berlin Heidelberg GmbH, 1939.

FARINA, E. *Desenvolvimento conceitual de um módulo de potência para agricultura*. Dissertação (Mestrado) — Univesidade Federal de Santa Catarina, 2010.

FONSECA, A. J. H. *Sistematização do processo de obtenção das especificações de projeto de produtos industriais e sua implementação computacional*. Tese (Doutorado) — Universidade Federal de Santa Catarina, 2000.

GAO, W.; MA, B. J.; CAO, T. K.; LIU, Z. C. Resresearch and manufacturing of endless wire saw when cutting granite. *Key Engineering Materials*, 2008.

GE, P. Q.; ZHANG, L.; GAO, W.; LIU, Z. C. Development of endless diamond wire saw and sawing experiments. *Materials Science Forum*, v. 471-472, p. 481–484, 2004. Trans Tech Publications, Switzerland.

GUHA, M. *Collins English Dictionary (Reference edition)*. Glasgow: Collins, 2016.

GÖTTSCHING, P. *Systematische Untersuchungen zur Herstellung von Endlosdrähten zum Einsatz beim Drahtsägen*. Undergraduate Thesis - Technische Universität Berlin, 2017.

HALBERG, H. Approaches to modeling of recrystallization. *Metals*, v. 1, n. 1, p. 16–48, 2011.

HARDIN, C. W. *Fixed abrasive diamond wire saw slicing of single crystal SiC wafers and wood*. Dissertação (Masters Thesis) — North Carolina State University, Department of mechanical and aerospace engineering, 2003.

HODSEN, J. B.; HODSEN, J. B. *Continuous wire saw loop and method of manufacture thereof*. US patent, US 6065462 A, Colorado Springs, Colo., May 2000.

IEA. *Report IEA PVPS T1-34:2018*. International Energy Agency, 2018.

JIA, F.; SAN, H.; KOH, L. Global solar photovoltaic industry: an overview and national competitiveness of taiwan. *Journal of Cleaner Production*, v. 126, n. 1, p. 550 – 562, 2016.

KANNE, J. W. R. Solid-state resistance upset welding: a process with unique advantages for advanced materials. *Advanced Joining Technologies for new materials*, 1994.

KEARNS, W. H. *Welding Handbook: Resistance and Solid-State Welding and Other Joining Processes*. Seventh edition. American Welding Society: The Macmillan Press Ltd., 1980. (Seventh Edition, Volume 3).

KNOBLAUCH, R. *Diamond wire sawing of monocrystalline silicon*. PhD Thesis (Mechanical Engineering), Federal University of Santa Catarina, 2019.

KNOBLAUCH, R.; BOING, D.; WEINGAERTNER, W. L.; WEGENER, K.; KUSTER, F.; XAVIER, F. A. Investigation of the progressive wear of individual diamond grains in wire used to cut monocrystalline silicon. *Wear*, 2018.

KNOBLAUCH, R.; COSTA, J. V. M. R.; WEINGAERTNER, W. L.; XAVIER, F. A.; WEGENER, K. Endless diamond wire saw for monocrystalline silicon cutting. *Proceedings of 59th Ilmenau Scientific Colloquium*, Ilmenau, Deutschland, 2017.

KNOBLAUCH, R.; SILVEIRA, C. A. da; CAMPOS, J. E. S. de; WEINGAERTNER, W. L.; XAVIER, F. A.; WEGENER, K. Test rig for welding diamond wires into a loop. *Proc. of the Fifth Intl. Conf. Advances in Civil, Structural and Mechanical Engineering*, Zurich, Switzerland, 2017.

KUMAR, A.; MELKOTE, S. N. Diamond wire sawing of solar silicon wafers: a sustainable manufacturing alternative to loose abrasive slurry sawing. *Procedia Manufacturing*, v. 21, p. 549–566, 2018.

LIENERT, T. J.; BABU, S. S.; SIEWERT, T. A.; ACOFF, V. L. *ASM Handbook: Welding fundamentals and processes*. Ohio: ASM International, 2011. (ASM Handbook, Volume 06A). ISBN 9781613446607.

LYTVYNOV, L. 13 - aluminum oxide. In: FORNARI, R. (Ed.). *Single Crystals of Electronic Materials*. Cambridge: Woodhead Publishing, 2019, (Woodhead Publishing Series in Electronic and Optical Materials). p. 447 – 485. ISBN 978-0-08-102096-8.

MAZUTE, J. *Estudo de mecanismo dosador de manivas para plantadora de mandioca*. Dissertação (Mestrado) — Universidade Federal de Santa Catarina, 2014.

MENG, J. F.; GE, P. Q.; LI, J. F. The surface quality of monocrystalline silicon cutting using fixed abrasive diamond endless wire saw. *International Journal of Computer Applications in Technology*, 2007.

MENG, J. F.; GE, P. Q.; LI, J. F.; GAO, W. Removal mechanism in wire-sawing of hard-brittle material. *Materials Science Forum*, 2004.

MENG, J. F.; GE, P. Q.; LI, J. F.; ZHOU, R. Research of endless wire saw cutting of al₂O₃/TiC ceramics. *Key Engineering Materials*, 2006.

MöLLER, H. J. Wafering of silicon crystals. *physica status solidi (a)*, v. 203, n. 4, p. 659–669, 2006.

MöLLER, H. J. Chapter two - wafering of silicon. In: WILLEKE, G. P.; WEBER, E. R. (Ed.). *Advances in Photovoltaics: Part 4*. Amsterdam: Elsevier, 2015, (Semiconductors and Semimetals). p. 63 – 109. ISBN 0080-8784.

MöLLER, H. J.; FUNKE, C.; RINIO, M.; SCHOLZ, S. Multicrystalline silicon for solar cells. *Thin Solid Films*, v. 487, p. 179–187, 2005.

PAHL, G.; BEITZ, W.; FELDHUSEN, J.; GROTE, K.-H. *Engineering Design*. 3. ed. London: Springer-Verlag London, 2007.

PEREIRA, M. *Metodologia de projeto para sistemas mecânicos de precisão reconfiguráveis*. Tese (Doutorado) — Universidade Federal de Santa Catarina, 2004.

PHILLIPS, A. L. *Welding Handbook*. Sixth edition. London, UK: Macmillan Education, 1969. (Gas, Arc and Resistance, Section Two).

RAJI, N. A.; OLUWOLE, O. O. Recrystallization kinetics and microstructure evolution of annealed cold-drawn low-carbon steel. *Journal of Crystallization Process and Technology*, 2013.

RENZ, D.; VÖLKER, G.; MILLER, J. Internship report (Mechanical Engineering), *Rupture strength testing device for welded diamond wires*. University of Applied Sciences for Engineering and Economics (HTW) - Berlin, Germany, 2017.

ROZENFELD, H.; FORCELLINI, F. A.; AMARAL, D. C.; TOLEDO, J. C. de; SILVA, S. L. da; ALLIPRANDINI, D. H.; SCALICE, R. K. *Gestão de desenvolvimento de produtos: Uma referência para a melhoria do processo*. São Paulo: Editora Saraiva, 2006.

RWMA. *Resistance welding manual*. Revised fourth edition. Philadelphia, PA: Resistance Welder Manufacturers Alliance, 2003.

SBRAVATI, B. *Study of a method for laser beam welding of diamond wire saws*. Trabalho de Conclusão de Curso - Universidade Federal de Santa Catarina, 2014.

SCHINDLER, J.; JANOSEK, M.; MISTECKY, E.; RUZICKA, M.; CIZEK, L. A.; RUSZ, S.; SVENANEK, P. Effect of cold rolling and annealing on mechanical properties of hsla steel. *Archives of materials science and engineering*, v. 36, n. 1, p. 41–47, 2009.

STOETERAU, R. L. *Projeto de máquinas ferramentas: Introdução ao projeto de máquinas ferramentas modernas*. Universidade Federal de Santa Catarina: Editora UFSC, 2004.

SUBBIAH, S.; SAPTAJI, K.; ZAREPOUR, H. A study of linear vibration-assisted scratching on silicon and its impact on diamond wire wafering process. *Eur. Photovolt. Sol. energy Conf. Exhib.*, 2013.

TANNER, A. *Fertigung eines Endlosdrahtes zwecks Optimierung des Silizium-Schneidprozesses*. Dissertação (Mestrado) — Swiss Federal Institute of Technology Zurich, Institut für Werkzeugmaschinen und Fertigung IWF, 2015.

TEOMETE, E. *Mechanics of wire saw machining process: Experimental analyses and modeling*. Tese (Doutorado) — Iowa State University, 2008.

TEOMETE, E. Investigation of long waviness induced by the wire saw process. *Proceedings of the Institution of Mechanical Engineers, Part B: Journal of Engineering Manufacture*, v. 225, n. 7, p. 1153–1162, 2011.

TURRENTTINI, F. *Endless saw for cutting stone*. US patent, US 379835 A, Geneva, Switzerland. Patented in Belgium July 15, 1887, No. 77,959; in France October 29, 1887, No. 183,835, and in Italy December 31, 1887, No. 22,576/383., Mar. 1888.

VOORT, G. F. V. *ASM Handbook Volume 9: Metallography and Microstructures*. Ohio: ASM - American Society for Metals, 1985.

WU, H. *Fundamental Investigation of cutting of silicon for photovoltaic applications*. Tese (Doutorado) — Georgia Institute of Technology, 2012.

WU, H. Wire sawing technology: A state-of-the-art review. *Precision Engineering*, v. 43, p. 1 – 9, 2016. ISSN 0141-6359.

YU, X.; WANG, P.; LI, X.; YANG, D. Thin czochralski silicon solar cells based on diamond wire sawing technology. *Solar Energy Materials and Solar Cells*, v. 98, p. 337 – 342, 2012. ISSN 0927-0248.

ZIDANI, M.; BOUMERZOUG, Z.; BAUDIN, T.; PENELLE, R. Texture and evolution of recrystallization in low carbon steel wire. *Materials Science Forum*, v. 514-516, p. 554–558, 2006.

APPENDIX A – Quality Function Deployment (QFD)

Customer Requirements
(qfd.ods)

Row Number	Demanded Quality (a.k.a. "Customer Requirements" or "Whats")	Weight / Importance	Relative Weight
1	Be able to weld wires of different diameters	4	3,15
2	Be easy to set up	4	3,15
3	Have a mechanism for machining grooves for wire ends	5	3,94
4	Have a groove shaped for wire ends fixing	5	3,94
5	Have an abrasion resistant groove	4	3,15
6	Be able to pass electric current through the wire	5	3,94
7	Be able to ensure the correct wire ends positioning by constructive factors	5	3,94
8	Have a die opening setting	3	2,36
9	Be able to provide continuous force during welding	4	3,15
10	Have a way to configure the provided force	5	3,94
11	Be able to enable viewing of the weld joint	3	2,36
12	Have easy viewing of the welding result	3	2,36
13	Have an easy way to remove the welded wire	5	3,94
14	Have good performance	4	3,15
15	Be resistant	3	2,36
16	Be fine	2	1,57
17	Have rounded edges	2	1,57
18	Be made of materials available in the laboratory	3	2,36
19	Be cheap	3	2,36
20	Precise manufacturing	4	3,15
21	Be easy to manufacture	3	2,36
22	Have low manufacturing cost	2	1,57
23	Have short production time	2	1,57
24	Be manufactured in the laboratory	4	3,15
25	Be easy to assemble	3	2,36
26	Be simple to set up	3	2,36
27	Be simple to operate	5	3,94
28	Have accessible settings	4	3,15
29	Be able to position a camera	3	2,36
30	Have easy visibility of consumable items	3	2,36
31	Be able to reproduce quality welds	5	3,94
32	Be robust	5	3,94
33	Be able to maintain uniformity in weld consolidation	3	2,36
34	Be easy to maintain	3	2,36
35	Be of accessible materials	3	2,36

Relationship Between Requirements:
9 - Strong 3 - Moderate 1 - Weak

Column Number	1	2	3	4	5	6	7	8	9	10	11	12	13	14	15	16	17	18	19	20	21	22	23
Max Relationship Value in Column	419.69	205.51	192.91	139.37	167.72	219.11	251.18	525.2	462.2	297.4	293.7	301.57	279.53	257.49	359.84	178.74	194.49	178.74	159.84	289	291.1	305.51	277.66
Relative Weight	6.91	3.38	3.17	2.29	2.76	3.59	4.13	8.04	7.61	4.73	4.83	4.96	4.60	4.24	5.92	2.94	3.20	2.94	2.63	4.76	4.63	3.38	3.74
Difficulty (0=Easy to Accomplish, 10=Extremely Difficult)	10	3	1	3	3	3	4	7	7	6	8	9	6	10	5	2	4	2	1	3	3	3	3
Minimize (▼), Maximize (▲), or Target (x)	▲	▲	▼	▼	▲	▲	▲	▼	▼	▼	▼	▼	▲	▲	▲	▲	▼	▲	▲	▲	▲	▲	▼
Target or Limit Value	< 15% wire diameter	Maximum possible	Area of contact	Poor conductor	Resistive wiring	< wire harness	> 200 F.S. Ohm/cm	< 5 min	Be cheap	0 < d < 3mm	1 < F < 7 N	< 1 N	Maximum Possible	-	< 0.01mm	> wire fit	< 600x50mm	0 < F < 50N	> wire fit	> 150 HV	> 200 GPa	around 75 HV	< 400x300mm

Row Number	Max Relationship Value in Row	Relative Weight	Quality Characteristics (a.k.a. "Functional Requirements" or "How's")	1	2	3	4	5	6	7	8	9	10	11	12	13	14	15	16	17	18	19	20	21	22	23	
1	9	3.15	Be able to weld wires of different diameters	9	1	9	1	3	3	3	1	9	9	9	9	9	9	9	9	9	9	9	9	9	9	9	
2	9	3.15	Be easy to set up	9	1	1	1	3	9	9	9	1	9	1	1	3	9	9	3	3	1	1	1	1	1	3	
3	9	3.94	Have a mechanism for machining grooves for wire ends	9	1	1	1	1	1	9	3	1	1	1	1	3	9	9	3	9	9	3	3	3	3	3	
4	9	3.94	Have a groove shaped for wire ends fixing	9	9	1	1	1	1	9	9	1	1	1	1	3	1	1	1	3	1	1	1	1	1	3	
5	9	3.15	Have an abrasion resistant groove	3	9	1	1	1	1	9	3	9	1	1	1	1	1	1	1	1	3	3	1	1	1	1	
6	9	3.94	Be able to pass electric current through the wire	1	1	9	3	1	9	9	1	3	9	1	1	1	3	1	1	1	1	1	1	1	1	1	
7	9	3.94	Be able to ensure the correct wire ends positioning by constructive factors	9	3	1	1	1	3	1	9	3	3	1	1	3	1	9	3	1	3	1	9	9	3	1	
8	9	2.36	Have a die opening setting	3	1	1	1	1	1	1	9	3	9	1	1	3	3	9	1	1	1	1	1	9	9	1	3
9	9	3.15	Be able to provide continuous force during welding	1	3	1	1	1	3	1	1	9	1	9	9	3	1	1	1	1	1	1	1	3	1	1	
10	9	3.94	Have a way to configure the provided force	1	1	1	1	1	1	9	9	1	9	9	3	1	1	1	1	1	1	1	1	1	1	3	
11	9	2.36	Be able to enable viewing of the weld joint	3	1	1	1	1	1	1	3	3	3	1	1	1	9	1	1	1	1	1	1	1	1	1	3
12	9	2.36	Have easy viewing of the welding result	3	1	1	1	1	1	1	3	3	3	1	1	1	9	1	1	1	1	1	1	1	1	1	3
13	9	3.94	Have an easy way to remove the welded wire	1	1	1	1	1	1	1	9	3	3	1	1	1	1	1	1	1	3	1	1	1	1	1	3
14	9	3.15	Have good performance	3	1	3	3	3	3	3	9	1	3	9	3	1	9	3	1	3	1	3	1	9	9	9	1
15	9	2.36	Be resistant	9	3	1	1	9	3	1	1	9	1	3	3	9	1	9	3	1	1	1	1	9	9	9	1
16	9	1.57	Be fine	1	1	1	1	1	1	1	1	9	1	1	1	3	3	1	1	3	1	1	1	1	1	3	
17	3	1.57	Have rounded edges	1	1	1	1	1	1	1	1	3	1	1	1	1	1	1	1	1	1	1	1	1	1	1	1
18	9	2.36	Be made of materials available in the laboratory	1	1	1	1	1	1	1	1	9	1	1	1	1	1	1	1	1	1	1	1	1	1	1	3
19	9	2.36	Be cheap	1	3	3	1	1	1	1	1	9	1	1	3	3	1	1	1	1	1	1	1	1	1	1	3
20	9	3.15	Precise manufacturing	9	1	1	1	1	1	1	3	9	3	1	3	3	1	9	3	3	1	3	1	1	1	1	3
21	3	2.36	Be easy to manufacture	1	1	1	1	1	1	1	3	1	1	1	1	1	1	1	1	1	1	1	1	1	1	1	3
22	9	1.57	Have low manufacturing cost	3	1	1	1	1	1	1	1	9	1	1	3	3	1	3	1	3	1	1	1	1	1	1	3
23	9	1.57	Have short production time	1	1	1	1	1	1	1	1	9	1	1	1	1	1	1	1	1	3	1	1	1	1	1	3
24	9	3.15	Be manufactured in the laboratory	1	1	1	1	1	1	1	1	9	1	1	1	1	1	1	1	1	1	1	1	1	1	1	3
25	9	2.36	Be easy to assemble	1	1	1	1	1	1	1	9	1	1	1	1	3	3	1	1	3	1	1	1	1	1	1	3
26	9	2.36	Be simple to set up	9	1	1	1	1	1	1	9	3	3	3	1	3	3	9	3	3	3	3	1	9	3	1	3
27	9	3.94	Be simple to operate	3	1	1	1	1	1	1	9	3	3	3	3	3	3	9	3	3	3	3	3	3	3	1	1
28	9	3.15	Have accessible settings	3	1	1	1	1	1	1	9	3	3	3	1	1	3	3	1	3	1	1	1	1	1	1	3
29	9	2.36	Be able to position a camera	3	1	1	1	1	1	1	3	3	3	1	1	1	9	1	1	1	1	1	1	1	1	1	3
30	9	2.36	Have easy visibility of consumable items	1	1	1	1	3	3	1	9	3	3	1	1	1	9	1	1	1	1	1	1	1	1	1	3
31	9	3.94	Be able to reproduce quality welds	9	3	3	3	3	3	3	9	3	3	9	9	9	1	9	3	1	1	1	1	9	9	9	1
32	9	3.94	Be robust	9	3	3	3	3	3	3	3	3	3	9	9	9	1	1	1	1	1	1	1	3	3	1	1
33	9	2.36	Be able to maintain uniformity in weld consolidation	1	1	1	1	1	1	1	9	1	3	1	1	1	1	1	1	3	1	1	3	3	3	3	3
34	9	2.36	Be easy to maintain	1	3	3	3	3	3	3	1	9	1	1	1	3	3	1	1	1	1	1	1	3	3	3	3
35	9	2.36	Be of accessible materials	1	3	3	3	3	3	3	1	9	1	1	1	3	3	3	1	1	3	1	1	3	3	3	3

Correlations: Positive (+) or Negative (-)

HOQ 1 "Roof"
(qfd.ods)

Row Number	Column Number	1	2	3	4	5	6	7	8	9	10	11	12	13	14	15	16	17	18	19	20	21	22	23
	Quality Characteristics (a.k.a. "Functional Requirements" or "Hows")	Concentricity of the weld joint	Hardness of the wire contact region	Electrical contact resistivity	Thermal conductivity of electric contact	Mechanical resistance of electric contact	Electrical contact ductility	Electrical resistivity of the fit	Device preparation time	Manufacturing cost of the device	Distance from the electrical contacts to the joint	Upsetting force	Static friction of the welding motion actuator	Rigidity of the device	Opacity of materials near weld joint	Machining device adjustment precision	Positioning range of the machining device	Dimension of the machining device	Wire tensile force for machining	Machining path	Adjustment and moving parts hardness	Modulus of elasticity of adjustment and movement parts	Hardness of static parts	Overall dimension of the device
1	Concentricity of the weld joint																							
2	Hardness of the wire contact region	+																						
3	Electrical contact resistivity	-	-																					
4	Thermal conductivity of electric contact	-	-	+																				
5	Mechanical resistance of electric contact	-	-	+	+																			
6	Electrical contact ductility	+	-	+	+	+																		
7	Electrical resistivity of the fit	-	+	-	-	-	-																	
8	Device preparation time	+	+	+	-	-	+	-																
9	Manufacturing cost of the device	+	+	+	+	+	+	+	-															
10	Distance from the electrical contacts to the joint	-	-	+	+	+	+	-	+	-														
11	Upsetting force	-	-	+	+	+	+	-	+	+	-													
12	Static friction of the welding motion actuator	-	-	-	+	-	-	-	+	+	-	+												
13	Rigidity of the device	+	+	-	-	+	-	-	+	+	-	-	+											
14	Opacity of materials near weld joint	-	-	+	+	-	+	+	+	+	+	-	-	-										
15	Machining device adjustment precision	+	-	-	-	-	-	-	+	+	-	-	-	-	-									
16	Positioning range of the machining device	-	-	-	-	-	-	-	+	+	-	-	-	-	-	+								
17	Dimension of the machining device	-	-	-	-	-	-	-	+	+	-	-	-	+	-	+	+							
18	Wire tensile force for machining	-	+	-	-	-	-	-	+	+	-	-	-	-	-	+	+							
19	Machining path	-	+	-	-	-	-	-	+	+	-	-	-	-	-	+	+	+						
20	Adjustment and moving parts hardness	+	-	-	-	-	+	-	+	+	+	-	-	-	-	+	-	-	-	-				
21	Modulus of elasticity of adjustment and movement parts	+	-	-	-	-	+	-	+	+	+	-	-	+	-	+	-	-	-	-	+			
22	Hardness of static parts	+	-	-	-	-	-	+	+	+	-	-	-	-	-	+	-	-	-	-	+	+		
23	Overall dimension of the device	-	-	-	-	-	-	-	+	+	+	-	+	+	-	-	+	+	-	+	-	-	-	

APPENDIX B – Welding power supply

The welding power supply (Figure 70) uses the energy from the grid, meaning, an alternate voltage signal with a peak of 311 V and a frequency of 60 Hz. This voltage is decreased by a transformer, and consequently, the current is increased. The current is determined by the resistance of the system components and the wire itself.



Figure 70: Welding source.

An electronic component called TRIAC (Triode for Alternating Current) is used to regulate the amount of voltage allowed to pass from the common network to the transformer. This is used to indirectly control the current applied to the wire ends. This component can regulate a percentage of the alternate tension allowed to pass to the wires. This percentage is measured by the end to the beginning of a half sinusoidal sign (red part of the curve in Figure 71).

This percentage is also an input variable of the welding source. For example, if the percentage is set to a value B, only B% of the voltage signal, counting from the end to the beginning of the half sinusoidal cycle, will be transmitted to the wire. In Figure 72, point C represents 100%, point A 0%, and point B the amount that is transmitted to the wire. This pattern happens until the end of the welding time.

The other main input variable of the welding source is the time during which the higher tension is applied (welding time T_1). This is important because it defines how much power is transmitted to the wire ends to form the weld. In Figure 72, this time is represented as T_1 .

Apart from these two main variables (initial time T_1 and percentage of the tension signal C_1) a secondary set of variables can also be defined. After the weld, if the current is suddenly stopped, the wire, due to its low thermal capacitance, has a fast drop in its temperature.

To avoid that, the current (and by consequence, the temperature) is gradually decreased. The secondary set of variables are the rate of the current

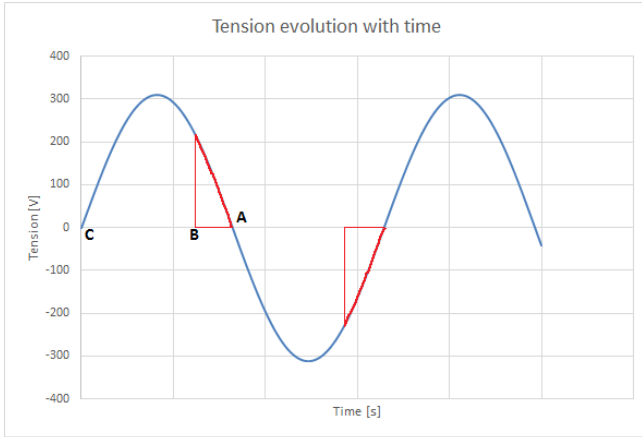


Figure 71: Sinusoidal Signal from the common network. Adapted from Campos (2016).

decrease, which can be decomposed into time of decayment and current (C_2 , T_2 , T_3 and T_4). A graph illustrating the process is shown on Figure 72.

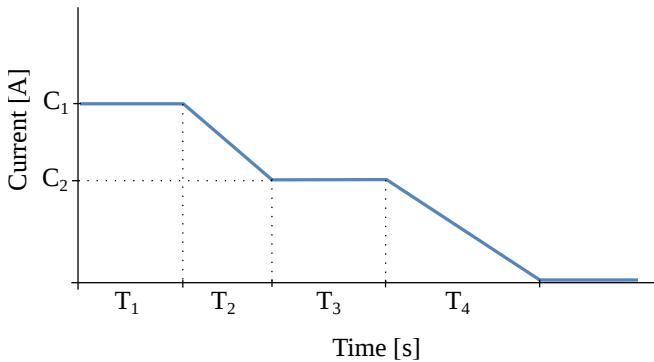


Figure 72: Variation of the Current with time.

In Figure 72, the level C_1 represents the weld current, which is applied into the wire for a time T_1 . After a certain time T_1 , the current begins to slowly decrease until it reaches the level C_2 . The rate of decayment is controlled by the variable T_2 . The current is maintained at the level C_2 until T_3 . It then starts to slowly decrease again until there's no more current. The rate of decayment of this last phase is controlled by T_4 . This system can indirectly control the wire's temperature at the weld, preventing it from becoming brittle.

APPENDIX C – Weld joints metallography

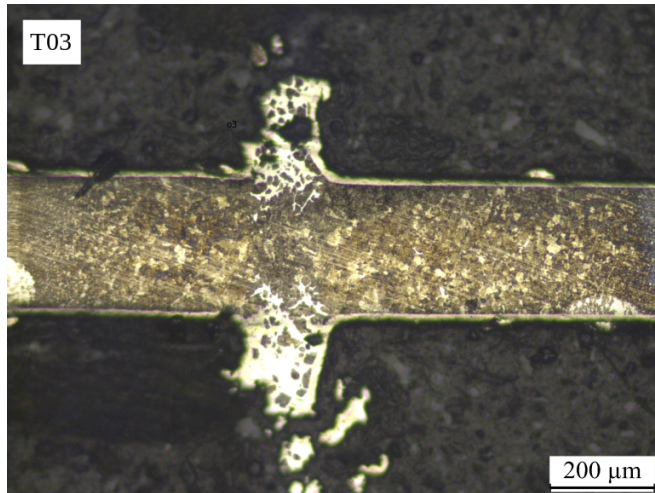


Figure 73: Metallography of the welded joint done with parameters T03.

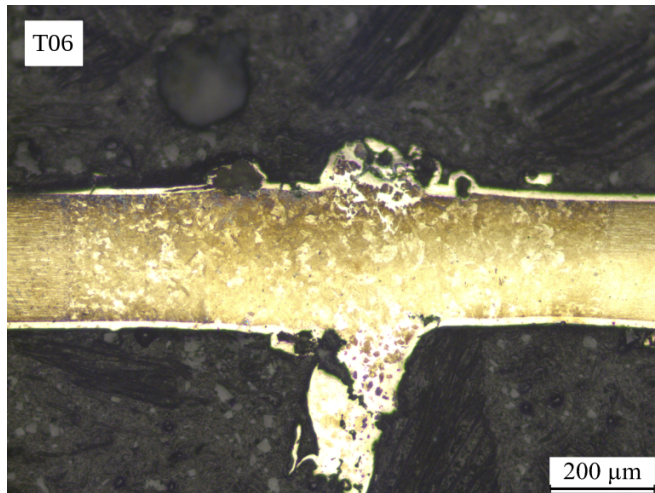


Figure 74: Metallography of the welded joint done with parameters T06.

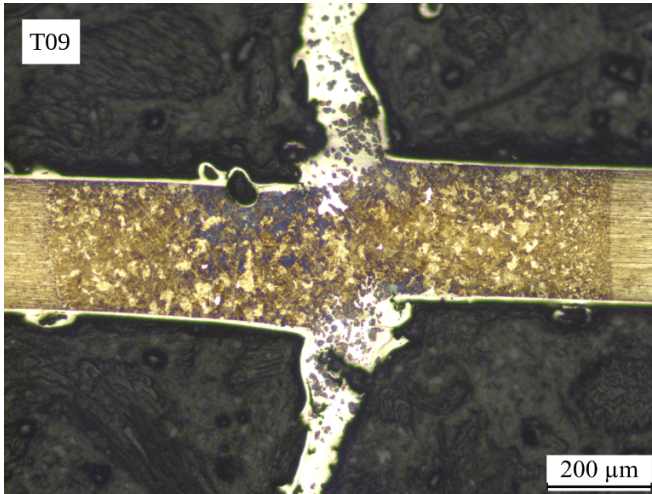


Figure 75: Metallography of the welded joint done with parameters T09.

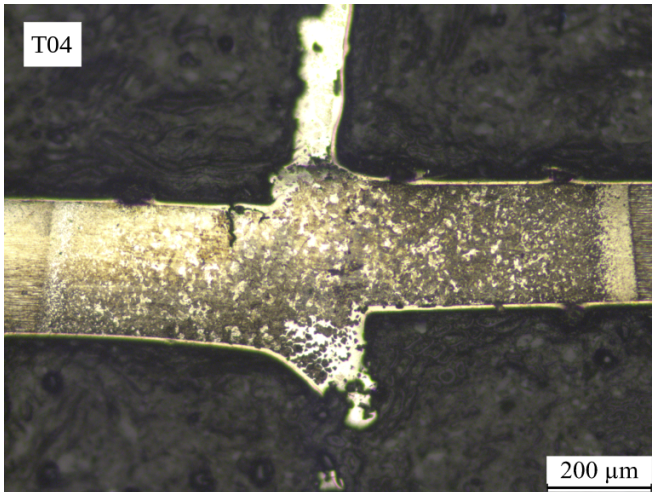


Figure 76: Metallography of the welded joint done with parameters T04.

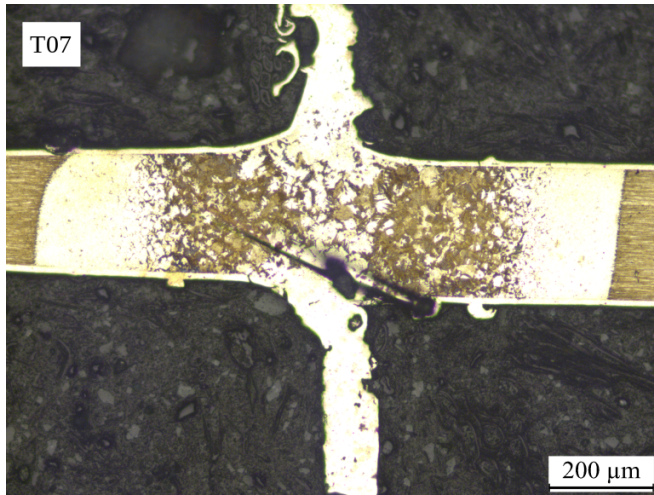


Figure 77: Metallography of the welded joint done with parameters T07.

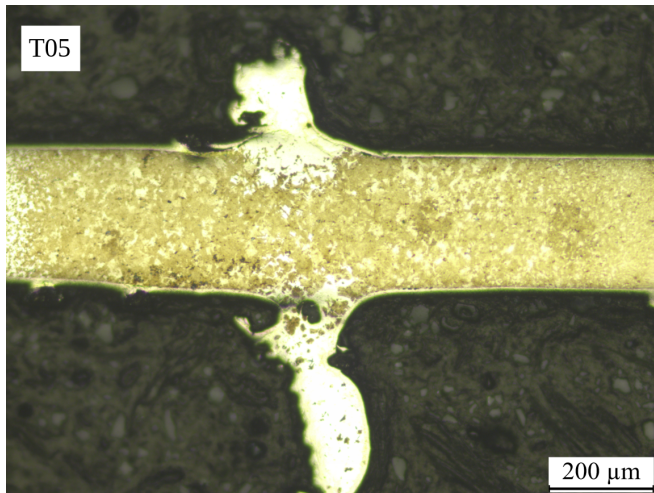


Figure 78: Metallography of the welded joint done with parameters T05.

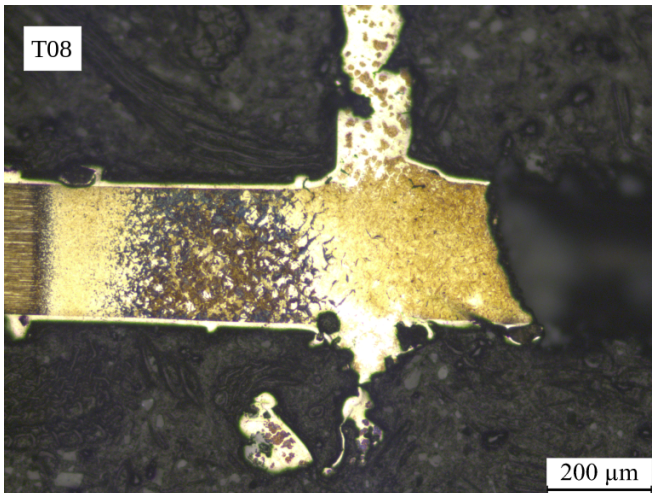


Figure 79: Metallography of the welded joint done with parameters T08.